Towards the structural characterization of proteins involved in peptidoglycan biosynthesis

Richting de structurele karakterisering van eiwitten die betrokken zijn bij de biosynthese van peptidoglycaan
(met een samenvatting in het Nederlands)

Proefschrift

ter verkrijging van de graad van doctor aan de Universiteit Utrecht op gezag van de rector magnificus, prof.dr. G. J. van der Zwaan, ingevolge het besluit van het college voor promoties in het openbaar te verdedigen op maandag 30 november 2015 des middags te 12.45 uur

door

Ioulia Nikolaidis

geboren op 25 januari 1982
te Oelde, Duitsland

Promotor:	Prof. dr. A. Killian
Copromotoren:	Dr. E. J. Breukink
	Dr. A. Dessen

This thesis was accomplished with financial support from the Netherlands Organisation for Health Research and Development (*Zorg Onderzoek Nederland Medische Wetenschappen*, ZonMw), grant number 205100001.

To my grandmother Gerda

Printing and Cover: Ridderprint BV, the Netherlands
ISBN: 978-94-6299-223-8

Contents

CHAPTER 1

INTRODUCTION

Partially based on: **Ioulia Nikolaidis, Sandy Favini-Stabile and Andréa Dessen.** Resistance to antibiotics targeted to the bacterial cell wall. Protein Sci. **2014** Mar; 23 (3): 243-259.

The cell wall is an essential structure for bacterial survival and unique to bacteria. It is the structural component of the cell envelope of almost all bacteria with the exception of *Mycoplasma* and a small group of highly specialized prokaryotes (Razin 1963, Errington 2013). This cell envelope is not only responsible for the structural rigidity, which is required to preserve cellular integrity against high differences in internal osmotic pressure, but also determines cellular shape and serves as a scaffold for anchoring numerous cell envelope components, such as proteins and polysaccharides (Neuhaus and Baddiley 2003, van Dam, Sijbrandi et al. 2007, Dramsi, Magnet et al. 2008). The structure of this macromolecule must nonetheless be highly dynamic, requiring constant remodeling and a tight regulation to enable both cell growth and division. Bacterial pathogens are today the most common cause for a wide range of illnesses, including infections of the skin and blood, pneumonia, tuberculosis and meningitis (Lovering, Safadi et al. 2012). Consequently, the cell wall biosynthetic pathway has been an optimal target for the development of antibiotics for over half a century.

1. 1 The bacterial cell wall: structure and chemical arrangement

Based on the chemical composition, the cell envelope of most bacteria falls into two major groups. Gram-positive bacteria are surrounded by a thick cell wall consisting of several layers of peptidoglycan (20-80 nm) located above the plasma membrane and forming the cell exterior. Perpendicular to these sheets are the teichoic acids and lipoteichoic acids, which are covalently linked to the peptidoglycan mesh (**Fig. 1** (A)). On the other hand, the cell wall of Gram-negative organisms is composed just of a single layer of peptidoglycan, sandwiched between the plasma and outer membrane (Beveridge 1981, Yao, Jericho et al. 1999). The inner leaflet of the outer membrane contains lipoprotein-complexes (Lpp or Braun's lipoprotein), which maintain the contact between the outer membrane and the murein sacculus in the periplasmic space (**Fig. 1** (B)).

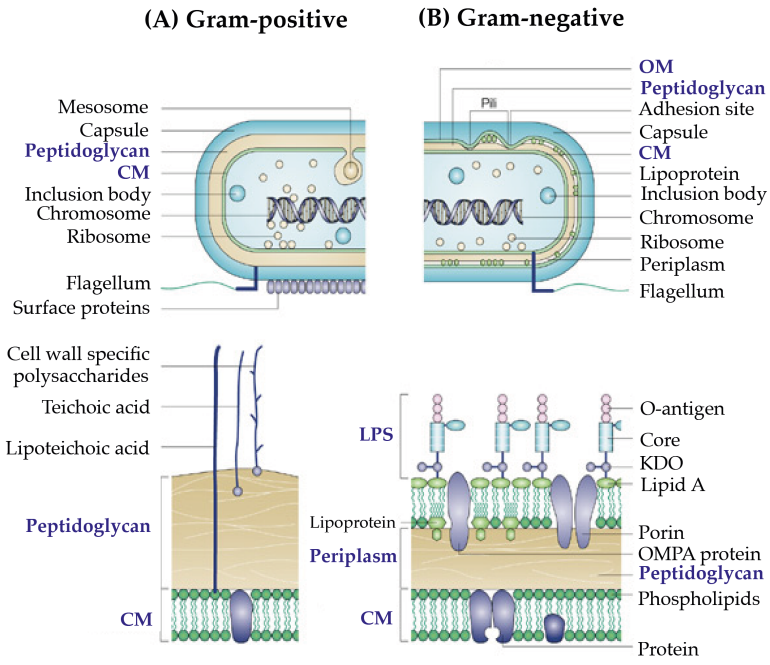

Fig. 1: Schematic representation of (A) Gram-positive and (B) Gram-negative cell envelop. Abbreviations: LPS, Lipopolysaccharide; CM, cytoplasmic membrane; OM, outer membrane. Adapted from (Lolis and Bucala 2003).

The major structural component of both cell walls is the peptidoglycan, also referred to as murein, which is conserved among eubacteria. This heteropolymer is a three-dimensional, cross-linked mesh, which is formed by linear glycan chains composed of alternating *N*-acetyl muramic acid (Mur*N*Ac) and *N*-acetyl glucosamine (Glc*N*Ac) units cross-linked by short peptides (van Heijenoort 2001, Vollmer, Blanot et al. 2008, Vollmer, Joris et al. 2008). The primary structure of the building block of the peptidoglycan is shown in **Fig. 2** (A).

In the mature peptidoglycan, the glycan chains are cross-linked by means of the peptide cross-bridges that extend from the lactyl segment of the Mur*N*Ac saccharide. The C3 lacyl moiety of Mur*N*Ac is substituted by a peptide subunit composed of D- and L-amino acids, most often consisting of L-Alanine, D-Glutamic

acid, *meso*-2,6-diaminopimelic acid (or L-Lysine), D-Alanine and D-Alanine, but can vary among bacterial species (**Fig. 2** (A)). The pentapeptide stem is present in the nascent peptidoglycan, however, during cross-linking reactions the terminal D-Alanine at position 5 gets generally cleaved off and is thus not present in the mature peptidoglycan. The stem peptides generally serve as a point of covalent attachment of cell envelope proteins to the murein and peptides from neighboring glycan chains can form cross-links with each other (Braun and Wolff 1970). The formation of cross-bridges occurs in most cases between the D-Alanine at position 4 and the diamino acid at position 3, either directly (Gram-negative bacteria; **Fig. 2** (B), top) or in some cases through a short peptide bridge (Gram-positive bacteria; **Fig. 2** (B), bottom) (Schleifer and Kandler 1972, Holtje 1998, Vollmer 2008).

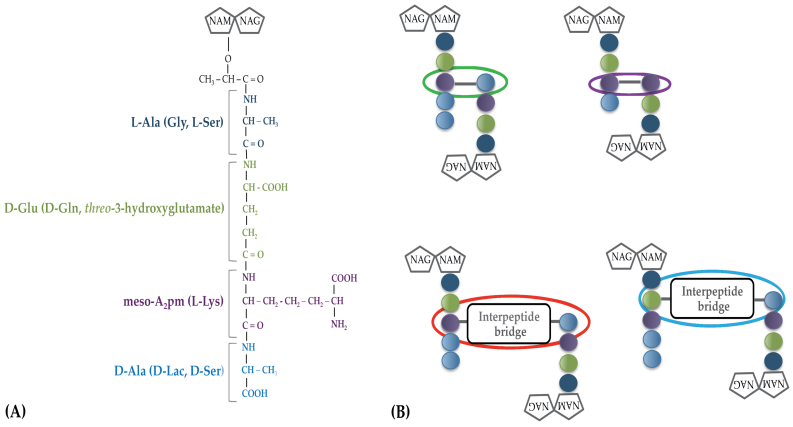

Fig. 2: Variations in peptidoglycan stem peptide. Chemical structure of the peptidoglycan building block. **(A)** The glycan chain is made of Glc*N*Ac and Mur*N*Ac in which the D-lactoyl group of Mur*N*Ac is substituted by peptide chains containing D- and L- amino acids (variations in chemical compositions are shown in brackets). **(B)** Peptidoglycan cross-linking reactions can be either directly, through 4-3 or 3-3 crosslinks (top; green circle and purple circle, respectively) or situated between position 3 and 4 or 2 and 4 of the stem-peptide (bottom; red circle and blue circle, respectively). Abbreviations: NAM, Mur*N*Ac; NAG, Glc*N*Ac. Adapted from (Vollmer 2012).

Notably, the architecture of peptidoglycan can show great diversity within and across bacterial species, whether in length of the glycan chains, extent and location of the stem peptide or composition of the interpeptide bridge. The repeating

disaccharide backbone shows only minor modifications during maturation of the cell wall, including mainly N-deacetylation of Glc*N*Ac and/or Mur*N*Ac, O-acetylation of the Mur*N*Ac moiety or enzymatic conversion of the terminal Mur*N*Ac residue to 1,6-anhydromuramic acid (Abrams 1958, Ghuysen 1968, Ward 1973, Vollmer and Tomasz 2000, Vollmer and Tomasz 2002, Vollmer 2008).

Nevertheless, the structure of the peptide side chains is much more variable, including differences in cross-links, variations in amino acids composition as well as diversity in interpeptide bridges.

Gram-positive bacteria, which are surrounded by a thick layer of murein, contain often an additional side chain linked to the third amino acid of the pentapeptide stem. These interpeptides are of various lengths and compositions, containing from one to seven amino acids in the L or D conformation (Schleifer and Kandler 1972). Nonribosomal peptidyl transferases belonging to the Fem protein family are responsible for the synthesis of these interpeptides (Rohrer and Berger-Bachi 2003). Fem transferases incorporate L-amino acids and glycine into the side chain through participation of aminoacyl-tRNAs and are known to be essential for the correct assembly of the peptidoglycan (Hegde and Blanchard 2003). Also a considerable amount of different macromolecules are attached to the stem peptide which are involved *e.g.* in cell wall biosynthesis and transport of nutrients into the cell. These proteins are generally attached to the murein sacculus by either covalent bonding or electrostatic association (Beveridge 1999).

However, despite the progress in the last decades in elucidating the fine structure of peptidoglycan, the complexity of its molecular architecture is still not fully understood. For understanding bacterial cell wall growth it is therefore an essential prerequisite to determine peptidoglycan architecture and its mechanism of intermolecular assembly.

1. 2 Peptidoglycan biosynthesis

The growth of peptidoglycan is a complex process, which involves the synthesis of the disaccharide pentapeptide subunits and their integration into the existing murein sacculus. The biosynthesis can be divided into three distinct stages: cytoplasmic, membrane and periplasmic steps (**Fig. 3**).

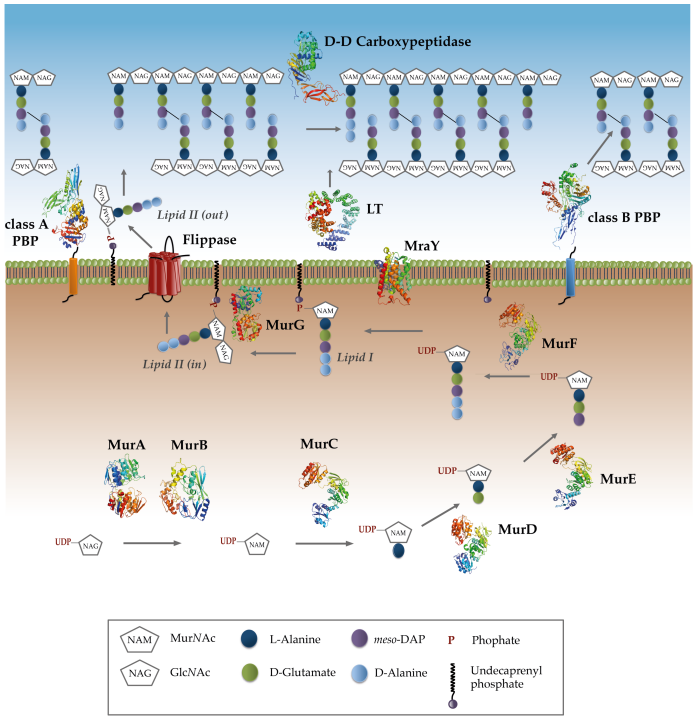

Fig. 3: Peptidoglycan biosynthesis. The synthesis of the peptidoglycan precursor, Lipid II, is initiated in the bacterial cytosol through the concerted action of six Mur enzymes (MurA to MurF) that act in a catalytic cascade (Macheboeuf, Contreras-Martel et al. 2006). The resulting soluble molecule, UDP-Mur*N*Ac-pentapeptide, becomes then associated to the cytoplasmic membrane through the action of an integral membrane protein, called MraY. This translocase couples undecaprenyl phosphate to UDP-Mur*N*Ac-pentapeptide to form Lipid I. MurG, a membrane associated glycosyltransferase, subsequently catalyzes the final cytoplasmic step through the transfer of a soluble Glc*N*Ac molecule to Lipid I resulting in the generation of Lipid II. This molecule is then *flipped* to the outside of the bacterial membrane, where it is acted upon by Penicillin-Binding Proteins (PBPs), which polymerize the glycan chains and cross-link the stem peptides. LT, Lytic transglycosylases.

THE CYTOPLASMIC STEPS: *Synthesis of UDP-MurNAc-pentapeptide*

The first step involves the assembly of the disaccharide-peptide monomer via a series of UDP precursors and lipid intermediates (van Heijenoort, 2001). The synthesis is catalyzed by the concerted action of Mur enzymes located in the

bacterial cytoplasm. MurA transfers the enolpyruvyl moiety from phosphoenolpyruvate (PEP) to UDP-Glc*N*Ac generating enolpyruvyl-UDP-Glc*N*Ac. The UDP-*N*-acetylenolpyruvylglucosamine reductase MurB subsequently catalyzes in a NADPH-dependent manner the reduction of enolpyruvyl-UDP-Glc*N*Ac to UDP-Mur*N*Ac (Barreteau, Kovac et al. 2008). The addition of the pentapeptide side chain to UDP-Mur*N*Ac occurs afterwards through a series of ATP-dependent amino ligases MurC-MurF resulting in the formation of UDP-Mur*N*Ac-pentapeptide.

THE MEMBRANE STEPS: *Assembly of Lipid I and II*

The following steps occur at the cytoplasmic side of the inner membrane, starting with the transfer of Mur*N*Ac-pentapeptide within the cytoplasm onto the undecaprenyl phosphate lipid carrier, resulting in the generation of Lipid I (**Fig. 4**, left) (Struve and Neuhaus 1965, Bouhss, Mengin-Lecreulx et al. 1999). This reversible process is catalyzed by the integral membrane protein MraY in a magnesium-dependent manner (Heydanek, Linzer et al. 1970, Bouhss, Crouvoisier et al. 2004, Chung, Zhao et al. 2013). The catalytic mechanism of MraY is believed to proceed via an active site nucleophile in either one-step or two-step reaction (Heydanek, Struve et al. 1969, Lloyd, Brandish et al. 2004, Lovering, Safadi et al. 2012). The recent crystal structure solution of *Aquifex aeolicus* MraY revealed that an Aspartate acts as the nucleophile on the phosphate group of undecaprenylphosphate (Chung, Zhao et al. 2013). Insertional inactivation of *mraY* in *Escherichia coli* and in the Gram-positive organism *Streptococcus pneumoniae* resulted in a lethal phenotype, demonstrating its essential function for cell viability (Boyle and Donachie 1998).

Concurrently, the glycosyltransferase MurG couples Glc*N*Ac to the C-4 hydroxyl of the Mur*N*Ac moiety of Lipid I, generating the undecaprenyl-pyrophosphoryl-Glc*N*Ac-Mur*N*Ac-pentapeptide or better known as Lipid II (**Fig. 4**, right corner) (Mengin-Lecreulx, Texier et al. 1991, van Heijenoort 2001, Bouhss, Trunkfield et al. 2008). In bacterial cells, MurG is peripherally associated to the cytoplasmic membrane, most likely via a hydrophobic patch that is surrounded by basic residues as shown in the crystal structure (Bupp and van Heijenoort 1993, Ha, Walker et al. 2000).

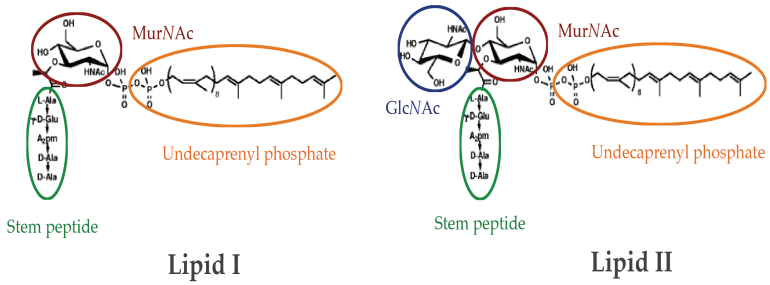

Fig. 4: Chemical composition of the two lipid intermediates, Lipid I (left) and Lipid II (right). Adapted from (van Heijenoort 2007).

MurG follows a sequential ordered Bi-Bi mechanism in which UDP-GlcNAc binds first in the C-terminal domain, whereas the primary acceptor-binding domain for Lipid I is located N-terminal (Chen, Men et al. 2002, Hu, Chen et al. 2003, van Heijenoort 2007, Lovering, Safadi et al. 2012). Lipid II remains anchored to the inner leaflet of the cytoplasmic membrane until it gets translocated to the outside of the bacterial membrane.

The enzymes involved in the synthesis of the complete disaccharide peptide monomer are well known, but the identity of the protein which is responsible for the transport of Lipid II across the cytoplasmic membrane has been controversial.

THE FLIPPASE

Two candidates have been proposed as mediating Lipid II translocation: FtsW/RodA/SpoVE–like or MurJ-like proteins.

Potential transporters of peptidoglycan subunits are essential, inner membrane proteins which have to be conserved among peptidoglycan producing bacteria. FtsW, an integral membrane protein whose gene is located within the *division and cell wall* (dcw) cluster in most bacterial species, has been suggested for a number of years as being responsible for Lipid II translocation across the cytoplasmic membrane (Holtje 1998, Bouhss, Trunkfield et al. 2008, Vollmer and Bertsche 2008).

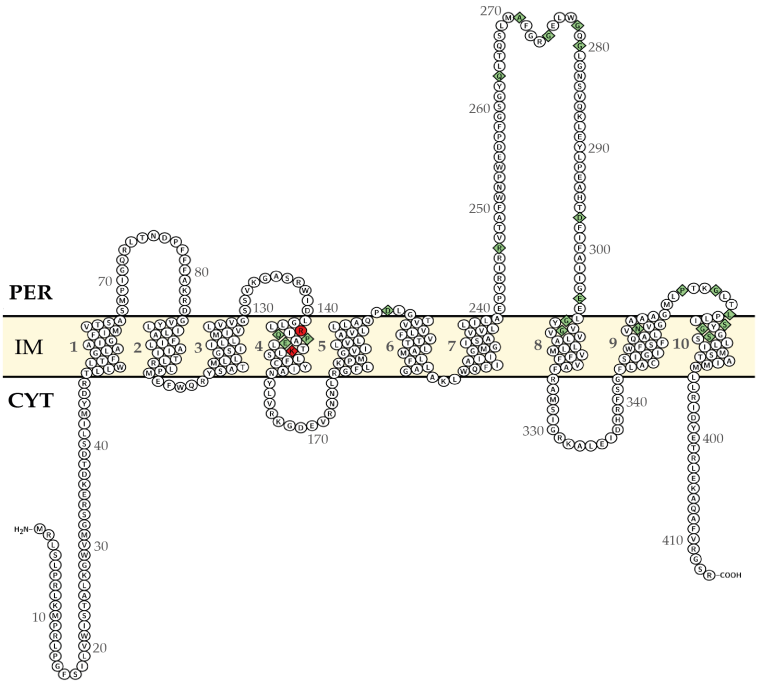

Fig. 5: Topology model of *Escherichia coli* FtsW. FtsW consists of ten predicted transmembrane helices, a large periplasmic loop between transmembrane helix 7 and 8, and both the N- and C-terminal extremities are predicted to face the cytoplasm. Conserved residues are shown in green and amino acids that are required for the activity are shown in red. Abbreviations: PER, periplasm; IM, inner membrane; CYT, cytoplasm.

It is an essential protein during cell division and daughter cell formation (Boyle, Khattar et al. 1997). FtsW has ten predicted membrane spanning helices (**Fig. 5**) and belongs to the SEDS protein family (**S**hape, **E**longation, **D**ivision and **S**porulation), which includes also two known homologs that share 30% identity: (1) **RodA** which is necessary for cell wall synthesis during cell elongation of rod-shaped cells, and (2) **SpoVE**, that is key for cell wall synthesis during spore-formation (*e.g.* in *Bacillus subtilis*) (Ikeda, Sato et al. 1989, Joris, Dive et al. 1990). Mohammadi and colleagues recently presented convincing evidence that transport of Lipid II requires the presence of FtsW. The authors used a fluorescence resonance energy transfer

(FRET)-based assay in which cell-derived vesicles containing an fluorescent 7-nitro-2,1,3-benzoxandiazol-4-yl (NBD)-labeled Lipid II in the inner leaflet of the membrane were incubated with a membrane-impermeable tetramethylrhodamine cadaverine (TMR)-labeled vancomycin acceptor, so that FRET occurred only after Lipid II translocation (Mohammadi, van Dam et al. 2011). Vesicles which derived from *E. coli* strains overexpressing FtsW, showed an increase in transbilayer movement of Lipid II compared to vesicles derived from wild-type cells. Conversely, vesicles derived from *E. coli* strains depleted of FtsW showed a decrease in Lipid II translocation. Direct evidence of the involvement of FtsW in Lipid II translocation could be demonstrated by a dithionite reduction assay in which the co-reconstitution of FtsW and NBD-Lipid II in model membranes led to increased accessibility of NBD-Lipid II for dithionite, hence confirming a direct role of FtsW in the transport of Lipid II (Mohammadi, van Dam et al. 2011).

Furthermore, the mechanism of Lipid II translocation seems to be ATP independent, with the subsequent polymerization step being considered the driving force for unidirectional translocation (van Dam, Sijbrandi et al. 2007, Mohammadi, van Dam et al. 2011). In addition, as peptidoglycan biosynthesis requires a continuous insertion of new material into the growing cell wall at a high rate, translocation of Lipid II has to match this speed and thus has to be in order of seconds (van Heijenoort, Gomez et al. 1992, van Dam, Sijbrandi et al. 2007, Sanyal and Menon 2009). This could be also successfully confirmed by the abovementioned fluorescent-based assays in which Lipid II translocation was fully accomplished within few seconds after addition of the quenching reagent (Mohammadi, van Dam et al. 2011).

All bacteria that possess a cell wall composed of peptidoglycan seem to possess at least one member of the SEDS family, which are completely absent in cell wall lacking organisms such as *Mycoplasma genitalium* and *Methanococcus janasschii* (Ikeda, Sato et al. 1989, Henriques, Glaser et al. 1998). Furthermore it is thought that each SEDS seem to functionally associate with its cognate class B Penicillin-Binding-Protein (PBP) and thus it is likely that Lipid II translocation to the exterior surface is coupled to the *downstream* synthesis of the cell wall by PBPs (Noirclerc-Savoye, Morlot et al. 2003, van Dam, Sijbrandi et al. 2007, Mohammadi, van Dam et al. 2011). Whether a (direct) coupling exists between the synthesis of Lipid II and its transport is unclear and remains to be determined. Fraipont and colleagues showed previously by *in vivo* FRET experiments as well as *in vitro* co-immunoprecipitation of FtsW and PBP3 that these two proteins directly interact with each other and form a

discrete subcomplex in *E. coli* (Fraipont, Alexeeva et al. 2011). Furthermore, site-directed mutagenesis experiments revealed the requirement of the periplasmic loop located between transmembrane segments 9 and 10 for the recruitment of PBP3 to the septum (Pastoret, Fraipont et al. 2004). This loop seems also to play an indirect role in interaction with the main peptidoglycan synthase PBP1B (Di Lallo, Fagioli et al. 2003, Karimova, Dautin et al. 2005, Fraipont, Alexeeva et al. 2011). Nevertheless, an FtsW-PBP3-PBP1B trimeric complex could not be detected by co-immunoprecipitation, probably due to weak or transient interaction.

MurJ on the other hand is composed of fourteen predicted transmembrane domains and belongs to the multidrug/oligo-saccharidyl-lipid/polysaccharide (MOP) exporter superfamily (Sham, Butler et al. 2014). Depletion of *E. coli* MurJ results in inhibition of peptidoglycan biosynthesis, leading to accumulation of peptidoglycan precursors in the cytoplasm of *E. coli* followed by lysis of the cell (Inoue, Murata et al. 2008, Ruiz 2008, Butler, Davis et al. 2013). Butler and colleagues used a combination of *in silico* modeling and *in vivo* approaches to demonstrate that *E. coli* MurJ shows high degrees of structural similarities to proteins belonging to the MATE (Multidrug and toxic compound extrusion) family, including transporters which translocate hydrophobic and amphipathic toxic compounds across the cytoplasmic membrane (Kuroda and Tsuchiya 2009, Butler, Davis et al. 2013). The structural model is organized similar to MATE protein structures, with two 6-helical bundles forming a V-shaped structure providing a central cavity and two lateral portals (**Fig. 6**) (Butler, Davis et al. 2013).

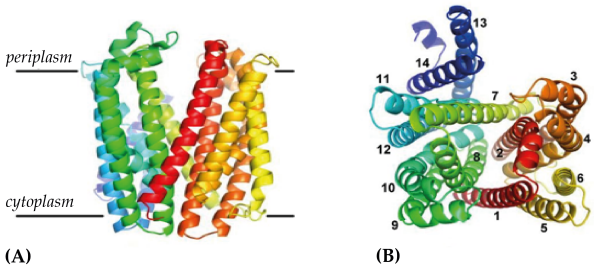

Fig. 6: Structural model of *Escherichia coli* MurJ generated by I-TASSER. **(A)** Front view of MurJ from membrane plane. **(B)** View from the top of the structural model with transmembrane domains numbered 1-14 (Butler, Davis et al. 2013).

This hydrophilic cavity contains several charged residues which are essential for the function of MurJ (Butler, Davis et al. 2013). Sham and colleagues developed recently an *in vivo* activity assay, which uses the toxin colicin M (ColM) to specifically cleave flipped Lipid II in the periplasm, resulting in the generation of soluble product PP-M_{pep5}-G which can be afterwards detected by high-performance liquid chromatography (Sham, Butler et al. 2014). The authors claim that when comparing wild-type MurJ with a MurJ-inactivated mutant only negligible amounts of PP-M_{pep5}-G could be detected and thus conclude that MurJ is essential for the translocation of Lipid II in *E. coli* (Sham, Butler et al. 2014).

However, flippase activity of the proposed candidates, be it FtsW or MurJ, could be only confirmed in one of the developed activity assays, either by the *in vitro* or the *in vivo*, but not simultaneously in both (Mohammadi, van Dam et al. 2011, Sham, Butler et al. 2014). Therefore, the identity of the protein mediating Lipid II translocation remains controversial and has to be further explored by additional biochemical approaches.

THE PERIPLASMIC STEPS: *Polymerization and incorporation*

Once Lipid II is flipped to the outside of the bacterial membrane, it can be subsequently incorporated into the peptidoglycan sacculus by enzymes which polymerize the disaccharide units (transglycosylation) and cross-link the stem peptides (transpeptidation) (**Fig. 7**) (van Heijenoort 2001, Vollmer and Bertsche 2008).

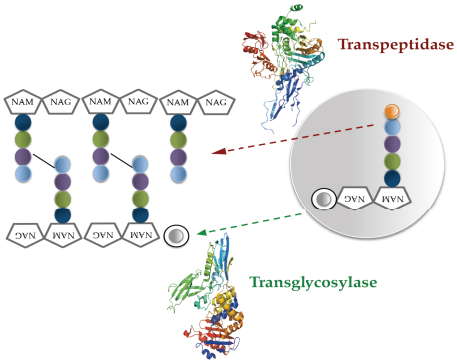

Fig. 7: Polymerization of the nascent peptidoglycan by transglycosylation and transpeptidation. The transglycosylation reaction involves the formation of a β-1,4-glyosidic bond

between the Mur*N*Ac and the Glc*N*Ac moiety of a disaccharide unit. Transpeptidation of the stem peptide occurs in two steps: **1)** The D-Alanine-D-Alanine at the end of the pentapeptide chain is cleaved, forming an enzyme-substrate intermediate and release of terminal D-Alanine and **2)** transfer of its peptidyl moiety to the free amino group of the diamino acid at position 3 of a nearby peptide; usually *meso*-2,6-diaminopimelic acid m-A_2pm, or L-Lysin. Adapted from (Vollmer and Holtje, 2000).

PENICILLIN-BINDING-PROTEINS (PBPs)

Key enzymes of this stage are PBPs. These proteins belong to the family of Active-site Serine Penicillin-recognizing Enzymes (ASPRE), which are characterized by the presence of a Penicillin-Binding (PB) domain with three structural conserved motifs: the active site SXXK and the two triads (S/Y) XN and (K/H)(S/T) G (**Fig. 8** (B)) (Zapun, Contreras-Martel et al. 2008). Each bacterial species possesses generally multiple PBPs, which can be commonly divided into two major classes (Ghuysen 1991, Goffin and Ghuysen 1998).

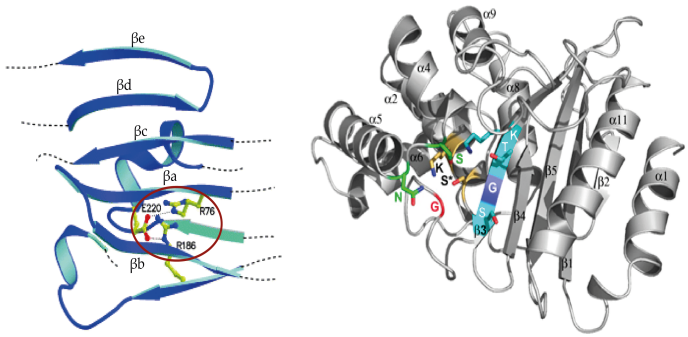

Fig. 8: (A) Close-up of the N-terminal region of *Streptococcus pneumoniae* PBP2x. The conserved residues (here **E**220, **R**76 and **R**186) are located mostly on β-strands and are circled in red. Adapted from (Macheboeuf, Contreras-Martel et al. 2006). **B) *Bacillus subtilis* PBP4a with its PBP domain and conserved motifs of the active site.** Motif SXXK shown in yellow, motif (S/Y) XN in green and motif (K/H)(S/T) G in cyan (Sauvage, Kerff et al. 2008).

The first class comprises high-molecular-mass (HMM) PBPs which are multi-domain enzymes containing a cytoplasmic tail, a membrane binding domain and a two

domain structure which is interspaced by a flexible β-sheet rich linker (Macheboeuf, Contreras-Martel et al. 2006, Lovering, de Castro et al. 2007, Sauvage, Kerff et al. 2008). Based on the structure and catalytic entities of their N-terminal domain, HMM PBPs can be further subdivided into two classes, A and B (Ghuysen 1991, Goffin and Ghuysen 1998, Sauvage, Kerff et al. 2008).

Class A HMM PBPs are bifunctional enzymes harboring both, a transglycosylase as well as a transpeptidase domain. This two-domain structure enables these enzymes to catalyze the sequential elongation of glycan chains and formation of cross-links between the peptides. Exemplified are these enzymes by *S. pneumoniae* PBP1A and PBP1B (**Fig. 9**, top). In *E. coli* these enzymes are considered to be major bifunctional transpeptidase/ transglycosylase enzymes, since inactivation of both proteins results in a lethal phenotype, whereas the presence of just one ensures cell viability (Kato, Suzuki et al. 1985, Yousif, Broome-Smith et al. 1985).

Class B HMM PBPs are monofunctional enzymes, resembling a typical three-domain structure composed of the active site (transpeptidase domain) sandwiched between an elongated N-terminal domain (nPB domain) and a helical rich domain at the C-terminal end of the protein containing just transpeptidase activity (**Fig. 9**, middle). Originally the nPB domain was thought to be a domain implicated in gathering other proteins involved in peptidoglycan synthesis, but its function was never demonstrated. Another possibility could be that this domain serves more as a pedestal, pointing the catalytic region of the protein away from the membrane to the nascent peptidoglycan (Holtje 1998, Macheboeuf, Contreras-Martel et al. 2006). At least for *E. coli* PBP3 it could be demonstrated that the nPB domain is required for the folding and/or stability of the PB module and thus functions as an intramolecular chaperone (Goffin, Fraipont et al. 1996).

Additionally it could be shown, that this nPB domain is highly variable and can range from 60 to 400 amino acids (Macheboeuf, Contreras-Martel et al. 2006). Goffin and Ghuysen identified through sequence analysis three conserved motifs within this domain which serve as an anchor point for stabilization of the N-terminal domain: (**R**GX_3DRNG), (**R**XYPXG) and (GX_2GX**E**X_3D) (**Fig. 8**) (Goffin and Ghuysen 2002). *E. coli* possesses two class B HMM PBPs, PBP2 and PBP3, which are essential during cell wall elongation and cell division, respectively. Inactivation of PBP2 results in termination of cell elongation and formation of round cells whereas loss of

PBP3 leads to the formation of long non-septate filaments (Osborn and Rothfield 2007).

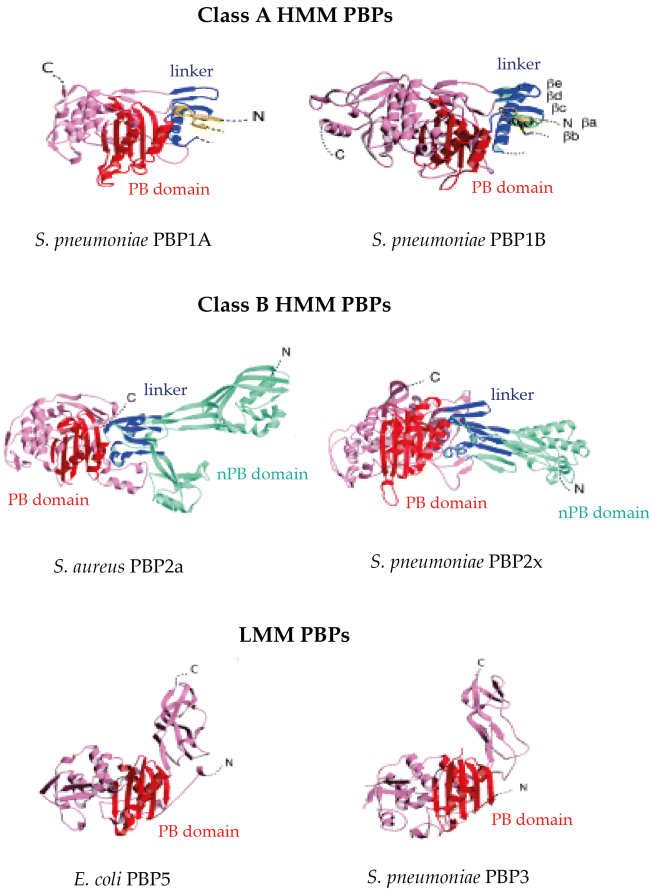

Fig. 9: Crystal structures of HMM and LMM PBPs. Both classes share a similar fold of the PB domain, which is composed of a five-stranded β-sheet fold packed by helices on both sides. Adapted from (Macheboeuf, Contreras-Martel et al. 2006).

Low-molecular mass (LMM) PBPs on the other hand belong to the second class. These proteins have mainly D-D-carboxypeptidase activities (hydrolysis of the D-Alanine-D-Alanine bond) (*e.g. E. coli* PBP5; **Fig. 9**, bottom, left) and are implicated in the degree of cross-linking, maturation and turnover of the cell wall, but are not

essential for peptidoglycan biosynthesis (Sauvage, Kerff et al. 2008). LMM PBPs possess an elongated, β-sheet rich C-terminal domain, which separates the catalytic region from the membrane associated amphipathic helix.

However, despite the fact that LMM PBPs are not essential for murein synthesis, they play an important role during peptidoglycan breakdown and are further discussed in the next section.

1. 3 Peptidoglycan growth, turnover and recycling

The highly dynamic structure of the peptidoglycan requires constant remodeling during growth and cell division. As the murein sacculus enlarges during these stages, meshes have to be cleaved to enable incorporation of new material (Schwarz, Asmus et al. 1969, Holtje, Mirelman et al. 1975, Holtje and Tuomanen 1991). This step has to be well coordinated and requires tight regulation, as uncontrolled cleavage could lead to lysis. To date, the mechanism of peptidoglycan growth is still a subject of speculation. Höltje proposed that bacteria integrate new material into the growing peptidoglycan layer by a two-step mechanism, also referred to as the 3-for-1 model (**Fig. 10**) (Holtje 1998).

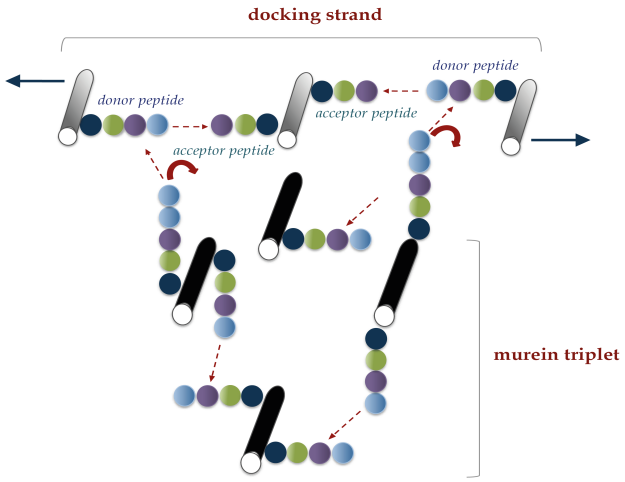

Fig. 10: Cell wall growth following the 3-for-1 model. The glycan strands of the pre-existing peptidoglycan are represented in grey, whereas the three newly synthetized strands are shown in outline. Adapted from (Holtje 1998).

In this model three newly synthesized peptidoglycan strands are covalently attached just underneath the existing murein sacculus. Later on, the old peptidoglycan strand is removed and the new segment can be inserted. This mechanism ensures that insertion of new material into the murein sacculus only occurs if the pre-existing peptidoglycan was successfully hydrolyzed, thus allowing a safe enlargement of the stress-bearing sacculus. Accordingly, cell wall growth requires not only the activity of murein synthases, but also the participation of enzymes, which are capable of cleaving specific bonds within the murein sacculus (Holtje 1998). Cell wall growth seems therefore to be directed by the interaction of theses proteins in different multi-enzyme complexes, which are recruited by intracellular elements of the bacterial cytoskeleton acting as a scaffold (Daniel and Errington 2003, Kruse, Bork-Jensen et al. 2005, Mohammadi, Karczmarek et al. 2007, Kawai, Daniel et al. 2009, White, Kitich et al. 2010, Dominguez-Escobar, Chastanet et al. 2011, Garner, Bernard et al. 2011). While peptidoglycan incorporation during elongation occurs along the lateral wall of the cell ('dispersed' elongation) and is driven by the actin-like protein MreB, septal peptidoglycan synthesis requires the tubulin-like protein FtsZ, which recruits first the elongation complex to the midcell ('preseptal' elongation) through polymerization into a ring-like structure just underneath the inner membrane (FtsZ-ring), followed by complete septal ring constriction and daughter cell separation (**Fig. 11**) (de Pedro, Quintela et al. 1997, Aarsman, Piette et al. 2005, Aaron, Charbon et al. 2007, Varma, de Pedro et al. 2007, Fenton and Gerdes 2013).

Consequently, during each stage of sacculus growth, these multi-enzyme complexes require the presence of hydrolases that cleave the sacculus and provide space for the incorporation of new material. These peptidoglycan hydrolyzing enzymes can be divided into three major groups: the carboxy- and endopeptidases, the *N*-acetylmuramyl-L-alanine amidases and last but not least the glycosidases, which comprise β-*N*-acetylhexoamidases, lysozymes as well as lytic transglycosylases (**Fig. 12**). Of special interest is the autolytic system of *E. coli*, which includes beside amidases and endopeptidases also glycosidases of the lytic transglycosylase-type (Holtje 1998).

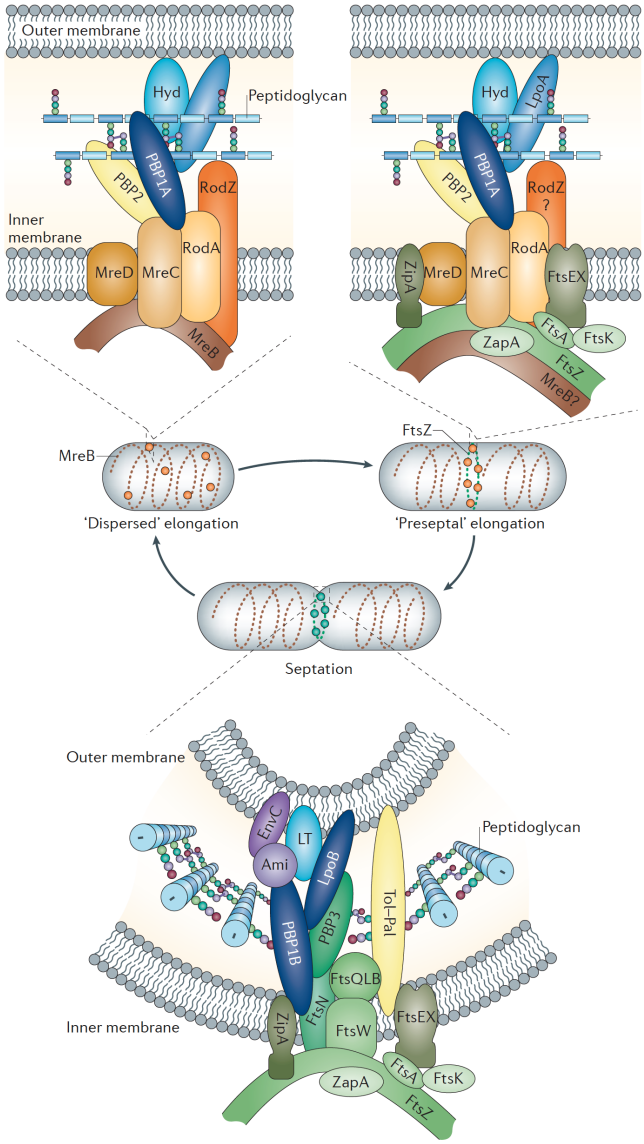

Fig. 11: Model of assembly of multi-enzyme complexes during lateral wall and septal peptidoglycan synthesis in *E. coli* (Typas, Banzhaf et al. 2012). During 'dispersed' cell wall elongation (upper left panel), translocation of peptidoglycan precursors (**RodA**) is followed by their incorporation by peptidoglycan synthases (**PBP2** and **PBP1A**) at the filament of **MreB**. The complex consists also of membrane proteins (**MreD**, **MreC**, **RodZ**), which control or position the PBPs and hydrolases (**Hyd**) that are required to cleave nascent peptidoglycan. Later, in the 'preseptal' stage of

elongation (upper right panel), **FtsZ** polymerizes into a ring-like structure (FtsZ-ring) and recruits the elongation complex and early division proteins (**FtsA**, **ZipA**, **ZapA**, **FtsE/X** as well as **FtsK**) at midcell. The final stage involves generation of a septum, resulting in daughter cell separation. Late division proteins (**FtsQLB**, **FtsW**, **PBP3**, **PBP1B** and **FtsN**), amidases (**Ami**) and their activators, as well as the **Tol-Pal** complex are assembled into the divisome.

LYTIC TRANSGLYCOSYLASES (LTs)

LTs represent the major class of muramidases in Gram-negative species and act on peptidoglycan with the same substrate specificity as lysozyme; cleaving the β-1,4 glycosidic bond between Glc*N*Ac and Mur*N*Ac (Holtje, Mirelman et al. 1975, Templin, Edwards et al. 1992). However, LTs do not catalyze a hydrolysis reaction; instead these enzymes cleave of the glycosidic bond generating glycan strands with 1,6-anhydroMur*N*Ac (anhMur*N*Ac) termini.

At least one soluble LT (Slt70) and six membrane-bound LTs (MltA-F) have been identified in *E. coli*. To date, crystal structures of several LTs have been solved (van Asselt, Dijkstra et al. 1999, van Asselt and Dijkstra 1999, van Asselt, Thunnissen et al. 1999, Leung, Duewel et al. 2001, van Straaten, Dijkstra et al. 2005, Powell, Liu et al. 2006, Fibriansah, Gliubich et al. 2012, Nikolaidis, Izore et al. 2012, Artola-Recolons, Lee et al. 2014).

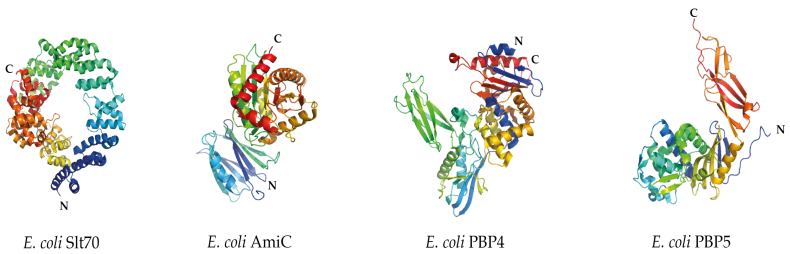

Fig. 12: Crystal structures of peptidoglycan hydrolases. Represented are structures from the three main groups of peptidoglycan hydrolyzing enzymes: glycosidase Slt70 (van Asselt, Thunnissen et al. 1999), *N*-acetylmuramyl-L-alanine amidase AmiC (Rocaboy, Herman et al. 2013), D,D-endopeptidase PBP4 (Kishida, Unzai et al. 2006) and D,D-carboxypeptidase PBP5 (Nicola, Peddi et al. 2005).

The structure of *E. coli* Slt70 consists of α-helices forming a doughnut-like shape with the catalytic domain on top, resembling structural similarities to goose-type lysozyme. Co-crystallization of Slt70 with anhMur*N*Ac revealed a specific recognition site for the peptide moiety of peptidoglycan, which is located at the interface of the catalytic domain (van Asselt, Thunnissen et al. 1999). This structure could confirm that Slt70 catalyzes the cleavage reaction at the anhMur*N*Ac termini of peptidoglycan (van Asselt, Thunnissen et al. 1999).

PEPTIDOGLYCAN TURNOVER AND RECYCLING

E. coli Slt70 as well as three other membrane-anchored LTs (MltA-B and MltF) have the ability to release a high amount of Glc*N*Ac-anhMur*N*Ac-peptide units, also referred to as muropeptides (Holtje, Mirelman et al. 1975, Engel, Smink et al. 1992, van Heijenoort 2011). Due to extensive growth, *E. coli* generates a massive turnover of approximately 40-50% per generation (Doyle, Chaloupka et al. 1988). These turnover products are generally accumulated in the periplasm, from where they can be efficiently reused by several recycling pathways (Goodell 1985, Holtje 1998, Johnson, Fisher et al. 2013). In *E. coli* the major pathway consists of the uptake of muropeptides via the AmpG permease (**Fig. 13**) (Holtje 1998, Cheng and Park 2002). Once transported to the cytoplasm, glucosamidase NagZ hydrolyzes the β-1,4 glycosidic bond (Votsch and Templin 2000), while amidase AmpD subsequently cleaves off the peptide moiety, generating Glc*N*Ac and anhMur*N*Ac. Surprisingly, AmpD is solely active on anhMur*N*Ac-peptides and not on other peptidoglycan precursors present in the cytoplasm (Jacobs, Joris et al. 1995). AmpD exhibits therefore strict substrate specificity and participates only in the intracellular recycling pathway of peptidoglycan turnover fragments (Jacobs, Joris et al. 1995, Genereux, Dehareng et al. 2004). The released anhMur*N*Ac will be afterwards further processed via the L,D-carboxypeptidase LdcA, which removes the C-terminal L-Ala and generates the murein tripeptide L-Ala-γ-D-Glu-*meso*-diaminopimelic acid (Templin, Ursinus et al. 1999). This tripeptide is directly channeled to the peptidoglycan biosynthesis pathway via the muropeptide ligase MpI, which catalyzes the addition of the tripeptide to UDP-Mur*N*Ac (Mengin-Lecreulx, van Heijenoort et al. 1996). This step results in the formation of UDP-Mur*N*Ac-tripeptide, key intermediate of the recycling pathway and substrate for MurF.

However, whereas AmpG permease exclusively transports sugar-containing muropeptides, oligopeptides can be also recycled via an alternative, minor recycling pathway, the Mpp/Opp system. This pathway utilizes turnover products released from the cell wall by amidases located in the periplasm. The generated tripeptides are taken up by the oligopeptide permease Opp, which requires the recruitment of the muropeptide binding protein MppA (Goodell 1985, Park, Raychaudhuri et al. 1998). As soon as these tripeptides reach the cytoplasm, a series of subsequent hydrolysis and ligation reactions (NagZ, AmpD, LdcA and MpI) result in the release of peptidoglycan precursors (UDP-Mur*N*Ac-tripeptide) for new incorporation into the cell wall (Holtje 1998, Johnson, Fisher et al. 2013).

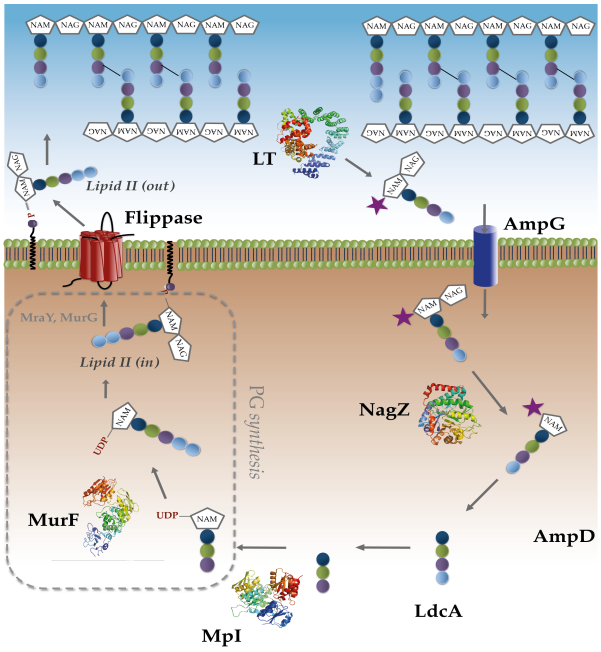

Fig. 13: Peptidoglycan (PG) turnover and recycling in *E. coli*. During bacterial growth and division, muropeptides are continuously liberated. The major path for recycling theses fragments is through the integral membrane protein AmpG. Through subsequent hydrolysis and ligation reactions, new peptidoglycan precursors are formed and are channeled directly to the peptidoglycan biosynthesis pathway by MurF. The purple star fused to *N*AM represents anhMur*N*Ac, the outlined rectangle highlights the cytoplasmic PG pathway.

More recently it was demonstrated that muropeptides play also a central role in the antibiotic resistance of bacteria. Muropeptides serve for bacteria as signal molecules that indicate the presence of cell wall targeting antibiotics. If the intracellular concentration of muropeptides increases, the bacterium activates its defense mechanism and triggers the induction of β-lactamases (Jacobs, Huang et al. 1994, Dietz, Pfeifle et al. 1997, Jacobs, Frere et al. 1997, Boudreau, Fisher et al. 2012). In Gram-negative organisms, two major pathways are responsible for the induction of β-lactamases: the AmpG–AmpR–AmpC pathway, and the BlrA/BlrB two component regulatory system (**Fig. 14**).

Regulation of AmpC depends on the relative concentrations of cytoplasmic anhydromuropeptides. In the absence of β-lactam pressure, UDP-Mur*N*Ac-pentapeptide is bound to the transcriptional regulator AmpR, which inhibits expression of AmpC (Jacoby 2009). Upon inhibition of PBPs by β-lactams, however, peptidoglycan biosynthesis is slowed down or blocked, while the activity of autolysins remains constant, resulting in accumulation of anhydromuropeptides in the periplasm. Muropeptides enter the cytoplasm through the AmpG permease, and their Glc*N*Ac moiety is hydrolyzed by NagZ (Votsch and Templin 2000, Cheng and Park 2002). The accumulation of anhydromuramyl peptides in the cytoplasm results in the displacement of UDP-Mur*N*Ac-pentapeptide from AmpR (Jacoby 2009). AmpC is thus expressed and subsequently secreted to the periplasm.

A different regulatory mechanism was identified in bacterial species of the genus *Aeromonas,* which control the expression of AmpC using a two component regulatory system consisting of the sensor kinase BlrB and the response regulator BlrA (**Fig. 14**). Both proteins are closely related to the *E. coli* CreBC two-component regulatory system, which is involved in the regulation of key metabolic pathways in response to nutrient deprivation (Avison, Horton et al. 2001). The inhibition of the TP activity of PBPs by β-lactams results in the accumulation of disaccharide pentapeptides in the periplasm, inducing autophosphorylation of the kinase domain of BlrB. Transfer of the phosphate moiety to BlrA causes binding of the response regulator to the promotor region upstream of the genes that code for the Amp, Cep, and Imi β-lactamases, inducing expression (Tayler, Ayala et al. 2010).

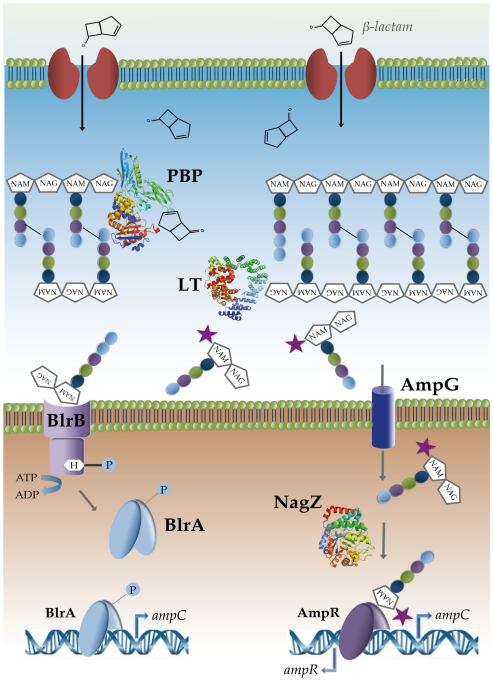

Fig. 14: Schematic model of AmpC β-lactamase induction in Gram-negative organisms. The AmpG-AmpR-AmpC pathway as well as the BlrA/BlrB two component regulatory system are indicated. The presence of β-lactams results in excessive breakdown of the murein sacculus and thus in accumulation of muropeptides. This accumulation causes either the activation of AmpR (AmpG-AmpR-AmpC pathway shown on the right) or the phosphorylation of BlrA (BlrA/BlrB two component regulators system shown on the left); in both situations, there is induction of the *ampC* gene. Abbreviations: LT, **L**ytic **T**ransglycosylases; PBP, **P**enicillin-**B**inding **P**rotein. Adapted from (Nikolaidis, Favini-Stabile et al. 2014).

1. 4 Towards the structural characterization of membrane proteins

Roughly one third of the genomes of most organisms encodes membrane proteins, which have been shown to play pivotal roles in a variety of cellular processes,

including transport, energy transduction, multidrug efflux, nutrient intake as well as protein export (Wallin and von Heijne 1998, Krogh, Larsson et al. 2001). This multitude of functions makes membrane proteins excellent targets for the development of new antimicrobial drugs (von Heijne 2007). However, structural studies of membrane proteins remain a considerable challenge due to the requirement of millligram quantities of pure, functional and homogeneous protein. Despite recent advances in the field of membrane protein structural biology, the number of currently available membrane protein structures remains rather small, representing just 1% of all protein structures in the Protein Data Bank (PDB). The highly amphipathic character and the overall low abundance of membrane proteins makes them inherently difficult to work with leading often to poor expression, limited stability, low purification yields and lack of well-ordered crystals (Grisshammer and Tate 1995, Seddon, Curnow et al. 2004). In general, significant efforts have to be invested to overcome each of these hurdles (**Fig. 15** (A)).

Once the protein of interest has been expressed at sufficient yields, it is usually nescessary to extract the protein from the lipid bilayer. Absolutely critical for this step are detergents, which have due to their unique, amphipathic nature the ability to disrupt the membrane and extract the protein of interest from the lipidic environment while protecting its hydrophobic surfaces (Carpenter, Beis et al. 2008, Linke 2009). Detergents are therefore invaluable tools in the study of membrane proteins and are required from the extraction of the protein until its final crystallization. Selecting the right detergent is one of the most crucial decisions and often requires, for each step, a detergent screening effort (see **Fig. 15** (A)). The choice of detergent has not only great impact on the functional integrity and stability of the membrane protein upon removal from the lipid bilayer, but also on crystallization success.

Crystallization of membrane proteins in the presence of detergents (*in surfo* method; **Fig. 15** (B)) requires that the detergent sufficiently protects the protein's hydrophobic surface while enabling potential crystal contacts to form (Ostermeier and Michel 1997). However, even if a detergent fulfills these requirements it may not lead to success. Detergents are not always able to adequately mimic the native membranes resulting often in limited stability of the protein. Consequently, significant efforts have been made to establish new techniques that allow the crystallization of membrane proteins in a more native environment (lipidic cubic

phase (LCP) and bicelles; see **Fig. 15** (B)) (Landau and Rosenbusch 1996, Faham and Bowie 2002).

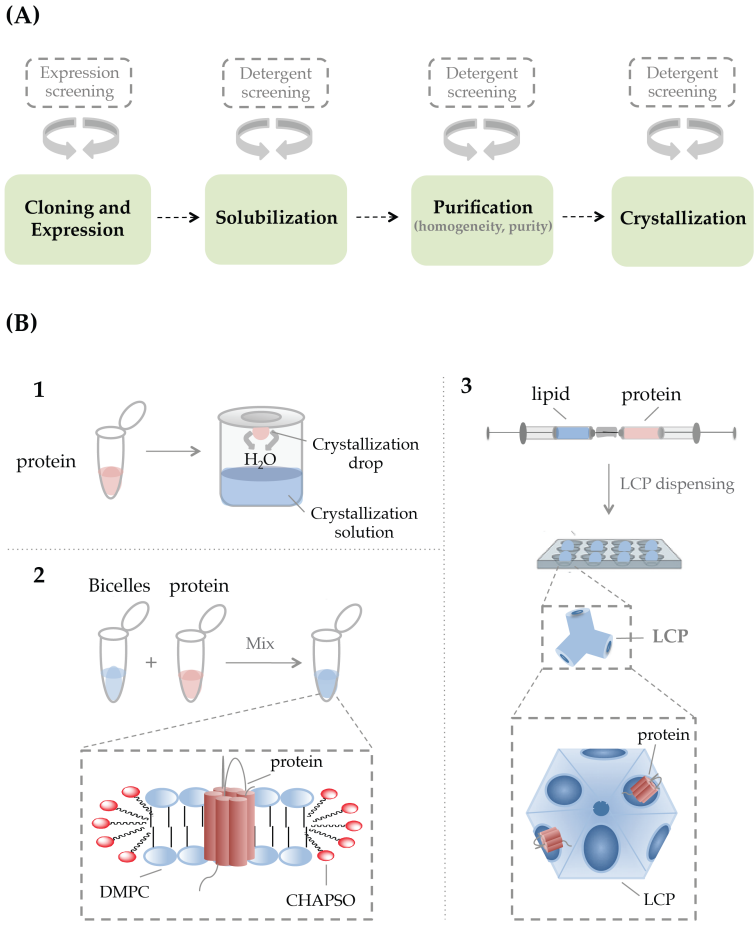

Fig. 15: (A) Flow chart of membrane protein expression, purification and crystallization. (B) Crystallization of membrane proteins using different crystallization methodologies. **(1)** Vapor diffusion crystallization in the presence of detergents (*in surfo*) and crystallization of membrane proteins from a lipid-based medium, such as **(2)** bicelles (typically DMPC (1,2-dimyristoyl-*sn*-glycero-3-phosphocholine) and CHAPSO (3-([3-cholamidopropyl]dimethylammonio)-2-hydroxy-1-propanesulphonate)) or **(3)** Lipidic cubic phase (LCP). The latter methods are based on the reconstitution of the membrane proteins in a more native-like environment.

Such approaches are based on the reconstitution of the membrane protein in a lipidic environment which may contribute to its enhanced stability and the formation of protein-protein contacts that are required for crystal nucleation and growth. The advantage of these approaches over the *in surfo* method is that both, hydrophobic as well as polar surfaces, can participate in the formation of crystal contacts.

Nevertheless, despite the fact that a panel of different crystallization approaches are currently available, the path towards obtaining diffraction-quality crystals still remains a non-trivial endeavor that requires substantial time and resources.

1. 5 Scope of the thesis

This thesis aimes at obtaining more insight into the complex process of peptidoglycan synthesis and regulation with the emphasis on **(1)** characterizing interactions between proteins that exert antagonistic functions during cell wall growth and **(2)** developing protocols for the purification and crystallization of Lipid II flippases. In **Chapter 2** surface plasmon resonance is used to characterize the interaction between *Pseudomonas aeruginosa* PBP2 and SltB1. Here it is shown that the interaction of these proteins is highly dependent on the presence of Ca^{2+}. Additionally, the structure of SltB1 is solved to high-resolution and shows that the protein carries an EF-hand motif that might participate in the interaction of SltB1 and PBP2. In **Chapter 3-5** the focus is on developing strategies to express, purify and crystallize a Lipid II transporter (SEDS proteins). In **Chapter 3** the expression of ten SEDS homologs is tested using different fusion tags, growth media and expression hosts. It is shown that fusion to Mistic allows the high-level expression of several SEDS proteins leading to expression yields that are sufficient for structural studies. In **Chapter 4** three SEDS proteins, that showed increased expression yields in the aforementioned expression screen, are solubilized and an extensive detergent exchange screening is performed. It is shown that all tested SEDS proteins are only stable in maltoside-based detergents. In addition, one SEDS protein, *S. pneumoniae* RodA, is purified to homogeneity and tested for activity, showing that the protein is able to induce Lipid II transport. In **Chapter 5** different methodologies are used to crystallize *S. pneumoniae* RodA. While the full-length protein failed to crystallize, a proteolytic resistant core domain of *S. pneumoniae* RodA crystallized in bicelles. Moreover, crystals were tested at the synchrotron for X-ray diffraction, pointing to

one condition that led to initial diffraction data. In **Chapter 6** the obtained results are summarized and discussed.

REFERENCES

Aaron, M., et al. (2007). "The tubulin homologue FtsZ contributes to cell elongation by guiding cell wall precursor synthesis in *Caulobacter crescentus*." Mol Microbiol **64**(4): 938-952.

Aarsman, M. E., et al. (2005). "Maturation of the *Escherichia coli* divisome occurs in two steps." Mol Microbiol **55**(6): 1631-1645.

Abrams, A. (1958). "O-acetyl groups in the cell wall of *Streptococcus faecalis*." J Biol Chem **230**(2): 949-959.

Artola-Recolons, C., et al. (2014). "Structure and Cell Wall Cleavage by Modular Lytic Transglycosylase MltC of *Escherichia coli*." ACS Chem Biol **9**(9): 2058-2066.

Avison, M. B., et al. (2001). "*Escherichia coli* CreBC is a global regulator of gene expression that responds to growth in minimal media." J Biol Chem **276**(29): 26955-26961.

Barreteau, H., et al. (2008). "Cytoplasmic steps of peptidoglycan biosynthesis." FEMS Microbiol Rev **32**(2): 168-207.

Beveridge, T. J. (1981). "Ultrastructure, chemistry, and function of the bacterial wall." Int Rev Cytol **72**: 229-317.

Beveridge, T. J. (1999). "Structures of gram-negative cell walls and their derived membrane vesicles." J Bacteriol **181**(16): 4725-4733.

Boudreau, M. A., et al. (2012). "Messenger functions of the bacterial cell wall-derived muropeptides." Biochemistry **51**(14): 2974-2990.

Bouhss, A., et al. (2004). "Purification and characterization of the bacterial MraY translocase catalyzing the first membrane step of peptidoglycan biosynthesis." J Biol Chem **279**(29): 29974-29980.

Bouhss, A., et al. (1999). "Topological analysis of the MraY protein catalysing the first membrane step of peptidoglycan synthesis." Mol Microbiol **34**(3): 576-585.

Bouhss, A., et al. (2008). "The biosynthesis of peptidoglycan lipid-linked intermediates." FEMS Microbiol Rev **32**(2): 208-233.

Boyle, D. S. and W. D. Donachie (1998). "mraY is an essential gene for cell growth in *Escherichia coli*." J Bacteriol **180**(23): 6429-6432.

Boyle, D. S., et al. (1997). "ftsW is an essential cell-division gene in *Escherichia coli*." Mol Microbiol **24**(6): 1263-1273.

Braun, V. and H. Wolff (1970). "The murein-lipoprotein linkage in the cell wall of *Escherichia coli*." Eur J Biochem **14**(2): 387-391.

Bupp, K. and J. van Heijenoort (1993). "The final step of peptidoglycan subunit assembly in *Escherichia coli* occurs in the cytoplasm." J Bacteriol **175**(6): 1841-1843.

Butler, E. K., et al. (2013). "Structure-function analysis of MurJ reveals a solvent-exposed cavity containing residues essential for peptidoglycan biogenesis in *Escherichia coli*." J Bacteriol **195**(20): 4639-4649.

Carpenter, E. P., et al. (2008). "Overcoming the challenges of membrane protein crystallography." Curr Opin Struct Biol **18**(5): 581-586.

Chen, L., et al. (2002). "Intrinsic lipid preferences and kinetic mechanism of *Escherichia coli* MurG." Biochemistry **41**(21): 6824-6833.

Cheng, Q. and J. T. Park (2002). "Substrate specificity of the AmpG permease required for recycling of cell wall anhydro-muropeptides." J Bacteriol **184**(23): 6434-6436.

Chung, B. C., et al. (2013). "Crystal structure of MraY, an essential membrane enzyme for bacterial cell wall synthesis." Science **341**(6149): 1012-1016.

Daniel, R. A. and J. Errington (2003). "Control of cell morphogenesis in bacteria: two distinct ways to make a rod-shaped cell." Cell **113**(6): 767-776.

de Pedro, M. A., et al. (1997). "Murein segregation in *Escherichia coli*." J Bacteriol **179**(9): 2823-2834.

Di Lallo, G., et al. (2003). "Use of a two-hybrid assay to study the assembly of a complex multicomponent protein machinery: bacterial septosome differentiation." Microbiology **149**(Pt 12): 3353-3359.

Dietz, H., et al. (1997). "The signal molecule for β-lactamase induction in *Enterobacter cloacae* is the anhydromuramyl-pentapeptide." Antimicrob Agents Chemother **41**(10): 2113-2120.

Dominguez-Escobar, J., et al. (2011). "Processive movement of MreB-associated cell wall biosynthetic complexes in bacteria." Science **333**(6039): 225-228.

Doyle, R. J., et al. (1988). "Turnover of cell walls in microorganisms." Microbiol Rev **52**(4): 554-567.

Dramsi, S., et al. (2008). "Covalent attachment of proteins to peptidoglycan." FEMS Microbiol Rev **32**(2): 307-320.

Engel, H., et al. (1992). "Murein-metabolizing enzymes from *Escherichia coli*: existence of a second lytic transglycosylase." J Bacteriol **174**(20): 6394-6403.

Errington, J. (2013). "L-form bacteria, cell walls and the origins of life." Open Biol **3**(1): 120143.

Faham, S. and J. U. Bowie (2002). "Bicelle crystallization: a new method for crystallizing membrane proteins yields a monomeric bacteriorhodopsin structure." J Mol Biol **316**(1): 1-6.

Fenton, A. K. and K. Gerdes (2013). "Direct interaction of FtsZ and MreB is required for septum synthesis and cell division in *Escherichia coli*." EMBO J **32**(13): 1953-1965.

Fibriansah, G., et al. (2012). "On the mechanism of peptidoglycan binding and cleavage by the endo-specific lytic transglycosylase MltE from *Escherichia coli*." Biochemistry **51**(45): 9164-9177.

Fraipont, C., et al. (2011). "The integral membrane FtsW protein and peptidoglycan synthase PBP3 form a subcomplex in *Escherichia coli*." Microbiology **157**(Pt 1): 251-259.

Garner, E. C., et al. (2011). "Coupled, circumferential motions of the cell wall synthesis machinery and MreB filaments in *B. subtilis*." Science **333**(6039): 222-225.

Genereux, C., et al. (2004). "Mutational analysis of the catalytic centre of the *Citrobacter freundii* AmpD N-acetylmuramyl-L-alanine amidase." Biochem J **377**(Pt 1): 111-120.

Ghuysen, J. M. (1968). "Use of bacteriolytic enzymes in determination of wall structure and their role in cell metabolism." Bacteriol Rev **32**(4 Pt 2): 425-464.

Ghuysen, J. M. (1991). "Serine β-lactamases and penicillin-binding proteins." Annu Rev Microbiol **45**: 37-67.

Goffin, C., et al. (1996). "The non-penicillin-binding module of the tripartite penicillin-binding protein 3 of *Escherichia coli* is required for folding and/or stability of the penicillin-binding module and the membrane-anchoring module confers cell septation activity on the folded structure." J Bacteriol **178**(18): 5402-5409.

Goffin, C. and J. M. Ghuysen (1998). "Multimodular penicillin-binding proteins: an enigmatic family of orthologs and paralogs." Microbiol Mol Biol Rev **62**(4): 1079-1093.

Goffin, C. and J. M. Ghuysen (2002). "Biochemistry and comparative genomics of SxxK superfamily acyltransferases offer a clue to the mycobacterial paradox: presence of penicillin-susceptible target proteins versus lack of efficiency of penicillin as therapeutic agent." Microbiol Mol Biol Rev **66**(4): 702-738, table of contents.

Goodell, E. W. (1985). "Recycling of murein by *Escherichia coli*." J Bacteriol **163**(1): 305-310.

Grisshammer, R. and C. G. Tate (1995). "Overexpression of integral membrane proteins for structural studies." Q Rev Biophys **28**(3): 315-422.

Ha, S., et al. (2000). "The 1.9 A crystal structure of *Escherichia coli* MurG, a membrane-associated glycosyltransferase involved in peptidoglycan biosynthesis." Protein Sci **9**(6): 1045-1052.

Hegde, S. S. and J. S. Blanchard (2003). "Kinetic and mechanistic characterization of recombinant *Lactobacillus viridescens* FemX (UDP-N-acetylmuramoyl pentapeptide-lysine N6-alanyltransferase)." J Biol Chem **278**(25): 22861-22867.

Henriques, A. O., et al. (1998). "Control of cell shape and elongation by the *rodA* gene in *Bacillus subtilis*." Mol Microbiol **28**(2): 235-247.

Heydanek, M. G., Jr., et al. (1970). "Initial stage in peptidoglycan synthesis. Mechanism of activation of phospho-N-acetylmuramyl-pentapeptide translocase by potassium ions." Biochemistry **9**(18): 3618-3623.

Heydanek, M. G., Jr., et al. (1969). "On the initial stage in peptidoglycan synthesis. 3. Kinetics and uncoupling of phospho-N-acetylmuramyl-pentapeptide translocase (uridine 5'-phosphate)." Biochemistry **8**(3): 1214-1221.

Holtje, J. V. (1998). "Growth of the stress-bearing and shape-maintaining murein sacculus of *Escherichia coli*." Microbiol Mol Biol Rev **62**(1): 181-203.

Holtje, J. V., et al. (1975). "Novel type of murein transglycosylase in *Escherichia coli*." J Bacteriol **124**(3): 1067-1076.

Holtje, J. V. and E. I. Tuomanen (1991). "The murein hydrolases of *Escherichia coli*: properties, functions and impact on the course of infections *in vivo*." J Gen Microbiol **137**(3): 441-454.

Hu, Y., et al. (2003). "Crystal structure of the MurG:UDP-GlcNAc complex reveals common structural principles of a superfamily of glycosyltransferases." Proc Natl Acad Sci U S A **100**(3): 845-849.

Ikeda, M., et al. (1989). "Structural similarity among *Escherichia coli* FtsW and RodA proteins and *Bacillus subtilis* SpoVE protein, which function in cell division, cell elongation, and spore formation, respectively." J Bacteriol **171**(11): 6375-6378.

Inoue, A., et al. (2008). "Involvement of an essential gene, *mviN*, in murein synthesis in *Escherichia coli*." J Bacteriol **190**(21): 7298-7301.

Jacobs, C., et al. (1997). "Cytosolic intermediates for cell wall biosynthesis and degradation control inducible β-lactam resistance in gram-negative bacteria." Cell **88**(6): 823-832.

Jacobs, C., et al. (1994). "Bacterial cell wall recycling provides cytosolic muropeptides as effectors for β-lactamase induction." EMBO J **13**(19): 4684-4694.

Jacobs, C., et al. (1995). "AmpD, essential for both β-lactamase regulation and cell wall recycling, is a novel cytosolic N-acetylmuramyl-L-alanine amidase." Mol Microbiol **15**(3): 553-559.

Jacoby, G. A. (2009). "AmpC β-lactamases." Clin Microbiol Rev **22**(1): 161-182, Table of Contents.

Johnson, J. W., et al. (2013). "Bacterial cell-wall recycling." Ann N Y Acad Sci **1277**: 54-75.

Joris, B., et al. (1990). "The life-cycle proteins RodA of *Escherichia coli* and SpoVE of *Bacillus subtilis* have very similar primary structures." Mol Microbiol **4**(3): 513-517.

Karimova, G., et al. (2005). "Interaction network among *Escherichia coli* membrane proteins involved in cell division as revealed by bacterial two-hybrid analysis." J Bacteriol **187**(7): 2233-2243.

Kato, J., et al. (1985). "Dispensability of either penicillin-binding protein-1a or -1b involved in the essential process for cell elongation in *Escherichia coli*." Mol Gen Genet **200**(2): 272-277.

Kawai, Y., et al. (2009). "Regulation of cell wall morphogenesis in *Bacillus subtilis* by recruitment of PBP1 to the MreB helix." Mol Microbiol **71**(5): 1131-1144.

Kishida, H., et al. (2006). "Crystal structure of penicillin binding protein 4 (dacB) from *Escherichia coli*, both in the native form and covalently linked to various antibiotics." Biochemistry **45**(3): 783-792.

Krogh, A., et al. (2001). "Predicting transmembrane protein topology with a hidden Markov model: application to complete genomes." J Mol Biol **305**(3): 567-580.

Kruse, T., et al. (2005). "The morphogenetic MreBCD proteins of *Escherichia coli* form an essential membrane-bound complex." Mol Microbiol **55**(1): 78-89.

Kuroda, T. and T. Tsuchiya (2009). "Multidrug efflux transporters in the MATE family." Biochim Biophys Acta **1794**(5): 763-768.

Landau, E. M. and J. P. Rosenbusch (1996). "Lipidic cubic phases: a novel concept for the crystallization of membrane proteins." Proc Natl Acad Sci U S A **93**(25): 14532-14535.

Leung, A. K., et al. (2001). "Crystal structure of the lytic transglycosylase from bacteriophage lambda in complex with hexa-N-acetylchitohexaose." Biochemistry **40**(19): 5665-5673.

Linke, D. (2009). "Detergents: an overview." Methods Enzymol **463**: 603-617.

Lloyd, A. J., et al. (2004). "Phospho-N-acetyl-muramyl-pentapeptide translocase from *Escherichia coli*: catalytic role of conserved aspartic acid residues." J Bacteriol **186**(6): 1747-1757.

Lolis, E. and R. Bucala (2003). "Therapeutic approaches to innate immunity: severe sepsis and septic shock." Nat Rev Drug Discov **2**(8): 635-645.

Lovering, A. L., et al. (2007). "Structural insight into the transglycosylation step of bacterial cell-wall biosynthesis." Science **315**(5817): 1402-1405.

Lovering, A. L., et al. (2012). "Structural perspective of peptidoglycan biosynthesis and assembly." Annu Rev Biochem **81**: 451-478.

Macheboeuf, P., et al. (2006). "Penicillin binding proteins: key players in bacterial cell cycle and drug resistance processes." FEMS Microbiol Rev **30**(5): 673-691.

Mengin-Lecreulx, D., et al. (1991). "The *murG* gene of *Escherichia coli* codes for the UDP-N-acetylglucosamine: N-acetylmuramyl-(pentapeptide) pyrophosphoryl-undecaprenol N-acetylglucosamine transferase involved in the membrane steps of peptidoglycan synthesis." J Bacteriol **173**(15): 4625-4636.

Mengin-Lecreulx, D., et al. (1996). "Identification of the *mpl* gene encoding UDP-N-acetylmuramate: L-alanyl-gamma-D-glutamyl-meso-diaminopimelate ligase in *Escherichia coli* and its role in recycling of cell wall peptidoglycan." J Bacteriol **178**(18): 5347-5352.

Mohammadi, T., et al. (2007). "The essential peptidoglycan glycosyltransferase MurG forms a complex with proteins involved in lateral envelope growth as well as with proteins involved in cell division in *Escherichia coli*." Mol Microbiol **65**(4): 1106-1121.

Mohammadi, T., et al. (2011). "Identification of FtsW as a transporter of lipid-linked cell wall precursors across the membrane." EMBO J **30**(8): 1425-1432.

Neuhaus, F. C. and J. Baddiley (2003). "A continuum of anionic charge: structures and functions of D-alanyl-teichoic acids in gram-positive bacteria." Microbiol Mol Biol Rev **67**(4): 686-723.

Nicola, G., et al. (2005). "Crystal structure of *Escherichia coli* penicillin-binding protein 5 bound to a tripeptide boronic acid inhibitor: a role for Ser-110 in deacylation." Biochemistry **44**(23): 8207-8217.

Nikolaidis, I., et al. (2014). "Resistance to antibiotics targeted to the bacterial cell wall." Protein Sci **23**(3): 243-259.

Nikolaidis, I., et al. (2012). "Calcium-dependent complex formation between PBP2 and lytic transglycosylase SltB1 of *Pseudomonas aeruginosa*." Microb Drug Resist **18**(3): 298-305.

Noirclerc-Savoye, M., et al. (2003). "Expression and purification of FtsW and RodA from *Streptococcus pneumoniae*, two membrane proteins involved in cell division and cell growth, respectively." Protein Expr Purif **30**(1): 18-25.

Osborn, M. J. and L. Rothfield (2007). "Cell shape determination in *Escherichia coli*." Curr Opin Microbiol **10**(6): 606-610.

Ostermeier, C. and H. Michel (1997). "Crystallization of membrane proteins." Curr Opin Struct Biol **7**(5): 697-701.

Park, J. T., et al. (1998). "MppA, a periplasmic binding protein essential for import of the bacterial cell wall peptide L-alanyl-gamma-D-glutamyl-meso-diaminopimelate." J Bacteriol **180**(5): 1215-1223.

Pastoret, S., et al. (2004). "Functional analysis of the cell division protein FtsW of *Escherichia coli*." J Bacteriol **186**(24): 8370-8379.

Powell, A. J., et al. (2006). "Crystal structures of the lytic transglycosylase MltA from *N. gonorrhoeae* and *E. coli*: insights into interdomain movements and substrate binding." J Mol Biol **359**(1): 122-136.

Razin, S. (1963). "Osmotic Lysis of Mycoplasma." J Gen Microbiol **33**: 471-475.

Rocaboy, M., et al. (2013). "The crystal structure of the cell division amidase AmiC reveals the fold of the AMIN domain, a new peptidoglycan binding domain." Mol Microbiol **90**(2): 267-277.

Rohrer, S. and B. Berger-Bachi (2003). "FemABX peptidyl transferases: a link between branched-chain cell wall peptide formation and β-lactam resistance in gram-positive cocci." Antimicrob Agents Chemother **47**(3): 837-846.

Ruiz, N. (2008). "Bioinformatics identification of MurJ (MviN) as the peptidoglycan lipid II flippase in *Escherichia coli*." Proc Natl Acad Sci U S A **105**(40): 15553-15557.

Sanyal, S. and A. K. Menon (2009). "Flipping lipids: why an' what's the reason for?" ACS Chem Biol **4**(11): 895-909.

Sauvage, E., et al. (2008). "The penicillin-binding proteins: structure and role in peptidoglycan biosynthesis." FEMS Microbiol Rev **32**(2): 234-258.

Schleifer, K. H. and O. Kandler (1972). "Peptidoglycan types of bacterial cell walls and their taxonomic implications." Bacteriol Rev **36**(4): 407-477.

Schwarz, U., et al. (1969). "Autolytic enzymes and cell division of *Escherichia coli*." J Mol Biol **41**(3): 419-429.

Seddon, A. M., et al. (2004). "Membrane proteins, lipids and detergents: not just a soap opera." Biochim Biophys Acta **1666**(1-2): 105-117.

Sham, L. T., et al. (2014). "Bacterial cell wall. MurJ is the flippase of lipid-linked precursors for peptidoglycan biogenesis." Science **345**(6193): 220-222.

Struve, W. G. and F. C. Neuhaus (1965). "Evidence for an Initial Acceptor of Udp-Nac-Muramyl-Pentapeptide in the Synthesis of Bacterial Mucopeptide." Biochem Biophys Res Commun **18**: 6-12.

Tayler, A. E., et al. (2010). "Induction of β-lactamase production in *Aeromonas hydrophila* is responsive to β-lactam-mediated changes in peptidoglycan composition." Microbiology **156**(Pt 8): 2327-2335.

Templin, M. F., et al. (1992). "A murein hydrolase is the specific target of bulgecin in *Escherichia coli*." J Biol Chem **267**(28): 20039-20043.

Templin, M. F., et al. (1999). "A defect in cell wall recycling triggers autolysis during the stationary growth phase of *Escherichia coli*." EMBO J **18**(15): 4108-4117.

Typas, A., et al. (2012). "From the regulation of peptidoglycan synthesis to bacterial growth and morphology." Nat Rev Microbiol **10**(2): 123-136.

van Asselt, E. J., et al. (1999). "Crystal structure of *Escherichia coli* lytic transglycosylase Slt35 reveals a lysozyme-like catalytic domain with an EF-hand." Structure **7**(10): 1167-1180.

van Asselt, E. J. and B. W. Dijkstra (1999). "Binding of calcium in the EF-hand of *Escherichia coli* lytic transglycosylase Slt35 is important for stability." FEBS Lett **458**(3): 429-435.

van Asselt, E. J., et al. (1999). "High resolution crystal structures of the *Escherichia coli* lytic transglycosylase Slt70 and its complex with a peptidoglycan fragment." J Mol Biol **291**(4): 877-898.

van Dam, V., et al. (2007). "Transmembrane transport of peptidoglycan precursors across model and bacterial membranes." Mol Microbiol **64**(4): 1105-1114.

van Heijenoort, J. (2001). "Recent advances in the formation of the bacterial peptidoglycan monomer unit." Nat Prod Rep **18**(5): 503-519.

van Heijenoort, J. (2007). "Lipid intermediates in the biosynthesis of bacterial peptidoglycan." Microbiol Mol Biol Rev **71**(4): 620-635.

van Heijenoort, J. (2011). "Peptidoglycan hydrolases of *Escherichia coli*." Microbiol Mol Biol Rev **75**(4): 636-663.

van Heijenoort, Y., et al. (1992). "Membrane intermediates in the peptidoglycan metabolism of *Escherichia coli*: possible roles of PBP1b and PBP3." J Bacteriol **174**(11): 3549-3557.

van Straaten, K. E., et al. (2005). "Crystal structure of MltA from *Escherichia coli* reveals a unique lytic transglycosylase fold." J Mol Biol **352**(5): 1068-1080.

Varma, A., et al. (2007). "FtsZ directs a second mode of peptidoglycan synthesis in *Escherichia coli*." J Bacteriol **189**(15): 5692-5704.

Vollmer, W. (2008). "Structural variation in the glycan strands of bacterial peptidoglycan." FEMS Microbiol Rev **32**(2): 287-306.

Vollmer, W. (2012). "Bacterial outer membrane evolution via sporulation?" Nat Chem Biol **8**(1): 14-18.

Vollmer, W. and U. Bertsche (2008). "Murein (peptidoglycan) structure, architecture and biosynthesis in *Escherichia coli*." Biochim Biophys Acta **1778**(9): 1714-1734.

Vollmer, W., et al. (2008). "Peptidoglycan structure and architecture." FEMS Microbiol Rev **32**(2): 149-167.

Vollmer, W., et al. (2008). "Bacterial peptidoglycan (murein) hydrolases." FEMS Microbiol Rev **32**(2): 259-286.

Vollmer, W. and A. Tomasz (2000). "The *pgdA* gene encodes for a peptidoglycan N-acetylglucosamine deacetylase in *Streptococcus pneumoniae*." J Biol Chem **275**(27): 20496-20501.

Vollmer, W. and A. Tomasz (2002). "Peptidoglycan N-acetylglucosamine deacetylase, a putative virulence factor in *Streptococcus pneumoniae*." Infect Immun **70**(12): 7176-7178.

von Heijne, G. (2007). "The membrane protein universe: what's out there and why bother?" J Intern Med **261**(6): 543-557.

Votsch, W. and M. F. Templin (2000). "Characterization of a β-N-acetylglucosaminidase of *Escherichia coli* and elucidation of its role in muropeptide recycling and β-lactamase induction." J Biol Chem **275**(50): 39032-39038.

Wallin, E. and G. von Heijne (1998). "Genome-wide analysis of integral membrane proteins from eubacterial, archaean, and eukaryotic organisms." Protein Sci **7**(4): 1029-1038.

Ward, J. B. (1973). "The chain length of the glycans in bacterial cell walls." Biochem J **133**(2): 395-398.

White, C. L., et al. (2010). "Positioning cell wall synthetic complexes by the bacterial morphogenetic proteins MreB and MreD." Mol Microbiol **76**(3): 616-633.

Yao, X., et al. (1999). "Thickness and elasticity of gram-negative murein sacculi measured by atomic force microscopy." J Bacteriol **181**(22): 6865-6875.

Yousif, S. Y., et al. (1985). "Lysis of *Escherichia coli* by β-lactam antibiotics: deletion analysis of the role of penicillin-binding proteins 1A and 1B." J Gen Microbiol **131**(10): 2839-2845.

Zapun, A., et al. (2008). "Penicillin-binding proteins and β-lactam resistance." FEMS Microbiol Rev **32**(2): 361-385.

CHAPTER 2

Calcium-Dependent complex formation between PBP2 and lytic transglycosylase SltB1 of *Pseudomonas aeruginosa*

Ioulia Nikolaidis, Thierry Izoré, Viviana Job, Nicole Thielens, Eefjan Breukink and Andréa Dessen. Calcium-dependent complex formation between PBP2 and lytic transglycosylases SltB1 of *Pseudomonas aeruginosa*. Microbial Drug Resistance **2012** Jun; 18 (3): 298-305.

ABSTRACT

In Gram-negative bacteria, the bacterial cell wall biosynthetic mechanism requires the coordinated action of enzymes and structural proteins located in the cytoplasm, within the membrane, and in the periplasm of the cell. Its main component, peptidoglycan (PG), is essential for cell division and wall elongation. Penicillin-Binding Proteins (PBPs) catalyze the last steps of PG biosynthesis, namely the polymerization of glycan chains and the cross-linking of stem peptides, and can be either monofunctional or bifunctional. Their action is coordinated with that of other enzymes essential for cell wall biosynthesis, such as Lytic Transglycosylases (LT). Here, we have studied SltB1, an LT from *Pseudomonas aeruginosa*, and identified that it forms a complex with PBP2, a monofunctional enzyme, which requires the presence of Ca^{2+}. In addition, we have solved the structure of SltB1 to a high resolution, and identified that it harbors an EF-hand like motif containing a Ca^{2+} ion displaying bipyramidal coordination. These studies provide initial structural details that shed light on the interactions between the PG biosynthesis enzymes in *P. aeruginosa*.

INTRODUCTION

The bacterial cell wall is a complex three-dimensional structure that protects the cell from environmental stress and ensures its shape. It also plays a key role during the processes of cell division and bacterial cell wall elongation. Its main building block, the peptidoglycan (PG), is a three-dimensional mesh that envelopes the entire bacterial cell and is formed by polymerized chains of repeating disaccharide subunits (*N*-acetylglucosamine (Glc*N*Ac) and *N*-acetylmuramic acid (Mur*N*Ac)) cross-linked by stem peptides (Holtje 1998). Its biosynthesis is initiated in the bacterial cytoplasm, where Mur enzymes catalyze the formation of the UDP-Mur*N*Ac-stem peptide precursor. Concomitantly, this precursor is linked to an undecaprenyl phosphate, a step that is followed by the addition of the second amino sugar Glc*N*Ac (Bouhss, Trunkfield et al. 2008). This molecule, Lipid II, is subsequently translocated to the periplasmic space by integral membrane proteins of the SEDS (**S**hape, **E**longation, **D**ivision, and **S**porulation) family (Mohammadi, van Dam et al. 2011). Once in the periplasm, Lipid II is the substrate of Penicillin-Binding Proteins (PBPs), which

polymerize the alternating Mur*N*Ac and Glc*N*Ac chains (glycosyltransfer [GT]) and cross-link the interchain stem peptides (transpeptidation [TP]). Thus, PG formation requires the coordination of the activities of cytoplasmic, membrane-inserted, and periplasmic proteins (**Fig. 1**) (Sauvage, Kerff et al. 2008, Mattei, Neves et al. 2010).

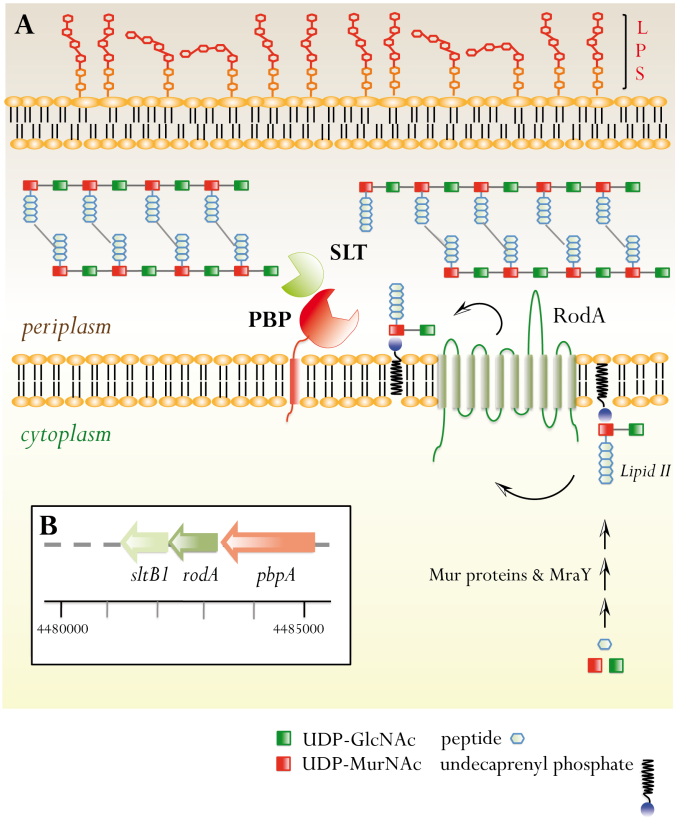

Fig. 1: Peptidoglycan (PG) synthesis. **(A)** PG synthesis initiates in the cytoplasm, through the action of six Mur proteins, resulting in the formation of UDP-*N*-acetylmuramic acid (Mur*N*Ac)-pentapeptide. MraY then attaches this soluble precursor to undecaprenyl phosphate, forming Lipid I. The glycosyltransferase MurG finalizes the cytoplasmic steps through attachment of UDP-*N*-acetylglucosamine (Glc*N*Ac) to Lipid I, resulting in the synthesis of Lipid II. This molecule is then transported across the cytoplasmic membrane to the periplasmic side by the flippase (*e.g.* RodA), where Penicillin-Binding Proteins (PBPs) and Lytic Transglycosylases (LTs) act upon it (Macheboeuf, Contreras-Martel et al. 2006). **(B)** The *P. aeruginosa* operon that carries genes encoding PBP2 and SltB1 also includes *rodA*, which codes for a Lipid II flippase.

High-molecular-mass (HMM) PBPs can either carry both GT and TP domains (class A), or catalyze only the TP reaction (class B). Low-molecular-mass (LMM) PBPs, on the other hand, can be either carboxypeptidases or endopeptidases, thus playing a role in the regulation of the level of PG cross-linking by cleaving peptide bonds within the stem peptide (Morlot, Pernot et al. 2005, Macheboeuf, Contreras-Martel et al. 2006, Sauvage, Kerff et al. 2008, Vollmer, Joris et al. 2008, Mattei, Neves et al. 2010). Notably, PG precursors are added by PBPs to the pre-existing PG in gaps in the cell wall generated by Lytic Transglycosylases (LTs) and endopeptidases, enhancing the turnover of old material, which suggests that such enzymes could be potentially involved in a macromolecular complex whose role is to coordinate the action of these antagonistic activities during the cell cycle (Scheurwater, Reid et al. 2008, Vollmer, Joris et al. 2008).

LTs have been grouped into four families according to amino-acid sequences and the conservation of motifs, and are either periplasmic or attached to the inner leaflet of the outer membrane through a lipoyl moiety. In *Escherichia coli*, at least seven different LTs have been identified and studied: Slt70, which is soluble, and six membrane-bound enzymes (MltA, MltB, MltC, MltD, MltE, and EmtA) (Vollmer, Joris et al. 2008). In support of the hypothesis that PBPs interact with LTs in a macromolecular complex, PBP2, a HMM class B enzyme, was shown to interact with MltA in *Neisseria meningitides* (Jennings, Savino et al. 2002); in *E. coli*, MltA immobilized on an affinity column was shown to recognize PBP1c, PBP2, PBP3, and PBP1b, the latter through an interaction with the structural protein MipA (Vollmer, von Rechenberg et al. 1999); and Slt70 was shown to bind to PBP3, PBP7, and PBP8 (Romeis and Holtje 1994). LTs have, thus, been shown to interact with HMM as well as LMM PBPs.

Pseudomonas aeruginosa is a major human pathogen, the causative agent of nosocomial infections, and a particular threat to immunocompromised and cystic fibrosis patients (Lyczak, Cannon et al. 2002). *P. aeruginosa* expresses a class B PBP (PBP2) within a gene cluster that also harbors the RodA flippase and a periplasmic transglycosylase (LT), SltB1 (Blackburn and Clarke 2001, Reid, Blackburn et al. 2006, Legaree and Clarke 2008). In order to further conduct the studies of Legaree and Clarke, who provided the first evidence regarding the interaction between PBP2 and SltB1 (Legaree and Clarke 2008), we purified both proteins independently and used **s**urface **p**lasmon **r**esonance (SPR) spectroscopy to show that the interaction between PBP2 and SltB1 requires the presence of Ca^{2+}. In addition, we solved the crystal

structure of *P. aeruginosa* SltB1 to a high resolution, which revealed that it carries an EF-hand-type Ca^{2+}-binding loop that could potentially play a role in the recognition of partner molecules such as PBP2. These results provide an initial framework for understanding the structural requirements for interactions between PG biosynthesis enzymes in *P. aeruginosa*.

MATERIALS AND METHODS

Cloning

Regions from genes *pbpA* and *sltB1*, corresponding to PBP2 (residue 39–646) and SltB1 (residue 40–341), respectively, were initially amplified from a clinical *P. aeruginosa* strain PAO1. SltB1 was cloned into the first site of a pETDuet-1 vector (*Eco*RI/*Hin*dIII), thus downstream from a hexahistidine tag, and a thrombin cleavage site was added to the vector by polymerase chain reaction. PBP2 was cloned into pET30b (*Nde*I/*Hin*dIII), resulting in a noncleavable C-terminal fusion to a hexahistidine tag.

Protein expression and purification

PBP2

E. coli BL21(DE3) STAR (Invitrogen) carrying the expression vector just described were grown at 37°C in Luria-Bertani medium (LB), supplemented with 15 mg/L kanamycin. Expression was induced by the addition of isopropyl β-D-1-thiogalactopyranoside (IPTG) to a final concentration of 0.4 mM at an optical density (OD) at 600 nm of 0.3 A.U., and the cells were harvested by centrifugation after overnight growth at 16°C. The pellet was resuspended in lysis buffer (50 mM NaH_2PO_4 pH 8.0, 300 mM NaCl, 10% glycerol, 20 mM imidazole, 1% 3-[(3-cholamidopropyl) dimethylammonio]-1-propanesulfonate [CHAPS]) and sonicated. Cell debris was removed by centrifugation, and the cleared lysate was incubated with Ni-chelating resin (GE Healthcare) pre-equilibrated in lysis buffer. Hexahistidine-tagged protein was retrieved by an imidazole gradient (20–500 mM). The fractions containing PBP2 were pooled and further purified by size-exclusion chromatography (Superdex 200 HR 10/30) equilibrated in 25 mM HEPES pH 7.5,

150 mM NaCl. The protein was concentrated in a 50 kDa cutoff concentrator (Vivaspin).

SltB1

E. coli BL21(DE3) C43 cells carrying the expression vector just described and the chaperone-expressing vector pG-KJE6 were grown at 37°C in LB, supplemented with 100 mg/L ampicillin and 34 mg/L chloramphenicol. The expression of the chaperones was induced by the addition of 0.5 mg/ml L (+) arabinose, 10 ng/ml tetracycline, and 20 mM benzyl alcohol at an OD_{600nm} of 0.4 A.U.; and cells were further grown at 16°C until an OD_{600nm} of 0.6 A.U. was reached. Expression of SltB1 was induced by the addition of IPTG to a final concentration of 0.2 mM, and bacteria were harvested by centrifugation after overnight growth at 16°C. The pellet was resuspended in lysis buffer (25 mM Tris-HCl pH 8.0, 250 mM NaCl, 10% glycerol, 20 mM imidazole, and 1% CHAPS), and the cells were disrupted by sonication. The lysate was clarified by centrifugation and incubated with Ni-chelating resin (GE Healthcare) pre-equilibrated in lysis buffer. Hexahistidine-tagged protein was retrieved by an imidazole gradient to 500 mM, which was followed by size-exclusion chromatography (Superdex 200 HR 10/30 in 25 mM HEPES pH 7.5, 150 mM NaCl) and ion exchange (Mono Q in 25 mM HEPES pH 7.5, 20 mM–1M NaCl gradient). For crystallization trials, the protein was further concentrated to 22 mg/ml in a 10 kDa cutoff concentrator (Vivaspin).

SPR experiments

Real-time monitoring of the interaction between PBP2 and SltB1 was performed through the immobilization of PBP2 onto a CM5 sensorchip (GE Healthcare) using a BIAcore 3000 instrument (GE Healthcare). Immobilization was performed at a flow rate of 10 µl/min in HBS-P buffer (10 mM HEPES pH 7.5, 150 mM NaCl containing 0.005% (v/v) surfactant P20). The flow cells of a CM5 chip were first activated with 70 µl of 0.2 M *N*-ethyl-*N'*- (diethylaminopropyl)-carbodiimide and 0.05 M *N*-hydroxysuccimide. Afterwards, soluble PBP (24 µg/ml in 10 mM acetate buffer pH 5.0) was injected over one of the activated flow cells until a level of 1,900 response units was reached. The un-reacted groups were then blocked by an injection of 70 µl of 1 M ethanolamine pH 8.5 over the two flow cells. One hundred microliters of the analyte (SltB1) was injected in HBS-P over the different flow cells at a flow rate of

30 µl/min, followed by 180 sec of dissociation. The background signal recorded on the control surface without immobilized protein served as a blank sensorgram for subtraction of the bulk refractive index background. Data were analyzed by the global fitting of both the association and dissociation phases for six SltB1 concentrations (ranging from 0.105 to 1.26 µM) simultaneously, using the BIAevaluation software (GE Healthcare).

Crystallization

Initial crystallization conditions were found using the high-throughput crystallization facility at the HTX lab (Partnership for Structural Biology, Grenoble). Crystals were obtained at 20°C in 1.9 M malonate pH 6.5. Subsequently, we manually produced diffraction quality crystals by mixing 1 µl SltB1 (20 mg/ml) and 1 µl precipitant (1.5 M malonate pH 6.5, 3 mM $CaCl_2$) as hanging drops in 24-well VDX™ plates (Hampton Research). The crystals were cryoprotected using mother liquor supplemented with 30% (vol/vol) glycerol.

Data collection and structure determination

Diffraction images of SltB1 crystals were collected at the European Synchrotron Research Facility (ESRF) beamline ID23-EH2. A native data set was collected to 1.8 Å. Images were processed and scaled with XDS (Kabsch 2010), revealing a $P3_221$ space group with one monomer per asymmetric unit. In order to obtain the phases, we performed a molecular replacement experiment by employing the coordinates of Slt35 from *E. coli* (lacking the first 18 amino acids (van Asselt and Dijkstra 1999); PDB code 1QUS) as a search model, using PHASER (Scheurwater, Reid et al. 2008). Automated protein model building and structure refinement were performed using ARP/wARP (Cohen, Ben Jelloul et al. 2008); leading to an *R*-factor of 0.178 (R_{free} 0.211). The structure was improved by several rounds of manual refinement using REFMAC 5.5 (Murshudov, Vagin et al. 1997) and model building using Coot (Emsley and Cowtan 2004). Data collection, structure solution, and refinement statistics can be found in **TABLE 1**.

TABLE 1. DATA COLLECTION, MOLECULAR REPLACEMENT, AND STRUCTURE REFINEMENT STATISTICS

Data set	
Wavelength (Å)	0.8726
Space group	P3(2)21
a (Å)	91.5
b (Å)	91.5
c (Å)	81.3
α=β (°)	90
γ (°)	120
Resolution (Å)	1.84
No. observed/unique reflections	709.980/34.561
Completeness (%)	99.8 (98.6)
Rsym (last shell)	6.4 (47.3)
I/σ(I) (last shell)	41.29 (8.41)
Molecular replacement	
Phaser RFZ	7.6
Phaser TFZ	15.1
Phaser LLG	170/186
Refinement	
Resolution (Å)	1.84
Rwork (%)	17.83
Rfree (%)	21.12
No. of protein atoms	2367
No. of solvent atoms	186
No. of Ca ions	1
rmsd, bond length (Å)	0.012
rmsd, bond angles (°)	1.204
Mean B factor (Å²)	24.106
Residues in most facvored/ allowed regions of Ramachandran plot (%)	100

rmsd, root mean square deviation.

RESULTS

The interaction between PBP2 and SltB1 is Ca^{2+} dependent

The production of recombinant SltB1 using a previously described method only yielded low amounts of soluble protein (Legaree and Clarke 2008). In order to circumvent this problem, we co-expressed SltB1 in the presence of molecular chaperones (DnaK, GroEL, DnaJ, GroES, and GrpE) and also performed chemical treatment of the growth media with the heat-shock inducer benzyl alcohol (Nishihara, Kanemori et al. 1998, de Marco, Vigh et al. 2005). These two modifications to the original expression protocol allowed us to obtain large amounts of highly soluble, pure SltB1 (**Fig. 2**) that was employed for both SPR experiments

and crystallization assays. PBP2 was expressed in *E. coli* and purified by using classical nickel affinity and gel filtration chromatographies.

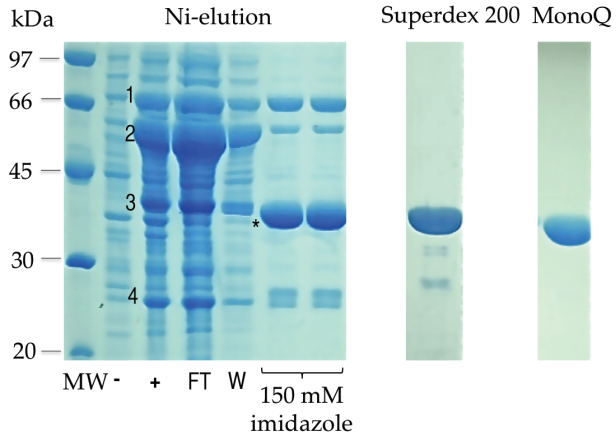

Fig. 2: SDS-PAGE analysis of co-expressed SltB1 with molecular chaperones and benzyl alcohol. Recombinant *Escherichia coli* BL21 (DE3) C43 were grown at 37°C and induced with isopropyl β-D-1-thiogalactopyranoside, tetracycline, L-arabinose, and benzyl alcohol. The majority of coexpressed chaperones could be removed during immobilized metal ion affinity chromatography purification (FT). Abbreviations: 1, DnaK; 2, GroEL; 3, DnaJ; 4, GrpE; *, SltB1; -, uninduced cells; +, induced cells; FT, flow through; W, wash fraction; MW, molecular weight marker.

We then investigated the interaction between PBP2 and SltB1 by SPR analysis. Increasing concentrations of recombinant SltB1, ranging from 0.105 to 1.26 µM, were injected over a CM5 sensor chip on which PBP2 was the immobilized ligand (**Fig. 3**). Analysis of the SPR-binding data using the BIAevaluation software showed that the best fit for the interaction between immobilized PBP2 and soluble SltB1 was provided by the Langmuir 1:1 reaction model, yielding values for the association rate constant (k_a) and dissociation rate constant (k_d) of 2.52×10^{4} $M^{-1}\times s^{-1}$ and 5.98×10^{-3} $M^{-1}\times s^{-1}$, respectively. The resulting apparent equilibrium dissociation constant (K_D) of 230 nM (X^2=1.07) was calculated from the k_d/k_a ratio and is comparable to that measured by Legaree and Clarke of 130 nM, in which a similar experiment was

performed, but with SltB1 immobilized on the sensor chip and PBP2 tested as the soluble analyte (Legaree and Clarke 2008).

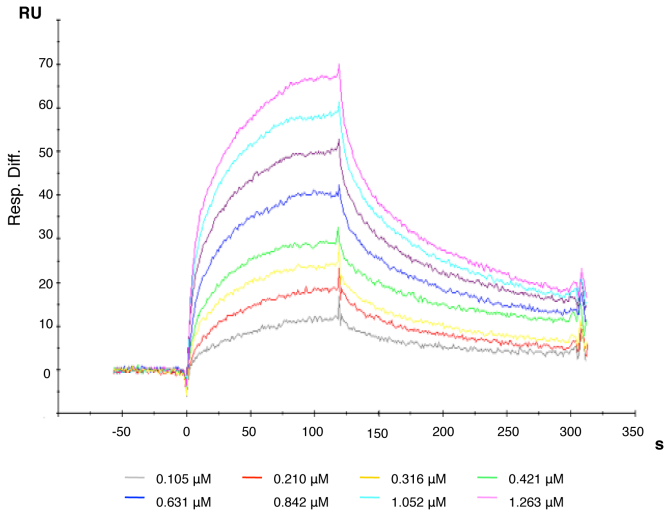

Fig. 3: Interaction of PBP2 with SltB1 demonstrated by SPR analysis. PBP2 was immobilized by coupling amino groups to a carboxylated dextran surface. SltB1 was injected for 180 s at concentrations ranging from 0.105 to 1.26 µM.

Interestingly, in our hands, this interaction was completely abolished when SltB1 was purified in the presence of 1 mM EDTA. Even at the highest concentration of tested analyte (6.34 µM), no interaction could be detected. The interaction between immobilized PBP2 and soluble SltB1 could only be recovered after the dialysis of SltB1 into a buffer containing 2.5 mM $CaCl_2$. This observation suggested that the interaction between SltB1 and PBP2 requires the presence of Ca^{2+}.

Crystal structure of SltB1

The structure of SltB1 was solved to 1.8 Å by performing a molecular replacement experiment using the structure of Slt35 from *E. coli* as a search model (van Asselt,

Kalk et al. 2000); a sequence comparison between SltB1 and Slt35 reveals that the two enzymes share 46% sequence identity (**Fig. 4**).

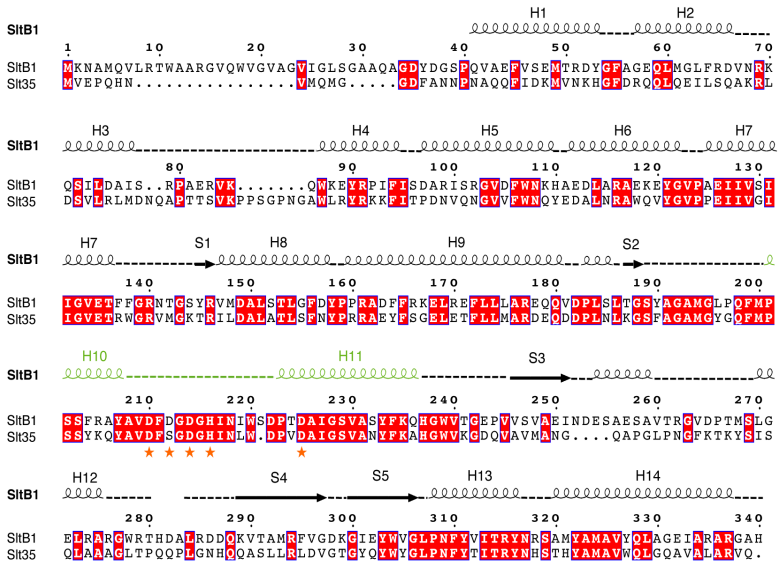

Fig. 4: Structural alignment of *Pseudomonas aeruginosa* SltB1 and *E. coli* Slt35. Identical residues are shown with a red background. The EF-hand-like motif is highlighted in green, whereas the interacting ligands are presented as orange stars. Secondary structure elements visualized in the SltB1 structure are indicate above the sequences. H, helix; S, sheet.

All residues included in the SltB1-expressing clone (40–341) were visible in the electron density map, with the exception of a loop formed by residues 281–283. The fold of the SltB1 monomer is very similar to that of Slt35 (a soluble, active form of the 40 kDa membrane-bound MltB (van Asselt, Kalk et al. 2000)); a comparison of the two structures reveals a root mean square deviation of 0.969 Å for 243 superimposed Cα atoms.

SltB1 harbors three major domains: an N-terminal α domain, a core domain that resembles the fold of lysozyme, and a C-terminal β-sheet domain (shown in blue, red, and green, respectively, in **Fig. 5** (A)).

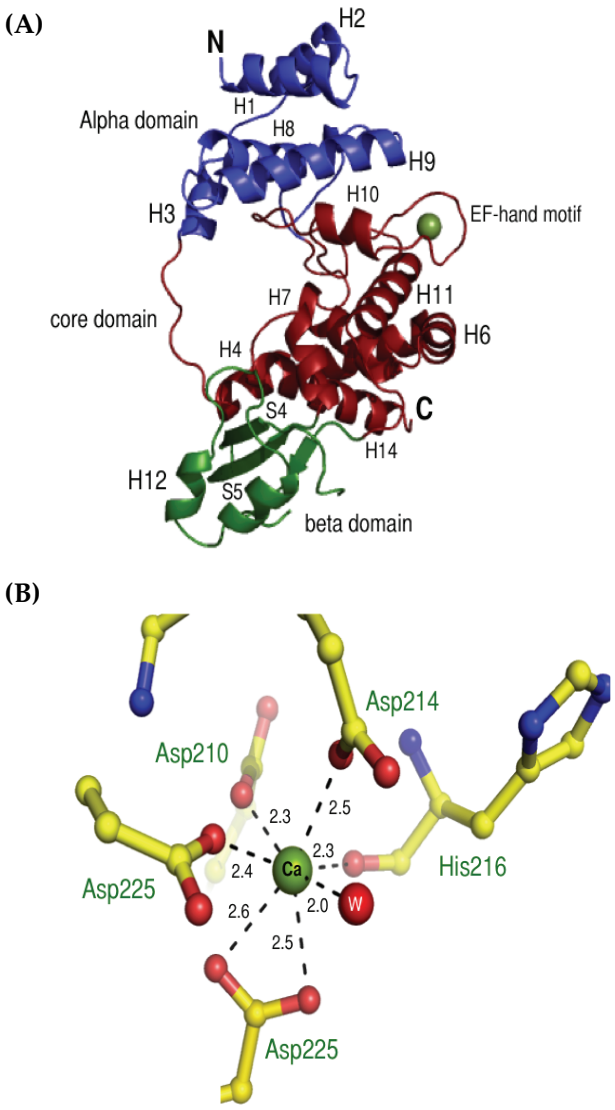

Fig. 5: Three-dimensional structure of SltB1. **(A)** the fold of SltB1 is highly alpha-helical and is made up of three interconnected domains referred to as the α (blue), core (red), and β (green) domains. **(B)** In the EF-hand-like motif, the Ca^{2+} ion is coordinated by six protein oxygen atoms and one water molecule (W) with an average distance of 2.3-2.6 and 2.0 Å, respectively. The coordination of the metal ion has tis typical bipyramidal configuration.

The α domain is formed by five helices, encompassing residues 40–78 (H1–H3) and 143–188 (H8 and H9). The β domain (residues 242–307) comprises one α helix (H12) and a small twisted β-sheet (S3–S5) packed against three helices (H4, H13, and H14) of the core domain. In this β domain, four residues (281–283) are missing from our model, due to the absence of electron density in the map, suggesting a high flexibility for this region.

The core domain consists of three segments comprising eight helices (H4-H7 residues 79–142; H10 and H11, residues 189–243; H13 and H14, residues 308–339). This domain is sandwiched between the α and β domains and is of particular interest, as it bears the putative catalytic site and an EF-hand like motif (see next).

Substrate and metal-binding regions

Superposition of the structure of *E. coli* Slt35 with our SltB1 structure shows that the catalytic acid/base in Slt35, Glu162, is located at the same position as Glu135 in SltB1, suggesting that the latter could play the role of catalytic acid/base in the *P. aeruginosa* enzyme. Furthermore, Glu135 is located in a groove that is present within the core domain, which, by analogy with the structure of other enzymes in the family, harbors the substrate-binding region (van Asselt, Kalk et al. 2000). In SltB1, the groove is mainly lined by aromatic residues (Tyr90, Phe94, Phe164, Phe165, Tyr190, Phe199, Tyr207, Tyr233, Tyr316, and Tyr322). Notably, the aromatic residues present in the groove of *E. coli* Slt35 were shown to be involved in PG recognition, and, thus, the involvement of the groove region for interaction with the substrate by SltB1 could also be possible.

The second segment of the core domain contains an EF-hand-like motif (green region in Fig. 4; residue 201–236), one of the most widespread calcium-binding folds, which is found in a number of metal-binding proteins. The EF-hand of SltB1 differs slightly from canonical EF-hand patterns. First, the EF-hand loop of SltB1 contains 15 residues instead of the typical 12-residue loop observed in canonical EF-hand proteins (Zhou, Yang et al. 2006). Second, the bidentate ligand at position 12 is, in fact, located at position 16 (Asp225). SltB1 can be, thus, classified as a class 4 EF-hand-like protein based on the classification of Zhou et al (Zhou, Yang et al. 2006).

E. coli Slt35 carries an EF-hand-type calcium-binding loop, and Ca^{2+} was shown to be important for stability of the molecule. In the SltB1 structure, presented here, the metal ion bound in the EF-hand loop could be successfully modeled as a

Ca^{2+}, which was also present in the crystallization solution. The Ca^{2+} ion is coordinated by six protein oxygen atoms (Oδ1 of Asp210, Oδ1 of Asp212, Oδ1 of Asp214, O of His216, Oδ1 and Oδ2 of Asp225) and one water molecule with an average distance of 2.3–2.6 and 2.0 Å, respectively (**Fig. 5** (B)). The water molecule is located between the Ca^{2+} ion and two other residues in the EF-hand loop, namely Asp225 and Asp214.

The amino acids that participate in metal coordination in the EF-hand motif are highly conserved (orange stars in **Fig. 4**), with the exception of the residue in an analogous position to that of His216, which can be Arg, Glu, or Lys, as the interaction is made with the backbone carbonyl (van Asselt and Dijkstra 1999). The coordination of the metal ion, therefore, represents the typical bipyramidal configuration for EF-hand-like motifs. Notably, in SltB1, the EF-hand loop is one of the regions that has the highest B-factors, revealing flexibility and a potential requirement for interaction with other protein partners for stabilization.

DISCUSSION

Proteins that are involved in the biosynthesis of PG have been postulated as being a part of a macromolecular complex that includes cytoplasmic, membrane-inserted, and periplasmic members. PBPs and LTs exert antagonistic functions within the PG biosynthesis process, namely Lipid II polymerization/cross-linking and glycan strand cleavage, and the regulation of their activities has been proposed to be facilitated by their proximal localization/direct interaction (Holtje 1998, Vollmer, Joris et al. 2008, Mattei, Neves et al. 2010).

In *P. aeruginosa*, PBP2 has been shown to play a key role in the rod-shaped morphology of the cell; deletion of the *pbpA* gene, which codes for PBP2, generates strains that display a spherical shape. In addition, such strains also display increased susceptibility to β-lactams, indicating that PBP2 plays a role in the development of resistance to such antibiotics (Legaree, Daniels et al. 2007). In this work, we have furthered the studies of Legaree and Clarke regarding the interaction between PBP2 and a molecular partner in the PG elongation process, SltB1, a LT (Legaree and Clarke 2008).

In order to perform these studies, it was necessary to develop a protocol to obtain large amounts of soluble SltB1. This was made possible by coexpressing SltB1 in the

presence of chaperones and of benzyl alcohol, but not by using the additives separately. It is conceivable that the addition of benzyl alcohol induced the expression of other endogenous chaperones (such as IbpA/B or ClpB), allowing them to work in concert with the plasmid-encoded chaperones GroEL-GroES and DnaK-DnaJ-GrpE in order to prevent aggregation and to mediate the correct refolding of SltB1 (de Marco, Vigh et al. 2005). Subsequently, we employed SPR spectroscopy to study the interaction between PBP2 and SltB1 in the absence and presence of calcium ions. Notably, binding was only detected in the presence of Ca^{2+}, suggesting that the metal could play a role in the stabilization of SltB1 and be potentially important for the interaction itself. Temperature-scanning circular dichroism and fluorescence spectroscopy experiments performed on purified *E. coli* Slt35 also revealed that Ca^{2+} played a role in the stabilization of the enzyme (van Asselt and Dijkstra 1999). It is also of note that the interaction between SltB1 and PBP2 was identified by using the soluble form of the PBP (which does not carry the transmembrane region), attesting to the fact that it is the periplasmic region of PBP2 which is involved in recognition of SltB1 (in agreement with Legaree and Clarke (Legaree and Clarke 2008)).

Our high-resolution structure of SltB1 reveals a three-domain fold that is highly similar to that of other soluble LTs, and, especially, Slt35 from *E. coli* (van Asselt, Kalk et al. 2000). The middle, core domain (**Fig. 5** (A)) displays a classic EF-hand fold with a Ca^{2+} ion coordinated by seven oxygen atoms (**Fig. 5** (B)) which is often seen in other EF-hand-carrying proteins (Michiels, Xi et al. 2002, Zhou, Yang et al. 2006). Markedly, eukaryotic proteins that carry multiple EF-hand regions often undergo conformational modifications on binding Ca^{2+}, an event that plays a role in signal transduction (Grabarek 2006, Zhou, Yang et al. 2006). It is conceivable that the requirement of Ca^{2+} for the interaction between SltB1 and PBP2 in *P. aeruginosa* reflects a conformational modification of the EF-hand of SltB1 on recognition of its partner; a detailed understanding of this process will require a solution to the high-resolution structure of the PBP2: SltB1 complex. However, our SPR studies indicated that SltB1 had to be in its metal-bound form in order to recognize PBP2, which suggests that this specific region could play a role in PBP recognition. Interestingly, Romeis and Höltje identified that *E. coli* PBP8, an endopeptidase, not only binds to Slt70 but also stimulates its activity and protects it from degradation, pointing to the interdependence of these proteins for optimal functionality (Romeis and Holtje 1994). Thus, the data presented here, combined with studies on LTs and PBPs from other

bacterial species, define an initial framework for the understanding of the relationship between these antagonistic enzymes in the cell-wall biosynthesis process.

ACKNOWLEDGEMENTS

The authors would like to thank J. Marquez and the HTX Lab team (Partnership for Structural Biology (PSB), France) for access to and help with high throughput crystallization, I. Bally (Institut de Biologie Structurale (IBS), PSB) for access to the SPR facility, and the European Synchrotron Radiation Facility (ESRF, PSB) for access to beamlines.

REFERENCES

Blackburn, N. T. and A. J. Clarke (2001). "Identification of four families of peptidoglycan lytic transglycosylases." J Mol Evol **52**(1): 78-84.

Bouhss, A., et al. (2008). "The biosynthesis of peptidoglycan lipid-linked intermediates." FEMS Microbiol Rev **32**(2): 208-233.

Cohen, S. X., et al. (2008). "ARP/wARP and molecular replacement: the next generation." Acta Crystallogr D Biol Crystallogr **64**(Pt 1): 49-60.

de Marco, A., et al. (2005). "Native folding of aggregation-prone recombinant proteins in *Escherichia coli* by osmolytes, plasmid- or benzyl alcohol-overexpressed molecular chaperones." Cell Stress Chaperones **10**(4): 329-339.

Emsley, P. and K. Cowtan (2004). "Coot: model-building tools for molecular graphics." Acta Crystallogr D Biol Crystallogr **60**(Pt 12 Pt 1): 2126-2132.

Grabarek, Z. (2006). "Structural basis for diversity of the EF-hand calcium-binding proteins." J Mol Biol **359**(3): 509-525.

Holtje, J. V. (1998). "Growth of the stress-bearing and shape-maintaining murein sacculus of *Escherichia coli*." Microbiol Mol Biol Rev **62**(1): 181-203.

Jennings, G. T., et al. (2002). "GNA33 from *Neisseria meningitidis* serogroup B encodes a membrane-bound lytic transglycosylase (MltA)." Eur J Biochem **269**(15): 3722-3731.

Kabsch, W. (2010). "Xds." Acta Crystallogr D Biol Crystallogr **66**(Pt 2): 125-132.

Legaree, B. A. and A. J. Clarke (2008). "Interaction of penicillin-binding protein 2 with soluble lytic transglycosylase B1 in *Pseudomonas aeruginosa*." J Bacteriol **190**(20): 6922-6926.

Legaree, B. A., et al. (2007). "Function of penicillin-binding protein 2 in viability and morphology of *Pseudomonas aeruginosa*." J Antimicrob Chemother **59**(3): 411-424.

Lyczak, J. B., et al. (2002). "Lung infections associated with cystic fibrosis." Clin Microbiol Rev **15**(2): 194-222.

Macheboeuf, P., et al. (2006). "Penicillin binding proteins: key players in bacterial cell cycle and drug resistance processes." FEMS Microbiol Rev **30**(5): 673-691.

Mattei, P. J., et al. (2010). "Bridging cell wall biosynthesis and bacterial morphogenesis." Curr Opin Struct Biol **20**(6): 749-755.

Michiels, J., et al. (2002). "The functions of Ca^{2+} in bacteria: a role for EF-hand proteins?" Trends Microbiol **10**(2): 87-93.

Mohammadi, T., et al. (2011). "Identification of FtsW as a transporter of lipid-linked cell wall precursors across the membrane." EMBO J **30**(8): 1425-1432.

Morlot, C., et al. (2005). "Crystal structure of a peptidoglycan synthesis regulatory factor (PBP3) from *Streptococcus pneumoniae*." J Biol Chem **280**(16): 15984-15991.

Murshudov, G. N., et al. (1997). "Refinement of macromolecular structures by the maximum-likelihood method." Acta Crystallogr D Biol Crystallogr **53**(Pt 3): 240-255.

Nishihara, K., et al. (1998). "Chaperone coexpression plasmids: differential and synergistic roles of DnaK-DnaJ-GrpE and GroEL-GroES in assisting folding of an allergen of Japanese cedar pollen, Cryj2, in *Escherichia coli*." Appl Environ Microbiol **64**(5): 1694-1699.

Reid, C. W., et al. (2006). "Role of arginine residues in the active site of the membrane-bound lytic transglycosylase B from *Pseudomonas aeruginosa*." Biochemistry **45**(7): 2129-2138.

Romeis, T. and J. V. Holtje (1994). "Specific interaction of penicillin-binding proteins 3 and 7/8 with soluble lytic transglycosylase in *Escherichia coli*." J Biol Chem **269**(34): 21603-21607.

Sauvage, E., et al. (2008). "The penicillin-binding proteins: structure and role in peptidoglycan biosynthesis." FEMS Microbiol Rev **32**(2): 234-258.

Scheurwater, E., et al. (2008). "Lytic transglycosylases: bacterial space-making autolysins." Int J Biochem Cell Biol **40**(4): 586-591.

van Asselt, E. J. and B. W. Dijkstra (1999). "Binding of calcium in the EF-hand of *Escherichia coli* lytic transglycosylase Slt35 is important for stability." FEBS Lett **458**(3): 429-435.

van Asselt, E. J., et al. (2000). "Crystallographic studies of the interactions of *Escherichia coli* lytic transglycosylase Slt35 with peptidoglycan." Biochemistry **39**(8): 1924-1934.

Vollmer, W., et al. (2008). "Bacterial peptidoglycan (murein) hydrolases." FEMS Microbiol Rev **32**(2): 259-286.

Vollmer, W., et al. (1999). "Demonstration of molecular interactions between the murein polymerase PBP1B, the lytic transglycosylase MltA, and the scaffolding protein MipA of *Escherichia coli*." J Biol Chem **274**(10): 6726-6734.

Zhou, Y., et al. (2006). "Prediction of EF-hand calcium-binding proteins and analysis of bacterial EF-hand proteins." Proteins **65**(3): 643-655.

CHAPTER 3

MISTIC as a fusion partner for high-level expression of bacterial flippases

ABSTRACT

The bacterial cell wall is an essential structure that preserves not only cellular integrity and protects the bacterium from mechanical damage but also from osmotic rupture or lysis. Synthesis of the bacterial cell wall requires the concerted action of several enzymes. A central process of this synthesis is the translocation of Lipid II across the cytoplasmic membrane to the periplasmic space. Members of the SEDS family are integral membrane proteins and have been long proposed as being responsible for Lipid II translocation. To understand the mode of action of Lipid II transport it is necessary to obtain detailed information about the atomic structure of the flippase. A prerequisite for structural studies is the production of sufficient amounts of properly folded protein. Herein we describe the successful use of Mistic as a fusion partner for high-level expression of several SEDS homologs, obtaining expression levels of 5 to 15 mg of protein/L of culture. Fusion of other tags led, upon expression of the recombinant proteins to low expression yields, degradation or even loss of cell viability. This is a major obstacle seen with the overexpression of foreign membrane proteins, caused mainly by the saturation of the host's protein translocation machinery. Mistic, however, has the ability to fold itself and its cargo protein into the lipid bilayer via direct association with the membrane and thus avoids overloading the membrane protein translocation machinery.

INTRODUCTION

The peptidoglycan is a unique structure of the bacterial cell wall and is essential for bacterial survival. Its macromolecular structure consists of alternating glycan chains composed of polymeric disaccharides Mur*N*Ac and Glc*N*Ac that are cross-linked by short peptides. One central event during the biosynthesis of peptidoglycan is the translocation of Lipid II from the inner to the outer leaflet of the cell. To date, the structure and function of several enzymes involved in peptidoglycan biosynthesis are well known, however, the identity of the protein mediating Lipid II translocation across the hydrophobic membrane remains controversial. FtsW, a multi-spanning membrane protein, belongs to the well-conserved SEDS protein family (**S**hape, **E**longation, **D**ivision and **S**porulation) that also includes RodA and SpoVE proteins, and has been proposed for decades to be responsible for Lipid II transport across the

membrane during cell division and daughter cell formation (Holtje 1998). SEDS proteins are highly conserved and present in all cell wall-containing bacteria. Recently, Mohammadi and colleagues presented evidence by using a dithionite reduction assay that FtsW has a direct role in Lipid II translocation, while Sham and co-workers suggested that this activity could be catalyzed by the inner-membrane protein MurJ (Mohammadi, van Dam et al. 2011, Sham, Butler et al. 2014). Nevertheless, to date only little is known about this translocation process and its regulation. Determination of the atomic structure of any flippase will provide insights into the molecular mechanism that underlies this fundamental process and is therefore a crucial prerequisite for advances in rationalized drug design.

However, membrane protein overexpression is a challenging task mainly caused by the complex requirements of membrane protein biogenesis. One of the major bottlenecks associated with the study of membrane proteins is therefore production of sufficient yields of properly folded protein. Due to their low abundance in natural biological membranes, expression in heterologous systems often leads to toxicity problems for the host or to inclusion body formation (Schlegel, Klepsch et al. 2010). The appropriate combination of bacterial strain, expression vector and optimized cell growth conditions can reduce these effects and allow the overproduction of the protein of interest. To date, numerous approaches have been developed to improve the yield and recovery of integral membrane proteins. Prokaryotic membrane proteins have proven to be most successfully expressed in *Escherichia coli* due to the ease of genetic manipulation and fast generation times. Recent studies have shown that overexpressing membrane proteins can be greatly improved if selecting *Escherichia coli* strains with strongly improved membrane protein overexpression characteristics, like the Walker strains C41 (DE3) and C43 (DE3), or by engineering chimera of the membrane protein of interest (Miroux and Walker 1996). The introduction of well-established fusion tags like thioredoxin (Trx), Mistic, the glycerol-conducting channel protein (GlpF) or poly Histidine (His) resulted frequently in optimized overexpression of recombinant membrane proteins (Therien, Glibowicka et al. 2002, Ishihara, Goto et al. 2005, Roosild, Greenwald et al. 2005, Neophytou, Harvey et al. 2007). As an alternative approach to circumvent the toxicity issues of overproducing foreign membrane proteins, cell-free expression systems have been recently developed that have the advantage of controlled expression conditions with no need to maintain cell viability. Successful overexpression of several membrane proteins, be it of prokaryotic or eukaryotic

origin, have been already reported (Ishihara, Goto et al. 2005, Klammt, Schwarz et al. 2005, Wuu and Swartz 2008, Tosi, Estrozi et al. 2014). However, cell-free expression systems are fairly expensive and also difficult to scale up.

Herein, we describe the successful overexpression of several SEDS proteins, obtaining a high to moderate expression level. The proteins were N-terminal fused to Mistic, a novel membrane-associated protein discovered in *Bacillus subtilis* (Roosild, Greenwald et al. 2005). Mistic is a unusual, highly hydrophilic protein representing a family of unique membrane-associating proteins that are composed of four transmembrane α-helices, which could particularly enhance the expression level of several, foreign membrane proteins when used as a fusion partner linked to their N-termini (Roosild, Greenwald et al. 2005, Kefala, Kwiatkowski et al. 2007, Dvir and Choe 2009, Chowdhury, Feng et al. 2012, Xu, Kong et al. 2013).

Surprisingly, Mistic lacks any identified signal sequence, which is recognized by the Sec translocon machinery and appears to fold autonomously into the lipid bilayer (Roosild et *al*, 2006). Overexpression of SEDS proteins in fusion with Mistic showed no limitation in biomass formation and thus no toxicity issues. Mistic is thought to chaperone the SEDS proteins into the membrane without assistance of the Sec translocon therefore limiting possible disturbance of the membrane protein biogenesis pathway.

MATERIALS AND METHODS

Construction of recombinant SEDS protein fusion constructs

The constructs used in the present study are shown in **Fig. 1**. SEDS proteins from different bacterial backgrounds (**TABLE 1**) were cloned systematically in fusion in either *E. coli*- or cell-free- based expression vectors (**Fig. 1**).

TABLE 1. List of selected SEDS proteins

PROTEIN NAME	ORGANSIM	Acc n° UNIPROT	Siza (kDa)	Topology
RodA	*S. pneumoniae*	Q97RK3	40	10 TM
FtsW	*E. coli*	P0ABG4	46	10 TM
RodA	*E. coli*	P0ABG7	40.5	9 TM
FtsW	*T. maritima*	Q9WY75	40.6	10 TM
RodA	*P. aeruginosa*	Q9X6V4	40	8 TM
FtsW	*B. subtilis*	O07639	43.7	10 TM
RodA	*B. subtilis*	P39604	43.3	10 TM
SpoVE	*B. subtilis*	P07373	40	10 TM
FtsW	*A. aeolicus*	O67212	51.7	10 TM
RodA	*A. aeolicus*	O66444	42.7	10 TM

The size of the each SEDS protein was calculated using the ExPASy tool ProtParam. Predictions of transmembrane domains (TM) were performed using the TMHMM server.

E. coli expression vectors

To test the expression of SEDS in *E. coli*, the ORFs coding for the selected SEDS were PCR amplified and inserted into the destination vectors pET30a and pET32a via *Hind*III and *Bam*HI sites, resulting in pET30a-F and pET32a-F, respectively. pLIM15 was created by removing the toxic *ccdB* expression cassette of vector pLIM14 (Noirclerc-Savoye, Gallet et al. 2010) and inserting the coding sequence of SEDS using *Nco*I-*Bam*HI sites. pGlpF-F was obtained by replacing the coding sequence of *mistic* in pLIM15 with the *glpF* expression cassette which was inserted as an *Nde*I-*Nco*I fragment.

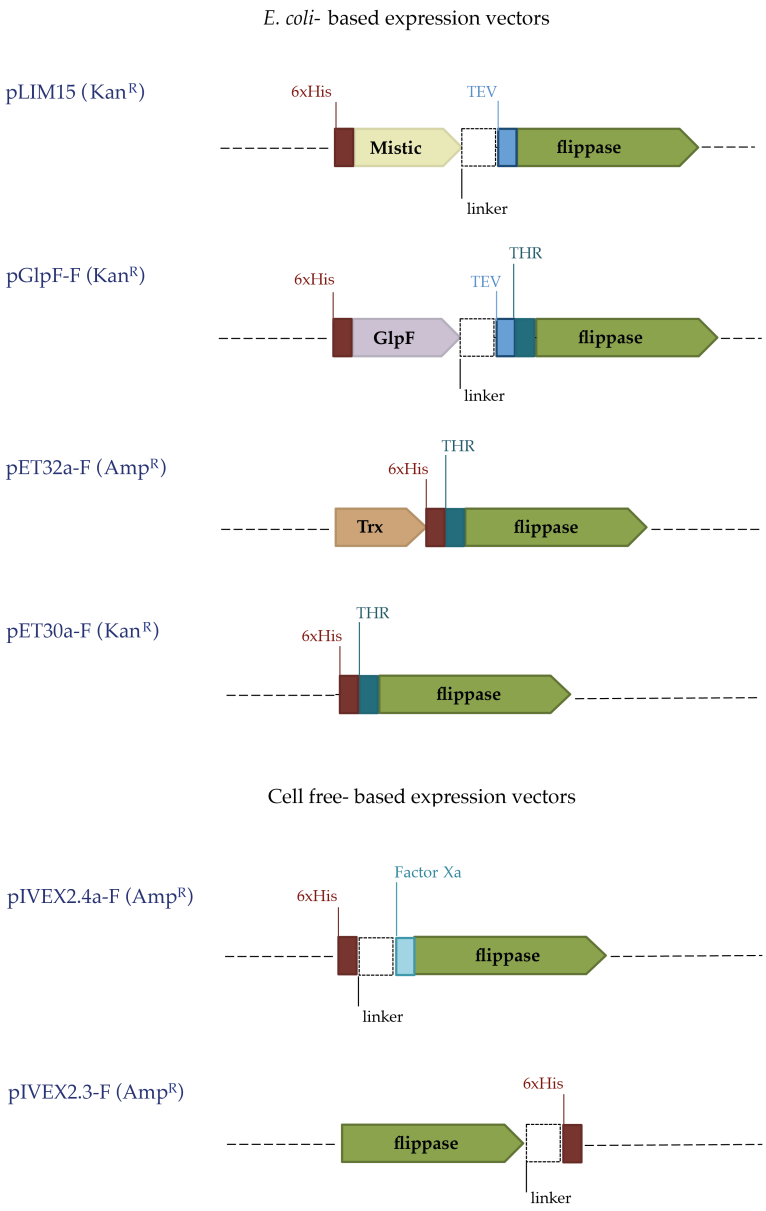

Fig. 1: Schematic diagram of SEDS fusion protein constructs. Abbreviations: Kan^R, kanamycin resistant; Amp^R, ampicillin resistant; TEV, **T**obacco **E**tch **V**irus cleavage site; THR, **thr**ombin cleavage site; Factor Xa, Factor Xa cleavage site.

Cell-free expression vectors

Vectors pIVEX2.4 and pIVEX2.3 were used for expression in the cell-free system. Genes encoding for *E. coli ftsW* and *Streptococcus pneumoniae rodA* were PCR amplified and transferred to the cell-free expression vectors via *Not*I/*Xho*I and *Nde*I/*Xho*I sites, resulting in pIVEX2.4-F and pIVEX2.3-F, respectively.

***E. coli*- based protein expression**

Expression vectors were used to transform *E. coli* BL21(DE3) C41, RIL and STAR (Invitrogen) competent cells. Expression tests were performed in 24-deep well plates containing 3 ml of either Luria-Bertani (LB), Terrific Broth (TB) or Minimal medium (M9). The cultures were inoculated with overnight pre-cultures at a 1/40th dilution and expression was induced by the addition of isopropyl β-D-1-thiogalactopyranoside (IPTG) to a final concentration of 0.5 mM at an OD_{600nm} of 1 A.U. After further growth for 3 hours at 37°C, the cells were harvested by centrifugation (6.000 rpm, 20 min, 4°C) and the cell pellet was resuspended in 150 µl TBS buffer (50 mM Tris (pH 7.5), 150 mM NaCl) containing lysozyme (Fluka), benzonase (Novagen) and BugBuster (Novagen) to a final concentration of 200 µg/ml, 25 units/ml and 0.5x, respectively. The cell suspension was incubated on a shaking platform for at least 20 minutes at room temperature and 10 µl aliquots were analyzed by Western blots.

Cell-free- based protein expression

For *in vitro* expression, 10 µg/ml of water-solubilized plasmid DNA (pIVEX2.3-F or pIVEX2.4a-F) were added to 50 µl final volume of reaction mixture in a 1.5 ml Eppendorf tube. The reaction mixture consisted of 1 mM amino acid mix, 0.8 mM ribonucleotides (guanosine-, uracil- and cytidine-triphospahte), 1.2 mM adenosine triphosphate, 55 mM HEPES pH 7.5, 68 µM folinic acid, 0.64 mM cyclic adenosine monophosphate, 3.4 mM dithiothreitol, 27.5 mM ammonium acetate, 80 mM creatine phosphate, 208 mM potassium glutamate, 16-24 mM magnesium acetate, 250 µg/ml creatine kinase, 27 µg/ml T7 RNA polymerase (produced in-house), 0.175 µg/ml tRNA, 20 µl/ml S30 *E. coli* extract (produced in-house). After preparation of the mixtures, samples were incubated at 30°C with agitation for 3 hours. Reaction

mixtures were afterwards pelleted by centrifugation and subsequently resuspended in 10 µl TBS buffer. Expression yields were analyzed by Western blot.

For expression of the plasmids in the presence of liposomes:

1 mg/ml liposomes were added to the cell free reaction mixtures, the following steps were the same as described above. The liposomes were prepared by dissolving the appropriate amount of lyophilized lipids (L-α-phosphatidycholine (Egg PC) and polar fraction of *E. coli* lipids, respectively; Avanti) in 100% chloroform, which was subsequently evaporated under liquid nitrogen stream followed by suspension in sterile water.

Western blot analysis

Total cell samples were separated by Sodium Dodecyl Sulfate- Polyacrylamide Gel Electrophoresis (SDS-PAGE) and transferred to nitrocellulose membranes by dry electro blotting. The nitrocellulose membrane was blocked with 5% Bovine Serum Albumine (BSA) in TBS complemented with 0.005% Tween 20 (TBST) for 2 hours at room temperature. After a short wash with TBST, the nitrocellulose membrane was incubated overnight at 4°C with monoclonal Anti-poly-Histidine-peroxidase antibodies (Sigma) at 1:2000 dilution in TBST. The next morning, the membrane was washed 3x with TBST and afterwards incubated with freshly prepared substrate solution (SIGMAFAST DAB with metal enhancer, Sigma) for color development. The amount of recombinant protein was quantified by comparison to known amounts of a control His-tagged protein loaded on the same blot.

RESULTS

SEDS proteins are integral membrane proteins containing between eight and ten predicted transmembrane (TM) domains. All bacteria that produce peptidoglycan carry at least one member of the SEDS protein family. The aim of this study was to identify constructs which allow high-level expression of SEDS proteins sufficient enough for structural studies. Therefore, we chose ten different homologs of SEDS proteins from different bacterial backgrounds (**TABLE 1**) and expressed them in two expression systems using various fusion tags. Following the cloning of the selected SEDS proteins into the different overexpression cassettes (**Fig. 1**), small-scale

expression screens were performed in triplicate for all chimeras using *E. coli* as the host, and only for two of the ten chosen homologs protein expression was tested with the cell-free system. Expression levels of the target protein were analyzed by Western blot, using the His-tag sequence to reveal the presence of the overexpressed target protein. Expression levels are given in mg of protein/L of culture (see **TABLE 2**).

Expression in E. coli

Expression of SEDS proteins from pET30a-F (N-terminal fusion of His-tag) yielded only for three out of the ten tested homologs in detectable expression of the full-length protein (**Fig. 2**). For homologs RodA and FtsW from *Bacillus subtilis* as well as RodA from *S. pneumoniae* weak expression of the target protein could be detected in all tested expression strains, except C41, which resulted in degradation of *B. subtilis* FtsW. However, expression of the other seven homologs resulted either in loss of cell viability or degradation of the target protein (see **Fig. 2**, *e.g. B. subtilis* SpoVE).
Expression of SEDS proteins in fusion to a His-tag seemed to be not sufficient to produce high yields of target protein. Growth was strongly hampered in the majority of cultures resulting in cell densities reduced by more than 50% compared to the control (OD_{600nm} of 0.6-1.1 compared to OD_{600nm} 2.4, respectively).
This effect could be sometimes reduced by using large-affinity tags, such as Trx, GlpF or Mistic, which showed great success as a fusion partner in expressing integral membrane protein (Roosild, Greenwald et al. 2005, Neophytou, Harvey et al. 2007, Chowdhury, Feng et al. 2012, Xu, Kong et al. 2013).

Trx is a thermostable, 12-kDa intracellular *E. coli* protein that is easily overexpressed and very useful as a tag in avoiding inclusion body formation of the recombinant protein (LaVallie, Lu et al. 2000). Using Trx as a fusion partner is thought to be advantageous due to its high aqueous solubility. To test the ability of Trx in enhancing the expression of SEDS proteins, we cloned the genes encoding for ten different SEDS proteins downstream of Trx, resulting in plasmids pET32.a-F. Anyhow, expression of these chimeras resulted under all tested conditions in failure of detecting any recombinant protein on a Western blot. Furthermore, overexpression of the recombinant proteins resulted not only to a extremely reduced log phase of the cultures when compared to the not induced strains, but also to an arrest in the stationary phase and shortly after to cell death (data not shown).

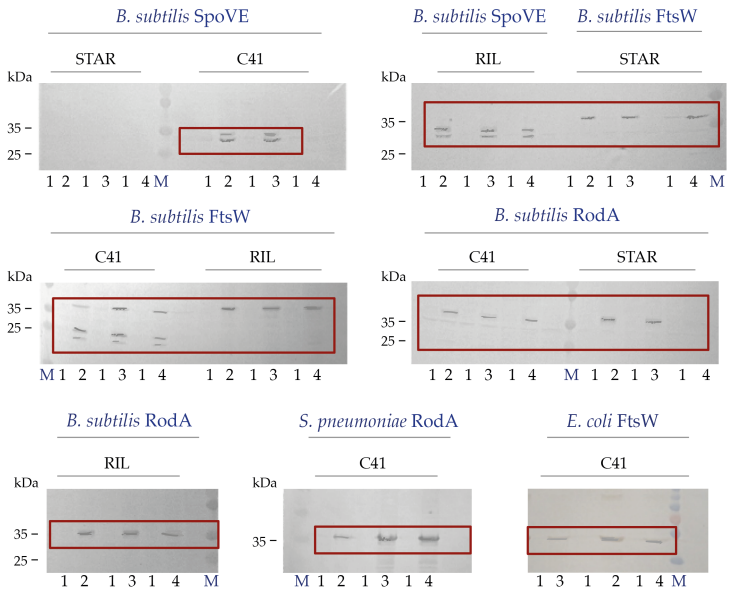

Fig. 2: Western blot analysis of cell extracts of His-SEDS fusions. Overexpressed proteins are shown in red rectangles. Abbreviations: 1, not induced cells; 2, expressed protein in TB medium; 3, expressed protein in LB medium; 4, expressed protein in M9 medium; M, marker.

The decrease of growth, followed by loss of cell viability, is most probably caused by the expression of the recombinant protein. Hence we tested another strategy in which we utilized a tag provided by an integral membrane protein native to its host.

GlpF, a highly expressed *E. coli* membrane protein, was used recently by Neophytou and colleagues as a fusion partner for the expression of several eukaryotic membrane proteins (Neophytou, Harvey et al. 2007). It is assumed that fusion of GlpF to the target protein ensures integration of the recombinant protein into the membrane via the Sec translocon. It must be noted, that choosing GlpF as a fusion partner to any integral membrane protein, requires that the N-terminus of the target protein is located in the cytosol, allowing correct topology of the target protein after insertion into the membrane (Neophytou, Harvey et al. 2007). As all tested SEDS homologs were predicted to have their N-termini on the cytoplasmic side of the membrane (as predicted by TMHMM), we tested the GlpF system by cloning the gene encoding for *glpF* upstream of the SEDS coding sequences, resulting in

plasmids pGlpF-F. Nevertheless, after extensive screening of all strains and conditions, expression of SEDS proteins in fusion to GlpF led unfortunately to the same result obtained with the Trx fusion. Loss of cell viability upon expression of the recombinant proteins could be caused due to destabilization of the membrane protein biogenesis pathway. The limiting capacity of the Sec translocon to process a massive load of nascent, heterologously expressed protein can drastically affect membrane integrity and cell functionality leading often to the activation of stress responses and eventually to cell death. To circumvent such an event, a system had to be used which successfully inserts recombinant expressed proteins into the host membrane without requiring recognition by the Sec translocon machinery.

Mistic, a small integral membrane protein recently discovered in *B. subtilis*, was shown to spontaneously fold into the inner membrane, in a Sec-independent manner. Roosild and colleagues described the successful use of Mistic as a fusion partner to promote facilitated membrane insertion of various cargo proteins (Roosild, Greenwald et al. 2005). Based on these facts it was assumed that fusion of Mistic to SEDS proteins could lead to improved expression of the recombinant proteins without destabilizing the protein translocation machinery. We therefore cloned the coding sequences of all ten SEDS homologs in fusion with the C-terminus of Mistic, resulting in plasmids pLIM15-F. Detectable amounts of full-length protein were obtained for six out of the ten tested SEDS protein fusions (see **Fig. 3** (A)). Mistic fusion significantly increased the yields of the recombinant proteins that were markedly higher than that of the His-tagged fusions (see **TABLE 2**). As shown in **Fig. 2** and **Fig. 3** (A), while FtsW from *Thermatoga maritima* and RodA from *Pseudomonas aeruginosa* and *E. coli* resulted in loss of cell viability when expressed as a His-tagged fusion, they were highly expressed by the Mistic method.

Furthermore, fusion of a His-tag to *S. pneumoniae* RodA, *E. coli* FtsW as well as *B. subtilis* FtsW resulted just in a weak expression of the recombinant protein; however, using Mistic as a fusion partner caused a tremendous boost in production of recombinant protein, which was, depending on the SEDS used, between 5-35 fold (see **TABLE 2**). Remarkably, fusion of Mistic to RodA from *S. pneumoniae* and FtsW from *T. maritima* enhanced the yield of recombinant expressed protein to a level that it was even clearly detectable by Coomassie-blue stain (**Fig. 3** (B)). Hence, Mistic seems to act like a membrane targeting signal sequence that enables the cargo protein to fold autonomously into the lipid bilayer and thus circumvent saturation of the translocation machinery. Fusion to Mistic has therefore the ability to greatly enhance

overexpression of SEDS proteins leading to significantly increased yields of the target protein without affecting cell viability.

TABLE 2. Protein yields obtained with the small-scale expression test

	E. coli based expression				Cell-free expression	
PROTEIN NAME	His-tag	Trx-tag	GlpF-tag	Mistic-tag	N-terminal His-tag	C-terminal His-tag
S. pneumoniae RodA	◆◆	⦸	⦸	◆◆◆◆◆	◆	⦸
E. coli FtsW	◆◆	⦸	⦸	◆◆◆◆	◆	⦸
E. coli RodA	⦸	⦸	⦸	◆◆◆◆	n.t	n.t
T. maritima FtsW	⦸	⦸	⦸	◆◆◆◆◆	n.t	n.t
P. aeruginosa RodA	⦸	⦸	⦸	◆◆◆◆	n.t	n.t
B. subtilis FtsW	◆◆	⦸	⦸	◆◆◆◆	n.t	n.t
B. subtilis RodA	◆◆	⦸	⦸	⦸	n.t	n.t
B. subtilis SpoVE	❖	⦸	⦸	⦸	n.t	n.t
A. aeolicus FtsW	⦸	⦸	⦸	⦸	n.t	n.t
A. aeolicus RodA	⦸	⦸	⦸	⦸	n.t	n.t

For each protein, the yield obtained is expressed in mg of target protein/liter of culture. Abbreviations: ⦸, not detectable; ❖, degraded; n.t, not tested; ◆, < 0.1 mg/L; ◆◆, 0.1-0.4 mg/L; ◆◆◆, 0.4-2 mg/L; ◆◆◆◆, 2-5 mg/L; ◆◆◆◆◆, 5-10 mg/L; ◆◆◆◆◆◆, > 10mg/L.

Cell-free expression

To test the ability of the cell-free system to express SEDS proteins, we chose to test only two candidates, *S. pneumoniae* RodA and *E. coli* FtsW, which could be also expressed in the *E. coli*- based system as His-tagged versions (**Fig. 2**) or fusions to Mistic (**Fig. 3**). The genes encoding for these two homologs were cloned either in fusion with an N-terminal or a C-terminal His-tag, resulting in plasmids pIVEX2.4a-F and pIVEX2.3-F, respectively.

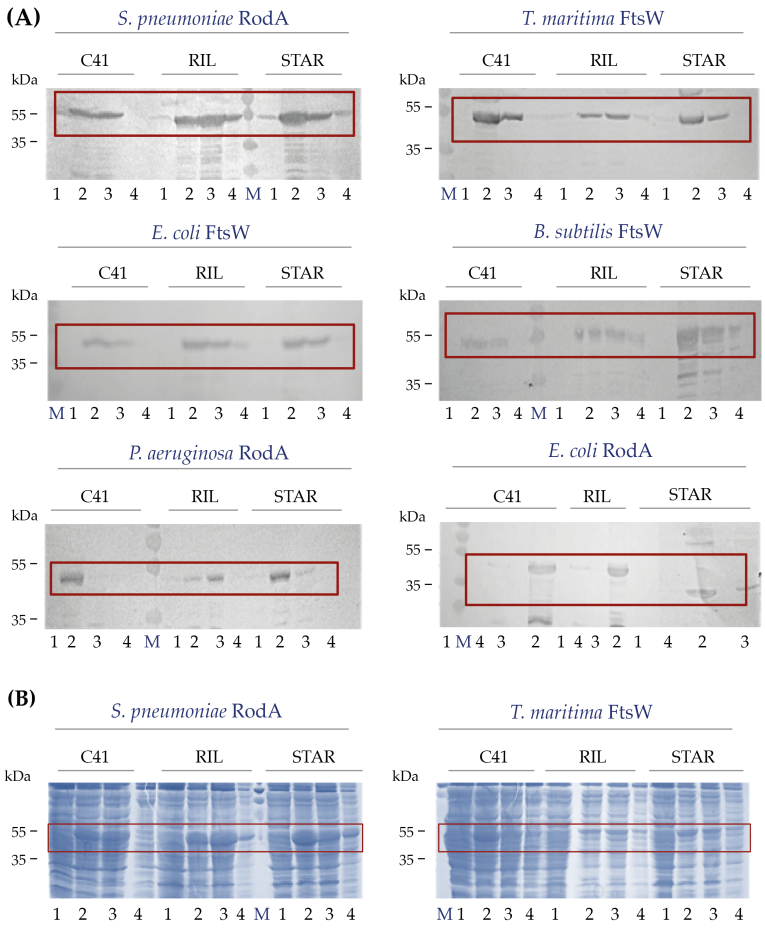

Fig. 3: Small-scale overexpression tests of SEDS proteins fused to Mistic. The cell extracts were analyzed by **(A)** Western blot or **(B)** coomassie-blue stain. Overexpressed proteins are shown in red rectangles. Abbreviations: 1, not induced cells; 2, expressed protein in TB medium; 3, expressed protein in LB medium; 4, expressed protein in M9 medium; M, marker.

Expression of these two homologs from plasmid pIVEX2.4a-F showed only barely detectable amounts of expressed protein on Western blots (**Fig. 4** (A)), whereas fusion of a His-tag to their C-termini led to no expression at all. As the standard expression reaction in the cell-free system is devoid of substantial amounts of

hydrophobic environments, like membranes or lipids, it was also tested, if the expression level of the two chosen target proteins could be increased in the presence of liposomes composed of defined lipids. However, addition of liposomes to the cell-free reaction did not increase expression of the SEDS proteins, expression was rather decreased (**Fig. 4** (B)). Moreover, expression of the SEDS proteins resulted in both tested conditions not only in yields that were below 0.1 mg/L, but also in the degradation of the expressed protein (**Fig. 4**).

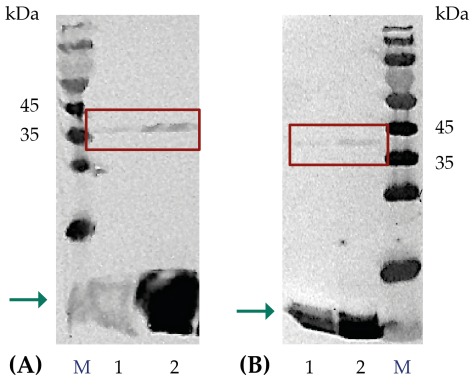

Fig. 4: Small-scale overexpression tests of SEDS proteins in cell-free system. The recombinant proteins (red rectangle) were either expressed **(A)** without liposomes or **(B)** in the presence of liposomes. Degradation products of the target proteins are indicated with a green arrow. Abbreviations: 1, *S. pneumoniae* RodA; 2, *E. coli* FtsW; M, marker.

We can exclude that this effect was caused by codon bias as we tested not only RodA of *S. pneumoniae*, but also FtsW from *E. coli*, which showed no significant difference in expression and degradation of the target protein. Whatever the case, as the expression of SEDS proteins in this system was not sufficient enough for further structural studies, we excluded the cell-free system as a system of choice.

DISCUSSION

Membrane proteins play crucial roles in a wide variety of biological processes, but irrespective of their prevalence, our knowledge and structural information of

membrane proteins is exceedingly scarce. Since the natural abundance of many membrane proteins is too low for structural studies, it is often necessary to express the protein of interest in a recombinant system to obtain sufficient amounts of properly folded protein. However, while to date various strategies exist for optimized expression of soluble proteins, overexpression of membrane proteins is a daunting task due to the unique amphipathic nature of their transmembrane domains. To overcome this major obstacle, overexpression of membrane proteins requires typically extensive screening till successful expression of the target protein is achieved. Finding ideal conditions for producing sufficient quantities of properly folded membrane protein is therefore very time consuming and generally accomplished by "trial and error"(Wagner, Baars et al. 2007).

In this study we evaluated the expression yields of ten homologs SEDS in two expression hosts using various fusion tags. Fusion to a conventional His-tag led only for four out of ten tested SEDS to weak expression of the target protein (see **Fig. 2** and **TABLE 2**). Overexpression of the other tested homologs strongly hampered growth resulting in loss of cell viability and cell death. The same result was obtained when SEDS proteins were fused to either Trx or GlpF. Our assumption is that overexpression of these chimera led to destabilization of the membrane protein biogenesis pathway caused by jamming the translocation machinery with non-native protein. Increasing evidence indicates that limiting the Sec translocon capacity is one of the major bottlenecks in the overexpression of foreign membrane proteins (Wagner, Bader et al. 2006, Wagner, Baars et al. 2007). Consequently, the host induces its stress responses and activates proteolytic systems that may lead to cell death.

To circumvent this obstacle, we utilized Mistic as a fusion partner. Overexpression of Mistic, be it alone or in fusion to foreign membrane proteins, lacks any toxicity issues associated with clogging the Sec translocon machinery due to its unique ability to autonomously insert the transmembrane domains of the target protein into the host's lipid bilayer (Roosild, Greenwald et al. 2005). Our data supports this hypothesis, since fusion of SEDS proteins to Mistic had a positive effect and significantly increased the expression yield 5-35 fold for six out of the ten tested homologs (see **TABLE 2**). Furthermore, overexpression of the recombinant proteins did not lead to reduced growth and had thus no effect on cell viability. Mistic seems to chaperone the SEDS proteins into the membrane without passing through the cellular translocon machinery, avoiding thus saturation of the membrane protein biogenesis pathway.

We were expecting to obtain similar results when expressing the SEDS *in vitro* as this system is devoid of any hydrophobic environments, like the cellular membrane. Surprisingly, expression of the two tested homologs resulted in very weak expression which was even lower than the expression yields obtained for the His-tagged fusions in the *E. coli*- based system. In addition to this, expression of the SEDS in the cell-free system resulted also in degradation of the protein in both tested conditions. Even after several optimization steps we were not able to express the SEDS in sufficient amounts which could further be used for structural studies.

Taken together, these observations show that only fusion of Mistic to the SEDS led to high-level production of recombinant protein, overcoming therefore the first hurdle towards the structural characterization of these proteins. Mistic demonstrated great ability to cope with the usual problems caused by expressing high amounts of recombinant membrane proteins and offers thus an inexpensive and powerful system for the overexpression of foreign membrane proteins.

ACKNOWLEDGEMENTS

We would like to thank V. Job and M. Noirclerc-Savoye (Institut de Biologie Structurale (IBS), France) for cloning *S. pneumoniae rodA* in pLIM15 and *E. coli ftsW* in pIVEX2.4a and pIVEX2.3. This work used the platforms of the Grenoble Instruct centre (ISBG; UMS 3518 CNRS-CEA-UJF-EMBL) with support from FRISBI (ANR-10-INSB-05-02) and GRAL (ANR-10-LABX-49-01) within the Grenoble Partnership for Structural Biology (PSB). We thank Lionel Imbert for assistance and access to the Cell-free platform.

REFERENCES

Chowdhury, A., et al. (2012). "Mistic and TarCF as fusion protein partners for functional expression of the cannabinoid receptor 2 in *Escherichia coli*." Protein Expr Purif **83**(2): 128-134.

Dvir, H. and S. Choe (2009). "Bacterial expression of a eukaryotic membrane protein in fusion to various Mistic orthologs." Protein Expr Purif **68**(1): 28-33.

Holtje, J. V. (1998). "Growth of the stress-bearing and shape-maintaining murein sacculus of *Escherichia coli*." Microbiol Mol Biol Rev **62**(1): 181-203.

Ishihara, G., et al. (2005). "Expression of G protein coupled receptors in a cell-free translational system using detergents and thioredoxin-fusion vectors." Protein Expr Purif **41**(1): 27-37.

Kefala, G., et al. (2007). "Application of Mistic to improving the expression and membrane integration of histidine kinase receptors from *Escherichia coli*." J Struct Funct Genomics **8**(4): 167-172.

Klammt, C., et al. (2005). "Evaluation of detergents for the soluble expression of α-helical and β-barrel-type integral membrane proteins by a preparative scale individual cell-free expression system." FEBS J **272**(23): 6024-6038.

LaVallie, E. R., et al. (2000). "Thioredoxin as a fusion partner for production of soluble recombinant proteins in *Escherichia coli*." Methods Enzymol **326**: 322-340.

Miroux, B. and J. E. Walker (1996). "Over-production of proteins in *Escherichia coli*: mutant hosts that allow synthesis of some membrane proteins and globular proteins at high levels." J Mol Biol **260**(3): 289-298.

Mohammadi, T., et al. (2011). "Identification of FtsW as a transporter of lipid-linked cell wall precursors across the membrane." EMBO J **30**(8): 1425-1432.

Neophytou, I., et al. (2007). "Eukaryotic integral membrane protein expression utilizing the *Escherichia coli* glycerol-conducting channel protein (GlpF)." Appl Microbiol Biotechnol **77**(2): 375-381.

Noirclerc-Savoye, M., et al. (2010). "Large scale purification of linear plasmid DNA for efficient high throughput cloning." Biotechnol J **5**(9): 978-985.

Roosild, T. P., et al. (2005). "NMR structure of Mistic, a membrane-integrating protein for membrane protein expression." Science **307**(5713): 1317-1321.

Schlegel, S., et al. (2010). "Revolutionizing membrane protein overexpression in bacteria." Microb Biotechnol **3**(4): 403-411.

Sham, L. T., et al. (2014). "Bacterial cell wall. MurJ is the flippase of lipid-linked precursors for peptidoglycan biogenesis." Science **345**(6193): 220-222.

Therien, A. G., et al. (2002). "Expression and purification of two hydrophobic double-spanning membrane proteins derived from the cystic fibrosis transmembrane conductance regulator." Protein Expr Purif **25**(1): 81-86.

Tosi, T., et al. (2014). "Structural similarity of secretins from type II and type III secretion systems." Structure **22**(9): 1348-1355.

Wagner, S., et al. (2007). "Consequences of membrane protein overexpression in *Escherichia coli*." Mol Cell Proteomics **6**(9): 1527-1550.

Wagner, S., et al. (2006). "Rationalizing membrane protein overexpression." Trends Biotechnol **24**(8): 364-371.

Wuu, J. J. and J. R. Swartz (2008). "High yield cell-free production of integral membrane proteins without refolding or detergents." Biochim Biophys Acta **1778**(5): 1237-1250.

Xu, Y., et al. (2013). "Improved membrane protein expression in *Lactococcus lactis* by fusion to Mistic." Microbiology **159**(Pt 6): 1002-1009.

CHAPTER 4

Towards the biochemical characterization of bacterial flippases

This work contributed to the following article: **Violaine Lantez, Ioulia Nikolaidis, Mathias Rechenmann, Thierry Vernet and Marjolaine Noirclerc-Savoye**. Rapid automated detergent screening for solubilization and purification of membrane proteins and complexes. Engineering in Life Science **2015**; 15 (1): 39-50.

ABSTRACT

The major constituent of the bacterial cell wall is peptidoglycan. Its biosynthesis is a complex, multistep process that requires the concerted action of several enzymes. One key event is the translocation of Lipid II across the cytoplasmic membrane. This process is thought to be mediated by multi-spanning membrane proteins that are members of the well-known SEDS protein family. Structural determination of any Lipid II flippase will not only provide insight into this essential translocation process but also open up ways for the development of new antimicrobial agents. In **Chapter 3** we described the successful overexpression of several SEDS proteins, obtaining a high to moderate expression level. Here, we have not only studied the effect of several detergents to extract and stabilize *Streptococcus pneumoniae* RodA, *Escherichia coli* FtsW and *Thermatoga maritima* FtsW, but also purified one of these homologs and demonstrated the importance of the solubilizing detergent in retaining the protein in a homogeneous and functionally active state. These studies provide therefore important biochemical details that are essential for the structural characterization of the Lipid II flippase.

INTRODUCTION

The peptidoglycan is a three-dimensional, cross-linked mesh, which is formed by linear glycan chains composed of alternating *N*-acetyl muramic acid (Mur*N*Ac) and *N*-acetyl glucosamine (Glc*N*Ac) units cross-linked by pentapeptidic chains. Its synthesis is initiated in the bacterial cytosol through the concerted action of six Mur enzymes (MurA to MurF) acting in a catalytic cascade, the integral membrane protein MraY and in the end the membrane associated glycosyltransferase MurG (Macheboeuf, Contreras-Martel et al. 2006). The resulting Lipid II is then 'flipped' to the outside of the bacterial membrane, where it is acted upon by PBPs which polymerize glycan chains and cross-link peptides (Vollmer, Blanot et al. 2008). The translocation of the amphipathic Lipid II across the cytoplasmic membrane is a key step in bacterial cell wall synthesis, but poorly understood. Recently Mohammadi and co-authors provided evidence that *Escherichia coli* FtsW functions as a specific transporter (flippase) for Lipid II. FtsW was capable to actively transport Lipid II across model and bacterial membranes, whereas other putative transporters, like

MurJ, did not show any 'flipping' activity (Mohammadi, van Dam et al. 2011). FtsW is a member of the well-conserved SEDS protein family, including also homologs RodA and SpoVE (Ikeda, Sato et al. 1989, Henriques, Glaser et al. 1998). These intergral membrane proteins harbour eight to ten separate membrane-spanning segments and are essential for cell wall growth during division, elongation and spore cortex formation, respectively (Ishino, Park et al. 1986, Joris, Dive et al. 1990, Boyle, Khattar et al. 1997, Khattar, Addinall et al. 1997, Holtje 1998). Conserved residues are mainly found in extracellular loops, whereas specific residues in the fourth transmembrane domain are essential for transport activity (Mohammadi, Sijbrandi et al. 2014).

However, despite its crucial role in the synthesis of peptidoglycan, the information about how the translocation process occurs is limited and requires further understanding. Determination of its three-dimensional structure will be therefore an essential tool towards understanding the function and mechanism of Lipid II transport on molecular level. Nevertheless, to achieve this goal several hurdles associated with the amphipathic nature of membrane proteins have still to be overcome.

The primary difficulty in the study of membrane proteins is to obtain high yields of the protein of interest (Grisshammer and Tate 1995, Seddon, Curnow et al. 2004). As most membrane proteins in their native environment are usually present at minute levels, it is not possible to extract adequate amounts from natural sources, requiring thus the expression of the membrane protein in recombinant systems (Tate 2001). This approach encounters several limitations, including inadequate membrane volume for the accommodation of the overexpressed protein and saturation of the translocation machinery (Miroux and Walker 1996, Wagner, Bader et al. 2006).

Once conditions are found that provide sufficient quantities of protein, the second difficulty is to isolate and purify the heterologously expressed protein from the lipid bilayer in a stable and functionally active form. However, as membrane proteins are composed mainly of highly hydrophobic membrane-spanning domains, extraction from the bilayer can cause aggregation or denaturation of the protein upon exposure to the aqueous environment. A pivotal role in the study of membrane proteins is played therefore by detergents, amphipathic molecules that have the ability to shield the hydrophobic surfaces of the protein by mimicking its native lipidic environment, while at the same time disrupting the membrane (Seddon, Curnow et al. 2004, Carpenter, Beis et al. 2008). Generally, solubilization of a

membrane protein requires high detergent concentrations (> critical micelle concentration (CMC) of the detergent used) to be able to disrupt the bilayer, resulting in the release of **P**rotein-**D**etergent **C**omplexes (PDC) (Prive 2007). As no 'universal' detergent is ideally suited for each membrane protein, a panel of detergents has to be screened for their ability to extract the protein. The choice of detergent is one of the most crucial decisions that must be made when designing a new purification protoctol for a membrane protein (Prive 2007, Carpenter, Beis et al. 2008). The ideal detergent should lead to successful recovery of soluble, homogeneous, stable and functional active protein (Carpenter, Beis et al. 2008).

Once this is achieved, the third and final drawback towards the atomic structure of a membrane protein is the ability to generate diffraction-quality crystals. The difficulty in crystallizing membrane proteins is due to the nature of the membrane protein itself as it contains amphipathic surfaces that are generally embedded in the bilayer (Caffrey 2003). However, upon addition of detergents the protein's native environment becomes destabilized, resulting in the release of PDCs. In this PDC the protein is surrounded by a flexible and dynamic detergent belt which not only serves as a shield that protects the hydrophobic transmembrane segments, but due to its nature also prevents the formation of well-ordered lattices (Prive 2007). To date several techniques exist to crystallize membrane proteins, but it is beyond the scope of the current chapter and will be discussed further on (**Chapter 5)**.

In a previous study (**Chapter 3**) we described the successful overexpression of several SEDS proteins in fusion to Mistic, a nonglobular membrane-associated protein recently identified in *Bacillus subtilis* (Roosild, Greenwald et al. 2005). Fusion of Mistic led to high production of recombinant homologs *Streptococcus pneumoniae* RodA (SpRodA), *E. coli* FtsW (EcFtsW) and *Thermatoga maritima* FtsW (TmFtsW), yielding expression levels of 5 to 15 mg of protein/L of culture.

In this report we describe the efficient solubilization of SpRodA, TmFtsW and EcFtsW from the *E. coli* membrane and the identification of detergents that have the ability to maintain the SEDS in a soluble and stable state after extraction and removal of the fusion tag. In addtion, we successfully purified high yields of functional and homogeneous SpRodA and demostrated that the choice of detergent used for the solubilization of the protein has a great impact on the stability and the activity of the protein.

MATERIALS AND METHODS

Detergents

All detergents used in this study were purchased from Affymetrix. Concentrations used for the solubilization and/or detergent exchange screenings are listed in **TABLE 1**.

Protein expression and solubilization

Expression plasmids coding for SpRodA, TmFtsW or EcFtsW in fusion with Mistic (see **Chapter 3**) were used to transform either *E. coli* BL21 (DE3) C41 or STAR (Invitrogen) competent cells. Cultures containing 1 L of TB medium were inoculated with a 1/40th dilution of overnight pre-cultures and expression of the recombinant membrane proteins was induced with 0.5 mM IPTG at an OD_{600nm} of 1 A.U. After further growth at 37°C for 3 hours, cells were collected by centrifugation (6.000 rpm, 20 min, 4°C) and resuspended in Buffer A (50 mM Tris pH 8, 200 mM NaCl, 10 % Glycerol) containing 1 mM protease inhibitors (phenylmethanesulphoylfluoride (PMSF), Aprotinin, Pepstatin and Leupeptin; Euromedex) and 200 µg/ml lysozyme (Fluka). Cell lysis was carried out by passing the sample six times through a pre-cooled cell disruptor (Constant Cell Disruption Systems) at 6.000 psi. After clarification by centrifugation (10.000 rpm, 10 min, 4°C), the membrane fraction was collected by ultracentrifugation (40.000 rpm, 60 min, 4°C). The membranes were afterwards resuspended in Buffer A and if necessary diluted to a final OD_{600nm} of 1 A.U. (parameter that enabled good detergent:protein ratios for subsequent solubilization). Membranes were solubilized by six different detergents at concentrations indicated in **TABLE 1.1** and incubated under gentle rotation for 60 min at 4°C. Non-solubilized material was removed by ultracentrifugation (40.000 rpm, 60 min, 4°C). Total and solubilized membranes (aliquots of 10 µl each) were separated by SDS-PAGE and visualized by Coomassie-blue staining.

Small-scale detergent exchange screening

All following automated steps were performed on a liquid Microlab STAR robot (Hamilton) controlled by the Venus software. Hereafter, we describe a detergent exchange protocol performed only for SEDS proteins solubilized in LAPAO.
Solubilized membranes were incubated with 2 ml of pre-equilibrated (Buffer A containing 0.5% LAPAO) Ni-NTA resin (Qiagen).
The following steps were performed by M. Noirclerc-Savoye (Institut de Biologie Structurale (IBS), Partnership for Structural Biology (PSB), France).
Subsequently, we dispensed 50 µl of this resin in each well of a Chromafil Multi 96 0.2 µM filter plate (Macherey Nagel) previously sealed with a silicon mat for 384 well PCR micro plate (Grosseron). The following wash and elution steps were performed by gravity flow. Each well was washed twice with 20 column volumes of Buffer B (Buffer A + detergents at concentrations corresponding to 2x or 5x their CMC (see **TABLE 1.2**)) supplemented with 50 mM imidazole. Elution of the proteins was achieved by incubation for 5 min with 100 µl Buffer B containing 300 mM imidazole and subsequent filtration for 2 s. The eluted proteins were collected in a 0.5 ml 96-well plate and analyzed by SDS-PAGE using XT-Criterion 26 well plates (Bio-Rad). Purified proteins were visualized by Coomassie-blue staining.

TABLE 1. List of all detergents used in this study

1. Solubilization

DETERGENT	CMC* mM (%)	CMC* %
FOS-choline 12 (FOS12)	1.5 (0.05)	1
n-Dodecyl-*β*-D-Maltopyranoside (DDM)	0.17 (0.009)	1
n-Octyl-*β*-D-Glucopyranoside (β-OG)	18 (0.53)	2
polyoxyethylene octyl phenyl ether (Triton X-100)	0.24 (0.016)	1
3-Laurylamido-N,N'-Dimethylpropyl Amine Oxide (LAPAO)	1.56 (0.052)	1
Sodium Lauroyl Sarcosine (Sarcosine)	14.4 (0.42)	1

2. Detergent exchange

DETERGENT	CMC* mM (%)	low / high CMC* mM
n-Dodecyl-*β*-D-Maltopyranoside (DDM)	0.17 (0.009)	0.34 / 0.85
n-Decyl-*β*-D-Maltopyranoside (DM)	1.8 (0.09)	3.6 / 9
n-Nonyl-*β*-D-Maltopyranoside (NM)	6 (0.28)	12 / 30
Decyl Maltose Neopentyl Glycol (DMNG)	0.036 (0.0034)	0.072 / 0.18
Lauryl Maltose Neopentyl Glycol (LMNG)	0.01 (0.001)	0.02 / 0.05
n-Octyl-*β*-D-Glucopyranoside (β-OG)	18 (0.53)	36 / 90
n-Tetradeyl-N,N-Dimethyl-3-Ammonio-1-Propanesulfonate (Anzergent 3-14)	0.16 (0.0056)	0.32 / 0.8
3-Laurylamido-N,N'-Dimethylpropyl Amine Oxide (LAPAO)	1.56 (0.052)	3.12/ 7.8
Tetraethylene Glycol Monooctyl Ether (C_8E_4)	8 (0.25)	16 / 40
Hexaethylene Glycol Monooctyl Ether (C_8E_6)	10 (0.39)	20 / 50
Octaethylene Glycol Monododecyl Ether ($C_{12}E_8$)	0.09 (0.005)	0.18 / 0.45
Polyoxythylene (9) Glycol Dodecyl Ether ($C_{12}E_9$)	0.05 (0.003)	0.1 / 0.25

* Approximate CMC in water at 20°C.

Cleavage of Mistic

In order to remove Mistic from purified SEDS proteins, a number of variables, such as the amount of TEV, temperature of incubation as well as time required for complete cleavage, were examined in a series of cleavage tests. All tested conditions were performed in the presence of Ethylenediaminetetraacetic acid (EDTA) and Dithiothreitol (DTT) to a final concentration of 0.5 and 1 mM, respectively. TEV protease (produced in-house, 30 kDa) was added to the reaction mixture at a protease to target protein ratio of 1 μg TEV protease to 4, 3 or 2 μg of target protein. Samples were afterwards incubated either for up to 4 h at room temperature (RT) or overnight at RT and 4°C. Aliquots of 10 μl were removed at 1, 2, 3 and 4 h as well as

after overnight incubation. Reactions were stopped by adding PMSF to the solution to a final concentration of 1 mM. Samples were afterwards separated by SDS-PAGE and cleavage efficiency was determined by comparing the uncleaved protein with the amount of remaining and/or cleaved product after incubation with the TEV protease.

Activity assay

Flippase activity assays were performed by T. Mohammadi in the E. Breukink Laboratory (University Utrecht, The Netherlands).
To assess the capability of SpRodA to actively transport Lipid II across model membranes we used a dithionite reduction assay as described previously (Mohammadi, van Dam et al. 2011). Briefly, the protein was reconstituted in large unilamellar vesicles (LUVs) containing fluorescently (NBD) labeled Lipid II by adding purified protein to solubilized LUVs in a 1:20.000 protein/phospholipid molar ratio. After gentle agitation for 1 h at 4°C, samples were incubated three times with a fresh 100 mg/ml Bio-Beads suspension (Bio-Rad) to remove the detergent. Vesicles were collected afterwards by subsequent ultracentrifugation (435.000 g for 30 min, 4°C) and resuspension in 10 mM HEPES-KOH pH 8, 100 mM NaCl, 5 mM KCl and 1 mM $MgSO_4$. The ability of RodA to translocate NBD-Lipid II from the inner to the outer leaflet of the LUVs was determined by calculating the percentage of NBD fluorescence remaining at the inner face of the LUVs and therefore not accessible for reduction by dithionite.

Preparative protein purification

SpRodA was expressed and membrane fractions were isolated as described above (**Protein expression and solubilization**). Subsequently, membranes were solubilized using the appropriate detergents as determined by the solubilization test and incubated further under gentle agitation for 60 min at 4°C. Non-solubilized material was removed by ultracentrifugation for 60 min at 40.000 rpm, 4°C.

Immobilized metal affinity chromatography (IMAC)

Solubilized membranes were incubated with pre-equilibrated (Buffer A + 50% of the detergent used for solubilization) Ni-NTA resin (3.5 ml for 100 ml of solubilized membranes). After gentle agitation overnight at 4°C, the Ni-NTA resin was packed in open Poly-Prep gravity-flow columns (Bio-Rad) and unbound proteins were removed by washing with 20 bed volumes of Buffer A containing 3.6 mM DM (Buffer C). Thereafter, the Ni-NTA resin was further washed with 10 bed volumes of Buffer C supplemented with 50 mM imidazole. Proteins were eluted by addition of 5 bed volumes of Buffer C containing 500 mM imidazole. After analysis of each IMAC purification step by SDS-PAGE, target protein containing fractions were transferred to a dialysis bag (molecular-weight cutoff (MWCO) 14 kDa). Dialysis was performed against Buffer C for 2 h at 4°C.

TEV cleavage

To remove Mistic from the target protein, we added TEV protease at a protease to target protein ratio of 1 µg TEV protease to 2 µg of target protein as determined by the cleavage test. The reaction was performed in the presence of 0.5 mM EDTA and 1 mM DTT for 3 h at RT and afterwards stopped by the addition of PMSF to a final concentration of 1 mM. After determination of successful cleavage of Mistic by SDS-PAGE, the TEV protease and Mistic were removed from the sample by further downstream applications.

Removal of Mistic and TEV

Subsequently, the cleaved protein was dialyzed against 25 mM Tris pH 8.5, 20 mM NaCl, 5% glycerol and 3.6 mM DM (Buffer D) for 2 h at 4°C. After dialysis, the sample was loaded onto a 1 ml HiTrap SP HP column (GE Healthcare) and washed with 25 bed volumes of Buffer D. Cleaved target protein was eluted by a linear gradient (20-30 bed volumes) of NaCl. Small aliquots from the flow through and elution steps were analyzed on SDS-PAGE.

Analytical Gel filtration

Fractions containing mostly pure protein were pooled and concentrated to 1 ml using Vivaspin 20 (MWCO 50 kDa) sample concentrator. Protein homogeneity was determined by loading the sample onto a Superdex 200 5/150 GL (GE Healthcare) using the ÄKTA FPLC chromatography system. Size exclusion chromatography was performed in Buffer D.

RESULTS

Studying membrane proteins has proven to be a challenging task due to their partially amphipathic nature and low natural abundance. Overexpression is therefore a necessity for most membrane proteins, but leads frequently to toxicity to the host. Finding suitable conditions for the overexpression of a particular membrane protein is therefore a prerequisite and requires extensive screening.

In a previous study (see **Chapter 3**) we demonstrated that fusion of Mistic to the N-terminus of several SEDS proteins allowed high-level production of the target proteins without disturbing the balance of the host. However, for further characterization of the protein, it is necessary to carefully remove the protein in its native form from the lipid bilayer. This is most effectively accomplished by using detergents. These amphipathic molecules contain both, a polar head group and a long hydrophobic carbon chain, forming above their CMC thermodynamically stable aggregates, also known as micelles. Extraction of the protein from the lipid bilayer requires generally an excess of detergent leading to dissolution of the membrane and incorporation of the protein into PDCs. To date a large number of detergents exist that are commercial available, but unfortunately no 'universal' detergent is ideally suited to solubilize all membrane proteins and has thus to be determined empirically. As a result, the choice of detergent is absolutely crucial for successful purification and stabilization of a given membrane protein.

We tested therefore several detergents for their ability to efficiently extract SEDS proteins from the lipid bilayer, performed an extensive detergent exchange screen to identify stabilizing detergents and carried out analyses on the solubilizing detergents capable of preserving protein function.

Solubilization tests

To investigate the efficiency of various detergents for the extraction of SpRodA and EcFtsW and TmFtsW, six detergents with different chemical properties were selected. These detergents (**TABLE 1.1**) include nonionic detergents, such as β-OG, DDM and Triton-X100, which are 'mild' detergents less likely to denature the protein, as well as some zwitterionic and anionic detergents like FOS12, LAPAO and Sarcosine, which are considered to be more harsh than nonionic detergents as they tend to destabilize the protein due to their charged character (Prive 2007). The detergent concentrations used for solubilization was for the majority of the detergents 1%, except for β-OG, a detergent with higher CMC, where 2% was used. Solubilization of the three tested SEDS proteins was performed simultaneously. Membrane dissolution could be detected directly by simple visual assessment of the turbidity of the solution. Addition of Sarcosine, LAPAO as well as FOS12 resulted already after short incubation with the detergent to an immediate decrease in sample turbidity associated with the transition from an intact membrane structure to dissolution of the membrane and formation of PDCs. The successful solubilization by these detergents was also assessed by SDS-PAGE (**Fig. 1**). The average solubilization efficiency was determined by scanning the Coomassie-stained gels and quantifying protein band intensities using the ImageJ software package (Schneider, Rasband et al. 2012). An intensity of 100% corresponds to total membranes. Among the six tested detergents, LAPAO was the most effective in extracting SEDS proteins from the lipid bilayer, resulting in solubilization efficiencies of about 95%. FOS12 and Sarcosine showed also high solubilization efficiencies of 85 to 90%, respectively.

DDM, Triton X-100 and β-OG showed on the contrary none or low capability of isolation, only 2-10% of the total protein could be solubilized using these detergents. We can conclude therefore that nonionic detergents were not very efficient, detergents with zwitterionic or anionic properties, such as LAPAO, FOS12 and Sarcosine, however, demonstrated excellent capabilities in solubilizing all three tested SEDS proteins. Sarcosine is known to effectively disrupt the cytoplasmic membrane of *E. coli* selectively (Filip, Fletcher et al. 1973), demonstrating thus high extraction efficiencies at very low CMC (~ 2.4 x CMC). Since zwitterionic detergents are known to be more effective in the solubilization of membrane proteins than nonionic detergents, it was also not surprising that this class of detergents showed

high solubilization efficiencies compared to nonionic detergents (le Maire, Champeil et al. 2000).

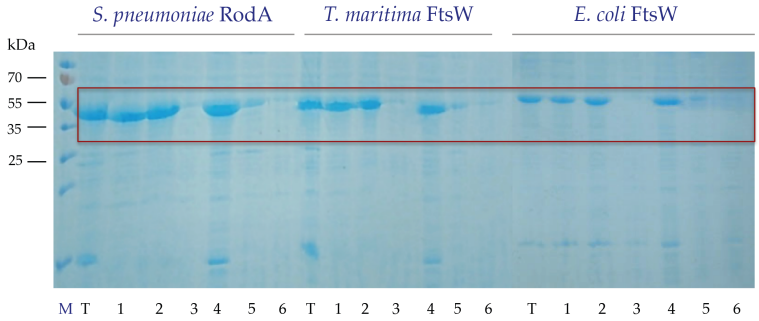

Fig. 1: Solubilization of SEDS proteins. Six detergents were systematically screened for their ability to solubilize SpRodA, TmFtsW and EcFtsW. The recombinant proteins (red rectangle) were solubilized for 1 hour with six different detergents. Abbreviations: T, total membrane protein; 1, FOS12; 2, Sarcosine; 3, Triton X-100; 4, LAPAO; 5, DDM; 6, β-OG; M, marker.

However, somehow unexpectedly, that DDM and β-OG showed very low solubilization efficiencies given their success in the structural characterization of several membrane proteins (Raman, Cherezov et al. 2006). A possible explanation for the poor solubilization with β-OG could be due to the relatively small micelle size of the detergent (~ 8-29 kDa), possibly not sufficient enough to protect the highly sensitive hydrophobic surface of the transmembrane segments.

Systematic detergent exchange screening

Solubilization of membrane proteins is generally achieved with an excess of detergent, as described for the tested SEDS proteins. This excess cannot only interfere with subsequent purification steps but also affect stability of the extracted protein. Therefore, following the identification of efficient detergents for the solubilization of SpRodA, EcFtsW and TmFtsW, we performed a second screen aimed at identifying detergents compatible with the stability of the protein and subsequent purification and crystallization. Detergent exchange was performed on membranes previously solubilized in 1% LAPAO as it was the most effective detergent for extraction of all

the three tested SEDS proteins. Solubilized membranes were incubated with Ni-NTA resin, washed extensively with 12 different detergents at two concentrations each and afterwards eluted in buffer containing the new detergent. As a positive control, LAPAO (the initial solubilizing detergent) was used during the purification. The imidazole-eluted samples were subsequently analyzed by SDS-PAGE and the amount of eluted protein was assessed by comparing protein band intensities to the positive control (**Fig. 2**). As the only parameters varying across the 24 conditions tested were the nature and concentration of the detergent, the presence of the His-tagged protein in the elution fraction was interpreted as evidence of protein stability and successful detergent exchange, whereas incompatible detergents caused protein precipitation on the resin and thus absence of the protein in the eluted fractions. With this approach we were able to identify detergents that were capable to exchange LAPAO and maintain the solubility of the tested SEDS proteins.

For SpRodA and TmFtsW protein recoveries were approximately 90-100% for detergents of the maltopyranoside family (DDM, DM and NM) as well as the zwitterionic detergent Anzergent 3-14, showing no detergent concentration dependency (see **Fig. 2** (A) and (B)). Also detergents of the maltose neopentyl glycol (MNG) family, like DMNG and LMNG, were able to maintain SpRodA and TmFtsW in a soluble state, resulting in protein recoveries of 50-100%, respectively (see **Fig. 2** (A) and (B)). Exchange of LAPAO for these six detergents showed no detergent concentration dependency, protein recoveries were for both tested detergent concentrations identical.

A similar result was observed for EcFtsW, whereas here protein recovery was affected by the amount of detergent used, for detergents DM and LMNG higher concentrations of detergent led to increased protein recovery (see **Fig. 2** (C)). In contrast, SpRodA, TmFtsW and EcFtsW showed heavy aggregation upon detergent exchange in alkyl PEGs, such as C_8E_4, C_8E_6, $C_{12}E_8$ and $C_{12}E_9$, as well as β-OG, resulting thus just in poor protein recoveries of 0-10% (see **Fig. 2** (A)-(C)). Detergent exchange of the three tested SEDS proteins showed therefore a similar profile, six out of the twelve tested detergents were capable in maintaining the proteins in soluble and stable form. Five of these detergents were sugar-based detergents of the maltopyranoside (NM, DM and DDM) and MNG family (LMNG and DMNG). Whereas each of these detergents contains various chain lengths, the head group is similar (maltose). This may indicate that the head group of the detergent has a great impact on the stability of the SEDS proteins.

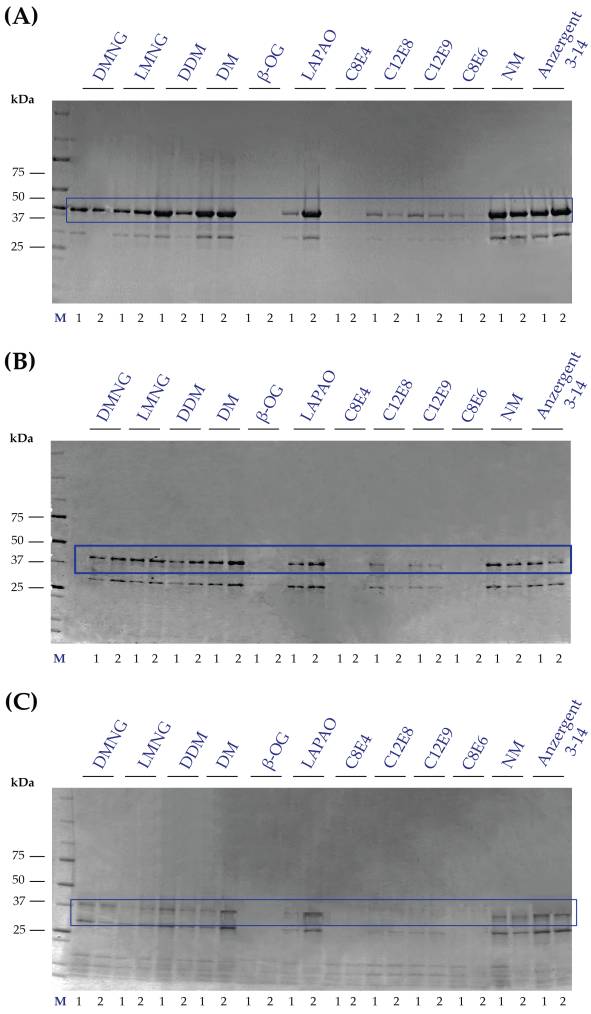

Fig. 2: Detergent exchange screening of SEDS proteins. **(A)** SpRodA, **(B)** TmFtsW and **(C)** EcFtsW were extensively washed with 12 different detergents at two concentrations each (see TABLE 1). Elution of the SEDS proteins (blue rectangle) from the Ni-NTA resin indicates successful detergent exchange. Proteins in high concentrations of DDM were diluted due to elution of the protein in 2x elution buffer. Each elution fraction indicated also contamination with SlyD (red arrow; identified by N-terminal sequencing), an *E. coli* protein that is known to have a high affinity for Ni-ions (Hottenrott, Schumann et al. 1997). Abbreviations: 1, 2 x CMC; 2, 5 x CMC; M, marker.

Maltoside-based detergents have been shown to be more effective in preserving the native structure of membrane proteins due to their mild properties in terms of protein aggregation and denaturation (Prive 2007). It is therefore not surprising that maltoside-based detergents show enhanced capabilities in stabilizing the SEDS proteins. Consequently, these detergents are to date the most successful detergents in the crystallization of several α-helical membrane proteins (Newstead, Ferrandon et al. 2008).

Cleavage of Mistic

After identification of a profile of the resilience of the SEDS proteins with respect to different detergents, we investigated in a further step if these detergents have the ability to maintain the proteins in stable form even after removal of Mistic. We therefore continued to perform TEV cleavage tests using the best behaving SEDS protein, SpRodA. This test was conducted on SpRodA purified in low concentrations of DM (**TABLE 1**). SpRodA was incubated at different protein to protease ratios for several hours at RT and overnight at 4°C. Cleavage efficiency was analyzed subsequently by SDS-PAGE (**Fig. 3**).

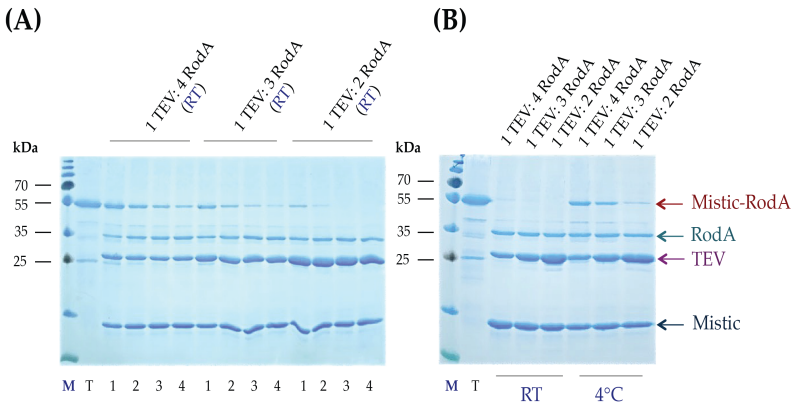

Fig. 3: TEV cleavage of SpRodA. The protein was incubated with three different protein/protease ratios **(A)** for up to 4 hours at room temperature (RT) or **(B)** overnight at RT and 4°C. Abbreviations: T, total protein; 1, 2, 3, 4, hours of incubation with TEV; RT, room temperature; M, marker.

For protein/protease ratios of 2:1, total cleavage of Mistic could be already observed after 3 hours of incubation at RT (**Fig. 3** (A)), whereas higher protein concentrations led only after overnight incubation to complete removal of Mistic (**Fig. 3** (B)). Cleavage at 4°C on the other hand showed low efficiency, for all tested protein/protease ratios approximately 5-20% of 'misticated' SpRodA was still uncleaved (see **Fig. 3** (B)).

We therefore concluded that cleavage at a protein/protease ratio of 2:1 for three hours at RT was the most efficient condition for complete removal of Mistic and was therefore chosen further to perform TEV cleavage on SpRodA and TmFtsW in the five nonionic detergents NM, DM, DDM, LMNG and DMNG as well as the zwitterionic detergents Anzergent 3-14 and LAPAO. EcFtsW was not included in this screen due to the very low recovery of the protein, resulting in difficult visualization of cleaved protein. Cleavage of SpRodA and TmFtsW was carried out therefore at the previously identified conditions and cleavage success was analyzed by comparing total protein with cleaved protein on a Coomassie-stained SDS-PAGE (**Fig. 4**).
Comparison of cleavage efficiencies and stability of the 'non-misticated' proteins, showed an identical profile for SpRodA and TmFtsW. Both proteins showed upon removal of Mistic a dramatic decrease of stability in zwitterionic detergents LAPAO and Anzergent 3-14, leading already after 2 hours of incubation with the protease to heavy precipitation of the sample. This was not completely surprising, since the charged character of zwitterionic detergents is not ideally suited for the stabilization of relatively fragile membrane proteins (Prive 2007).

This effect could not be observed in the presence of nonionic detergents. Cleavage of the two tested SEDS proteins in DMNG as well as in the two maltopyranoside detergents DDM and DM resulted in total tag removal already after 1-2 hours, whereas for NM and LMNG we identified residual fusion protein even after 3 hours, resulting in cleavage efficiencies of 80-90% (see **Fig. 4**). However, removal of Mistic in these detergents had no significant effect on the stability of the cleaved proteins, even after a period of one week at 4°C we could not observe any precipitation. Therefore, taking into consideration protein stability, cleavage efficiency and lack of protein aggregation of the cleaved product, we concluded that tag removal of SpRodA and TmFtsW in DDM and DM was more efficient and led to better results than the other tested detergents. These maltopyranoside detergents allowed us to obtain sufficient amounts of cleaved and stable protein at low incubation times.

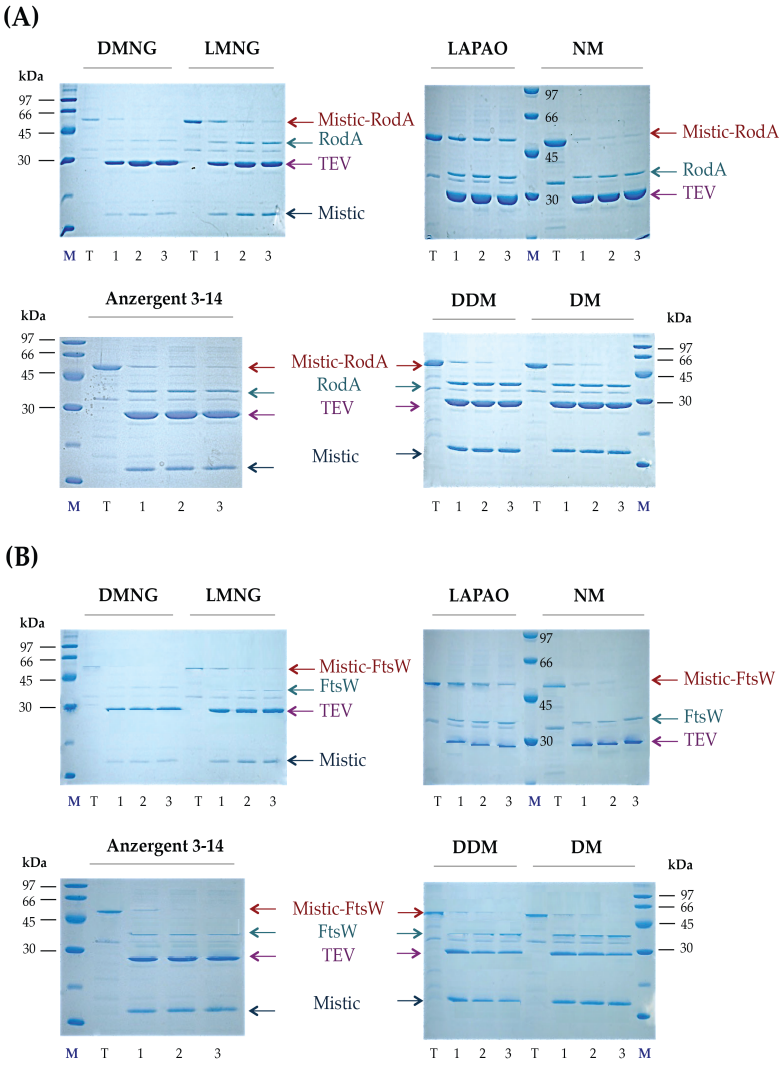

Fig. 4: TEV cleavage of SEDS proteins in different detergents. Cleavage of **(A)** SpRodA and **(B)** TmFtsW was performed at a protein/protease ratio of 2:1 for up to 3 hours at room temperature (RT). Cleavage efficiency was distinguished by comparing total protein with small aliquots from each time point. Abbreviations: T, total protein; 1, 2, 3, hours of incubation with TEV; M, marker.

These results indicated therefore that TmFtsW and SpRodA were upon removal of Mistic highly unstable in the presence of zwitterionic detergents leading to denaturation of the cleaved proteins. Maltoside-based detergents, however, did not affect stability of the cleaved proteins, suggesting that the mild properties of these detergents were more effective at inhibiting protein denaturation.

Purification of SpRodA in different detergents

Once we tested the ability of different detergents to extract the three tested SEDS proteins from the lipid bilayer and performed extensive detergent exchange screenings to identifiy detergents more suitable for maintaining the solubility and stability of the proteins, we continued with further purification steps. As structural studies require milligrams of pure, stable and homogeneous protein, we chose to proceed with the purification of a single candidate, SpRodA, as this SEDS protein was previously shown to yield high levels of overexpressed protein (see **Chapter 3**), solubility efficiencies of 85-95% (FOS12, Sarcosine and LAPAO) and stability in a panel of detergents (DMNG, LMNG, NM, DM and DDM). The purification pipeline included solubilization of SpRodA in detergents that demonstrated high efficiencies in extraction from the membrane (LAPAO, FOS12 and Sarcosine), followed by subsequent IMAC, cleavage of Mistic, ion-exchange chromatography to remove uncleaved protein, and finally size-exclusion chromatography (SEC) to determine homogeneity of the sample. The detergent of choice for the entire purification was DM, which not only has the ability to stabilize SpRodA +/- Mistic but also forms smaller micelles than DDM (DM ~ 22 kDa, DDM ~ 72 kDa). For downstream crystallization trials small micelles are advantageous as they do not exceed the molecular weight of SpRodA (+ Mistic ~ 61.5 kDa, - Mistic ~ 46 kDa) and have therefore the ability to enhance the likelihood of hydrophilic crystal contacts.

Solubilization of SpRodA in either LAPAO, FOS12 or Sarcosine and subsequent detergent exchange against DM by IMAC led to recoveries of 80% of pure protein for each of the tested detergents (**Fig. 5** (A)). Quantification of protein concentrations by NanoDrop resulted in total protein concentrations of 8, 7 and 6.5 mg for SpRodA solubilized in LAPAO, FOS12 and Sarcosine, respectively. Removal of Mistic was afterwards performed at conditions previously described in this study. Following cleavage, a reverse-IMAC chromatography was perfomed to separate cleaved SpRodA from the TEV protease and Mistic (both contain N-terminal

His-tags). Unfortunately, this approach failed since SpRodA bound unspecifically to the Ni-NTA resin, preventing therefore separation of the proteins (data not shown).

Another valuable and powerful technique that enables the separation of macromolecules relies on the difference between the net surface charge of the protein at a given pH. As the predicted pI of cleaved SpRodA is very basic (~ 9.67), we chose buffer conditions in which SpRodA specifically binds to a cation exchanger, whereas TEV and Mistic were retained in the flow through (see **Fig. 5** (B)). With this approach we were able to successfully separate SpRodA from TEV and Mistic, and we did not identify any residual contaminations of these proteins in the elution fractions (**Fig. 5** (B)). Whereas samples previously solubilized in FOS12 showed very pure SpRodA, solubilization in LAPAO and Sarcosine led to the co-purification of a contaminant at ~ 20 kDa, but fortunately not at a significant quantity (see **Fig. 5** (B)).

To further determine the homogeneity of the samples solubilized in the three different detergents, we performed SEC analysis to rapidly evaluate the quality of purified SpRodA (**Fig. 5** (C)). As the mobile phase was for all three samples identical, the presence of a single, well-defined peak indicated correctly folded and homogeneous SpRodA in the different detergents used for solubilization. Due to the presence of detergents binding to the membrane protein, the apparent molecular weight in gel filtration can be bigger and will have likely a shorter retention time relative to a molecular weight standard of the same mass. However, comparison of the elution peaks of SpRodA solubilized either in LAPAO, FOS12 and Sarcosine, showed clearly an effect of the solubilizing detergent on the stability of SpRodA. SEC analysis of SpRodA solubilized in LAPAO showed monodispersity judged from the appearance of a single peak in gel filtration (see **Fig. 5** (C)). The retention time was slightly shorter when compared to Ovalbumin (45 kDa), a molecular weight standard of approximately the same mass of SpRodA. This effect is probably due to DM micelles (~ 22 kDa) bound to SpRodA, resulting in PDCs of ~67 kDa.

On the other hand, we observed stability issues of SpRodA when solubilized in FOS12 and Sarcosine. The retention time of SpRodA solubilized in FOS12 was very short, resulting in elution of a broad peak shortly after the void volume (1.1 ml).

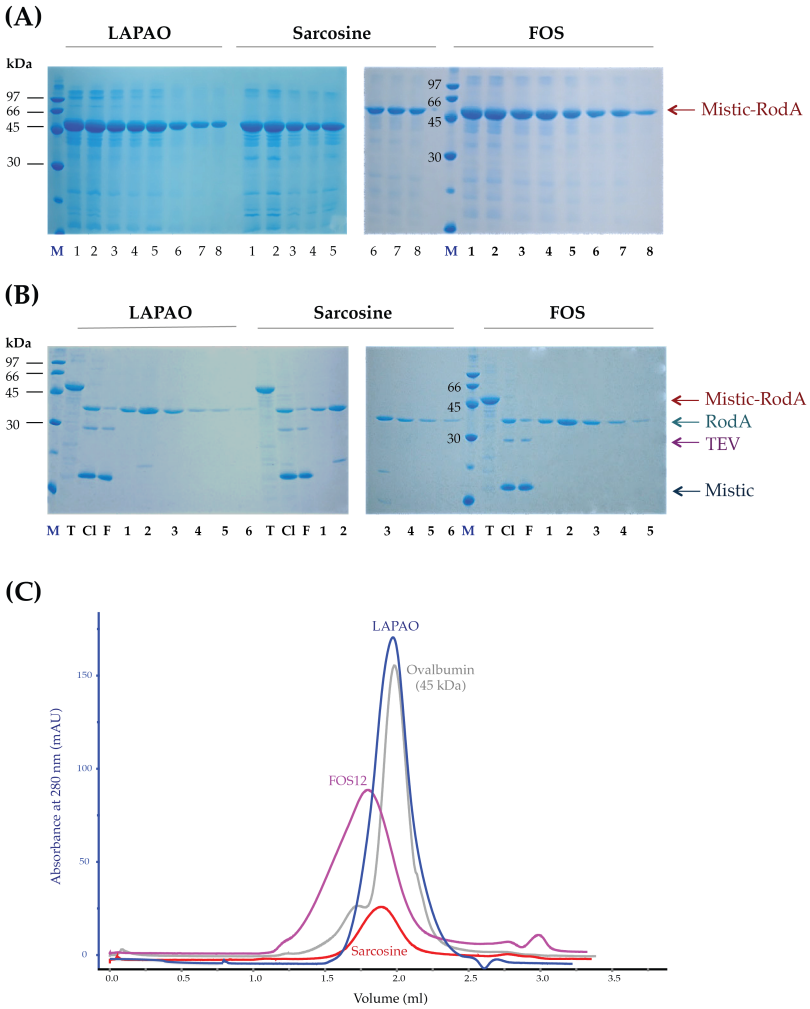

Fig. 5: Purification of SpRodA. Solubilization of SpRodA was performed either in LAPAO, FOS12 or Sarcosine. Detergent exchange against DM was achieved by **(A)** IMAC purification. Following cleavage of Mistic, SpRodA was further purified using **(B)** cation-exchange chromatography. Homogeneity of the samples was analyzed by **(C)** gel filtration. Abbreviations: T, total protein; Cl, cleaved protein; F, flow through; M, marker.

Over time this peak may have shifted completely to the void volume and, either way, indicated that SpRodA was prone to aggregation when solubilized in FOS12. This observation was not completely surprising, since Fos-choline detergents were reported to have the ability to extract and stabilize misfolded proteins (Leviatan, Sawada et al. 2010). Solubilization of SpRodA in Sarcosine led also to heavy aggregation; SEC analysis demonstrated a dramatic loss of protein, peak size was 7-fold decreased compared to SpRodA solubilized in LAPAO (see **Fig. 5** (C)). Since Sarcosine is known to be a very harsh detergent that tends to completely dissolute the inner membrane, it probably denatured the protein upon extraction from the membrane.

We concluded therefore, that solubilization of SpRodA in FOS12 or Sarcosine is not compatible with the correct fold of the protein, judged by the aggregation of SpRodA in these detergent, whereas LAPAO extracted SpRodA showed a monodisperse peak, indicating a well-folded and homogeneous protein sample.

LAPAO extracted SpRodA is active

The following experiments were performed by T. Mohammadi (University Utrecht, The Netherlands). To investigate whether the solubilizing detergent had an effect on the activity of SpRodA, we reconstituted 'misticated' as well as cleaved SpRodA into LUVs containing NBD-Lipid II. Vesicles containing no protein, *Streptomyces lividans* KcsA or *E. coli* FtsW were used as negative and positive controls, respectively, as reported previously by Mohammadi and colleagues (Mohammadi, van Dam et al. 2011).

After reconstitution of all proteins into vesicles, samples were assessed for their transport activity using the dithionite reduction assay. Comparison of 'misticated' SpRodA in all three detergents as well as cleaved SpRodA solubilized in FOS12 and Sarcosine showed no significant difference in the percentage of reduction of fluorescence upon addition of dithionite compared to empty vesicles and LUVs reconstituted with KcsA, and therefore suggesting no transbilayer movement of NBD-Lipid II (see **Fig. 6** (A)). Proteoliposomes containing cleaved SpRodA solubilized in LAPAO, however, showed a greater extent in fluorescence reduction (~ 70-75%) than for protein-free liposomes (~ 50%). This indicated that SpRodA solubilized with LAPAO had the ability to transport NBD-Lipid II across model membranes (**Fig. 6** (B)).

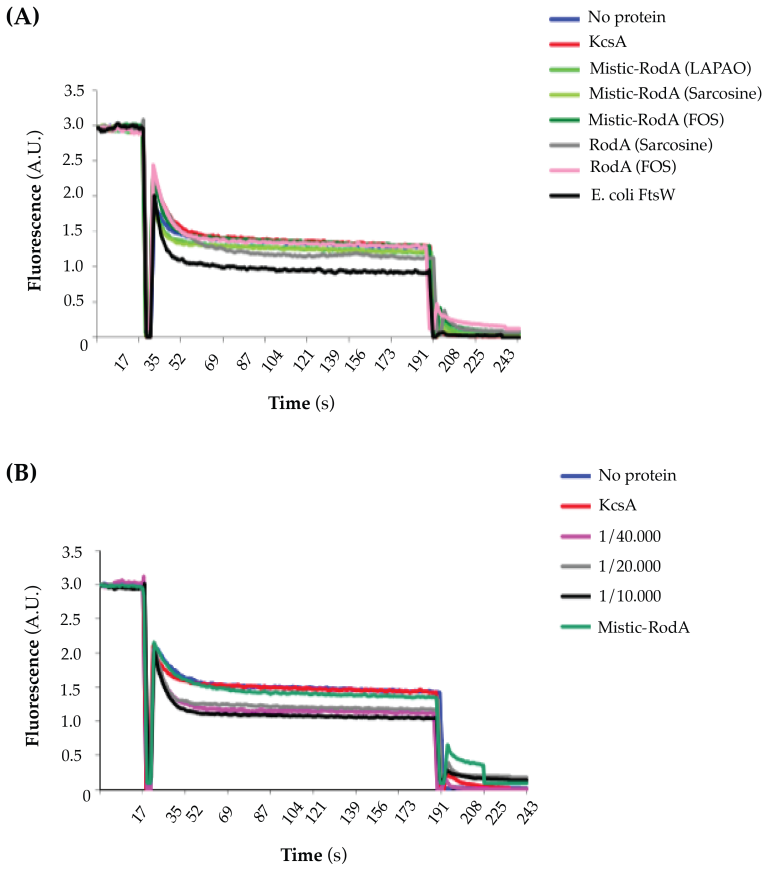

Fig. 6: Activity assays of 'misticated' and cleaved SpRodA solubilized in different detergents. LUVs containing NBD-Lipid II were reconstituted with **(A)** 'misticated' SpRodA extracted from the membrane in three different detergents and cleaved SpRodA solubilized in FOS12 and Sarcosine. Addition of dithionite led for all tested samples to a rapid decrease of fluorescence by ~ 50%. Proteoliposomes containing **(B)** cleaved SpRodA solubilized in LAPAO showed, on the contrary, a fluorescence reduction of ~ 70-75% compared to protein-free vesicles. Concentration dependency was not observed, as all three tested protein/phospholipid ratios led to the same percentage of quenched fluorescence. Complete quenching was achieved by addition of Triton X-100 to a final concentration of 0.1%. Empty vesicles and KcsA containing proteoliposomes were used as negative controls, whereas vesicles reconstituted with *E. coli* FtsW served as the positive control. Abbreviations: A.U., arbitrary units.

The different tested phospholipid/protein ratios led, however, to a similar extent of reduction by dithionite and thus in no decrease of protected NBD-Lipid II upon increase of SpRodA as was determined for *E. coli* FtsW (Mohammadi, van Dam et al. 2011).
Since SpRodA started to precipitate during storage at 4°C, we assumed that SpRodA was possibly prone to aggregation during the reconstitution process and independently of the amount of protein used at the start of the assay, only a specific pool remained active, ending up thus with an identical profile of transbilayer movement.

CONCLUSION

Detergents are a substantial tool in the study of membrane proteins that are required from the extraction of the protein till its final crystallization. Identification of suitable detergents with high stabilizing efficacy requires generally extensive screening. The data represented in this study provides not only a list of detergents with properties suitable for the high-level purification of SEDS proteins in homogeneous and functional form, but also the first biochemical evidence that RodA functions as a Lipid II flippase in *S. pneumoniae*. This information is therefore an essential prerequisite for further structural studies of bacterial flippases.

ACKNOWLEDGEMENTS

We would like to thank T. Mohammadi (University Utrecht, The Netherlands) for performing the activity assays on SpRodA samples.
This work used the platforms of the Grenoble Instruct centre (ISBG; UMS 3518 CNRS-CEA-UJF-EMBL) with support from FRISBI (ANR-10-INSB-05-02) and GRAL (ANR-10-LABX-49-01) within the Grenoble Partnership for Structural Biology (PSB). We thank M. Noirclerc-Savoye (IBS, PSB, France) for the detergent exchange screenings of TmFtsW, SpRodA and EcFtsW.

REFERENCES

Boyle, D. S., et al. (1997). "ftsW is an essential cell-division gene in *Escherichia coli*." Mol Microbiol **24**(6): 1263-1273.

Caffrey, M. (2003). "Membrane protein crystallization." J Struct Biol **142**(1): 108-132.

Carpenter, E. P., et al. (2008). "Overcoming the challenges of membrane protein crystallography." Curr Opin Struct Biol **18**(5): 581-586.

Filip, C., et al. (1973). "Solubilization of the cytoplasmic membrane of *Escherichia coli* by the ionic detergent sodium-lauryl sarcosinate." J Bacteriol **115**(3): 717-722.

Grisshammer, R. and C. G. Tate (1995). "Overexpression of integral membrane proteins for structural studies." Q Rev Biophys **28**(3): 315-422.

Henriques, A. O., et al. (1998). "Control of cell shape and elongation by the rodA gene in *Bacillus subtilis*." Mol Microbiol **28**(2): 235-247.

Holtje, J. V. (1998). "Growth of the stress-bearing and shape-maintaining murein sacculus of *Escherichia coli*." Microbiol Mol Biol Rev **62**(1): 181-203.

Hottenrott, S., et al. (1997). "The *Escherichia coli* SlyD is a metal ion-regulated peptidyl-prolyl cis/trans-isomerase." J Biol Chem **272**(25): 15697-15701.

Ikeda, M., et al. (1989). "Structural similarity among *Escherichia coli* FtsW and RodA proteins and *Bacillus subtilis* SpoVE protein, which function in cell division, cell elongation, and spore formation, respectively." J Bacteriol **171**(11): 6375-6378.

Ishino, F., et al. (1986). "Peptidoglycan synthetic activities in membranes of *Escherichia coli* caused by overproduction of penicillin-binding protein 2 and rodA protein." J Biol Chem **261**(15): 7024-7031.

Joris, B., et al. (1990). "The life-cycle proteins RodA of *Escherichia coli* and SpoVE of *Bacillus subtilis* have very similar primary structures." Mol Microbiol **4**(3): 513-517.

Khattar, M. M., et al. (1997). "Two polypeptide products of the *Escherichia coli* cell division gene ftsW and a possible role for FtsW in FtsZ function." J Bacteriol **179**(3): 784-793.

le Maire, M., et al. (2000). "Interaction of membrane proteins and lipids with solubilizing detergents." Biochim Biophys Acta **1508**(1-2): 86-111.

Leviatan, S., et al. (2010). "Combinatorial method for overexpression of membrane proteins in *Escherichia coli*." J Biol Chem **285**(31): 23548-23556.

Macheboeuf, P., et al. (2006). "Penicillin binding proteins: key players in bacterial cell cycle and drug resistance processes." FEMS Microbiol Rev **30**(5): 673-691.

Miroux, B. and J. E. Walker (1996). "Over-production of proteins in *Escherichia coli*: mutant hosts that allow synthesis of some membrane proteins and globular proteins at high levels." J Mol Biol **260**(3): 289-298.

Mohammadi, T., et al. (2014). "Specificity of the transport of lipid II by FtsW in *Escherichia coli*." J Biol Chem **289**(21): 14707-14718.

Mohammadi, T., et al. (2011). "Identification of FtsW as a transporter of lipid-linked cell wall precursors across the membrane." EMBO J **30**(8): 1425-1432.

Newstead, S., et al. (2008). "Rationalizing α-helical membrane protein crystallization." Protein Sci **17**(3): 466-472.

Prive, G. G. (2007). "Detergents for the stabilization and crystallization of membrane proteins." Methods **41**(4): 388-397.

Raman, P., et al. (2006). "The Membrane Protein Data Bank." Cell Mol Life Sci **63**(1): 36-51.

Roosild, T. P., et al. (2005). "NMR structure of Mistic, a membrane-integrating protein for membrane protein expression." Science **307**(5713): 1317-1321.

Schneider, C. A., et al. (2012). "NIH Image to ImageJ: 25 years of image analysis." Nat Methods **9**(7): 671-675.

Seddon, A. M., et al. (2004). "Membrane proteins, lipids and detergents: not just a soap opera." Biochim Biophys Acta **1666**(1-2): 105-117.

Tate, C. G. (2001). "Overexpression of mammalian integral membrane proteins for structural studies." FEBS Lett **504**(3): 94-98.

Vollmer, W., et al. (2008). "Peptidoglycan structure and architecture." FEMS Microbiol. Rev. **32**: 149-167.

Wagner, S., et al. (2006). "Rationalizing membrane protein overexpression." Trends Biotechnol **24**(8): 364-371.

CHAPTER 5

Crystallization of *Streptococcus pneumoniae* RodA

ABSTRACT

Despite recent technology advances, the structural characterization of membrane proteins remains a considerable challenge in the field of structural biology. One of the major hurdles is the production of well-ordered diffraction quality crystals. The long established detergent-based or *in surfo* approach is by far the most successful method to crystallize membrane proteins. However, in some cases the detergent not only prevents the formation of protein-protein contacts necessary for crystallization but also tends to destabilize the protein. Recently developed techniques involve therefore the crystallization of membrane proteins in a more native-like environment that is based on the self-assembling properties of detergents and lipids as mesophases (LCP) or disc-like micelles (bicelles). These methods proved to be of great utility in the structural determination of several membrane proteins. In the present study we investigated the capability of each approach to crystallize *Streptococcus pneumoniae* RodA, a member of the well-known SEDS protein family. While the full-length protein was not prone to crystallization, we identified a proteolytic resistant core domain of RodA that displayed increased stability and led to the successful crystallization of the protein in bicelles, allowing initial X-ray diffraction analysis by serial synchrotron crystallography.

INTRODUCTION

SEDS proteins play pivotal roles in the synthesis of peptidoglycan. They are required for the translocation of Lipid II across the cytoplasmic membrane. However, only little is known about the mechanism of Lipid II transport and its regulation. Detailed information about the three-dimensional structure is therefore required to understand this translocation process at a molecular level.

To date, X-ray crystallography is the most powerful and successful technique with which it is possible to yield reliable insight into the three-dimensional structure of any protein (Stroud 2011). Nevertheless, just 1% of all currently available structures in the Protein Data Bank (PDB) represent integral membrane proteins. The main reason for the paucity of membrane protein structures is due to their hydrophobicity, which makes their structural determination a daunting task. The major hurdles in obtaining the spatial structure of a membrane protein by X-ray

crystallography include not only the production and purification of sufficient quantities of protein, but also growth of well-ordered diffraction-quality crystals. However, the most critical step in the manipulation of membrane proteins is the necessity to remove the protein from their native lipidic environment by detergent solubilization (Landau and Rosenbusch 1996). These detergents are not always able to adequately mimic the native membranes resulting often in poor stability, rapid aggregation to amorphous structures and loss of important structural lipids or weakly bound subunits (Johansson, Wohri et al. 2009).

In surfo method

Nevertheless, membrane proteins have been traditionally crystallized as Protein-Detergent Complexes (PDCs), enabling manipulations similar to that of soluble proteins. This long-established detergent- or *in surfo*-based method, uses techniques such as vapor diffusion, microdialysis or microbatch to crystallize PDCs. A crucial prerequisite for *in surfo* crystallization is the ability of the protein to form protein-protein contacts in the presence of detergent micelles (Caffrey 2000, Caffrey 2003). Often, this crystallization approach generates type II crystals that are extremely fragile and have a large solvent content (**Fig. 1**). This is mainly caused by the presence of detergent micelles that cover the protein's hydrophobic region, allowing only interactions between the hydrophilic domains. To enable such hydrophilic interactions, detergent micelles should be ideally small enough to fit into the crystal lattice without interfering with protein-protein interactions, but large enough to sufficiently protect the protein's hydrophobic surface (Ostermeier and Michel 1997). The most critical step in obtaining well-ordered type II crystals is therefore the choice of detergent. Finding a suitable detergent that prevents protein aggregation while allowing in the same time the formation of crystal lattices requires generally extensive screening and does not always lead to success.

In meso crystallization

However, detergents are poor substitutes for the lipid bilayer membrane proteins are normally embedded in, and thus significant efforts were made to establish new crystallization techniques that are less aggressive and allow crystallization in a more native environment. Such approaches are the so-called bilayer or *in meso* techniques,

which include the bicelle, lipidic cubic phase (LCP) as well as the lipidic sponge phase crystallization. These methods circumvent the drawbacks of crystallization in detergent-micelles and make use of lipidic media, which more closely mimic the native environment of a membrane protein. *In meso* crystallization results generally in the production of small, but well-ordered crystals that contain a low solvent content. To date, all membrane proteins that were solved by an *in meso* crystallization approach generated type I crystals, in which the protein molecules are organized in a two-dimensional lattice by hydrophobic interactions stacked on top of each other by hydrophilic contacts (**Fig. 1**). Landau and Rosenbusch were the first to describe the successful crystallization of a membrane protein from a bilayer (Landau and Rosenbusch 1996). This bilayer, better known as LCP, has a complex molecular structure that forms spontaneously upon mixing a specific lipid with an aqueous buffer. Structurally, LCP can be described as a three-dimensional bicontinuous lipid bilayer that is interconnected by a system of water channels (Landau and Rosenbusch 1996). The idea was that this complex structure could serve as a crystallization matrix in which the reconstituted protein diffuses within its three-dimensional lattice and feeds crystal nuclei (Ostermeier and Michel 1997). This concept was validated by the structural determination of bacteriorhodopsin at high-resolution (Landau and Rosenbusch 1996). Despite this success, however, further membrane protein structures obtained by this approach failed to appear for a long time. The major reason for this was associated with the technical inability to work with an extremely viscous and sticky mesophase (Li and Caffrey 2011). This tide began to turn since the introduction of tools that allowed the manipulation of nanoliter volumes of 'toothpaste-like' media (Cheng, Hummel et al. 1998, Cherezov, Peddi et al. 2004, Caffrey and Cherezov 2009).

These technological developments proved to be of significance for the successful crystallization of membrane proteins within LCP. Since the structure determination of bacteriorhodopsin in 1996, the PDB has now included more than 174 membrane protein structures that have been solved using LCP as the hosting medium for crystal nucleation and growth (Cherezov, Clogston et al. 2002). Along with several structures of bacterial membrane proteins, the PDB entries also include high-resolution structures of various human G-protein-coupled receptors (GPCRs) (Pebay-Peyroula, Rummel et al. 1997, Katona, Andreasson et al. 2003, Cherezov, Rosenbaum et al. 2007, Hanson, Cherezov et al. 2008, Tiefenbrunn, Liu et al. 2011, Malinauskaite, Quick et al. 2014).

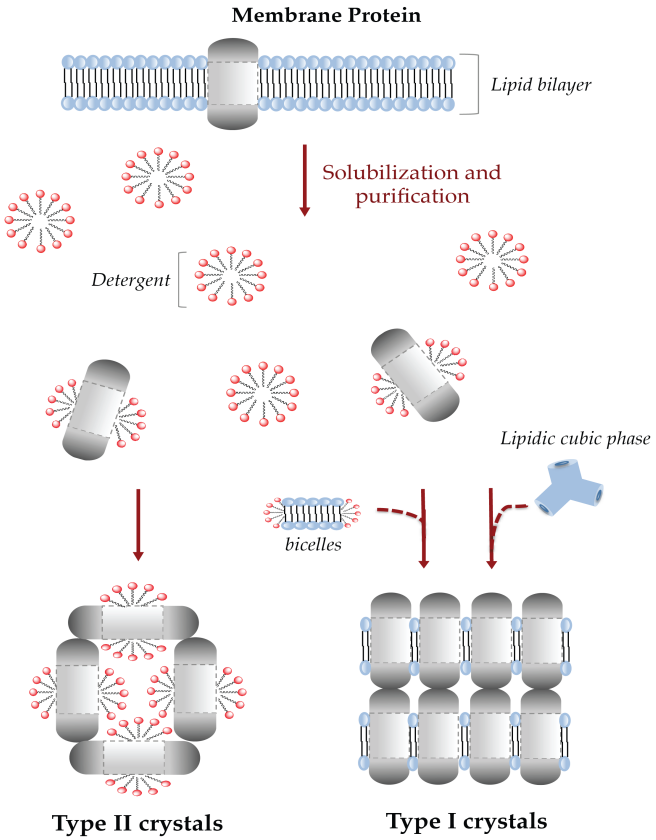

Fig. 1: Two types of membrane protein crystals. Type II crystals have detergent micelles covering the hydrophobic surface of the protein. Protein-protein interactions are limited to the polar surfaces of the protein (indicated in dark grey). Type I crystals on the other hand, can be formed by reconstituting the protein back in a lipidic environment, such as bicelles or lipidic cubic phase. These crystals are stacks of 2-dimensional sheets that are ordered in the third dimension by polar interactions.

Interestingly, proteins with large extramembrane domains were crystallized from a phase that differed from the conventional cubic phase. Under certain conditions, the cubic phase can transform into its liquid analogue that is referred to as the sponge phase (Cherezov, Yamashita et al. 2006, Wadsten, Wohri et al. 2006).

Within this swollen mesophase the bicontinuity of the cubic phase is still retained while its ordered structure is perturbed. This causes reduced bending rigidity of the highly curved bilayer and enlargement of the dimensions of the aqueous channels. The major advantage of these microstructural changes is that the increased water channel radius enables even proteins with relatively large hydrophilic domains to move within the mesophase and assemble into a crystal lattice (Wadsten, Wohri et al. 2006). The sponge phase has already supported the successful crystallization of several membrane proteins, including *e.g.* GPCRs, the reaction center from *Rhodobacter sphaeroides*, the light harvesting complex II from *Rhodopseudomonas acidophila* as well as *Escherichia coli* BtuB, which was the first β-barrel protein to be crystallized within a mesophase (Cherezov, Clogston et al. 2006, Cherezov, Yamashita et al. 2006, Wadsten, Wohri et al. 2006, Jaakola, Griffith et al. 2008). These statistics demonstrate therefore the great potential of this approach and support the hypothesis that the cubic phase, be it in its ordered or perturbed structure, provides a suitable crystallization matrix for growing highly ordered diffraction-quality crystals.

Recently, an alternative *in meso* approach was introduced that utilizes a more convenient lipidic host medium for the crystallization of membrane proteins. Bicelles are lipid-rich, bilayer discs that are formed through mixing a certain ratio of an amphiphile/short-chain phospholipid with a long-tail phospholipid (Ujwal and Bowie 2011, Ujwal and Abramson 2012). The interesting structural feature of a bicelle disc is that the lipids generate a central planar bilayer that is surrounded by a rim of detergent molecules protecting the apolar edges of the lipids. The morphology of bicelles can be therefore described as an intermediate between the typical mesophase and the classical detergent-micelle providing the benefits of both (Sanders and Prosser 1998). This unique system offers a native-like bilayer environment for the membrane protein while enabling ease of manipulation due to reduced viscosity (Moraes, Evans et al. 2014). Crystallization trials can be thus carried out similarly to that of PDCs using standard crystallization robotics. To date, several membrane protein structures have been reported that were successfully crystallized using bicelle formulations. This collection includes, in addition to structures of rhodopsins, structures of a GPCR and the voltage-dependent anion channel (VDAC) from *Mus musculus*, the latter being the first β-barrel protein crystallized within bicelles (Faham and Bowie 2002, Faham, Boulting et al. 2005, Rasmussen, Choi et al. 2007, Ujwal, Cascio et al. 2008).

In the current study we explored the capability of the aforementioned methods to crystallize *Streptococcus pneumoniae* RodA (SpRodA), a member of the well-conserved SEDS protein family. The data clearly indicated that full-length SpRodA failed to crystallize with each tested approach due to its limited stability. However, limited proteolysis experiments led to the identification of a proteolytic resistant core domain ($SpRodA_{1\text{-}255}$) that demonstrated increased stability, leading to its successful crystallization after reconstitution into bicelles. In addition, analysis of $SpRodA_{1\text{-}255}$ crystals by employing serial synchrotron crystallography resulted in the identification of one condition where crystals displayed diffraction.

MATERIALS AND METHODS

Auto-induction medium preparation

The defined medium is based on previously described methods (Studier 2005). The high cell density auto-induction medium contained (per liter): 924 ml ZY medium (10 g/L tryptone and 5 g/L yeast extract; Sigma), 1 ml 1 M $MgSO_4$ (Sigma), 50 ml 20xNPS at pH 6.75 (0.5 M $(NH_4)_2SO_4$, 1 M KH_2PO_4, 1 M Na_2HPO_4; Sigma), 10 ml 20% α-lactose (Sigma), 10 ml 50% glycerol (Sigma) and 5 ml 10% glucose (Sigma).

Construction of $SpRodA_{1\text{-}255}$

Site-directed mutagenesis was used to introduce a stop codon at position 766 in wild-type SpRodA (encoded on plasmid pLIM15, see **Chapter 3**), leading to an end in translation and the generation of a truncated version of SpRodA, further referred to as $SpRodA_{1\text{-}255}$.

Protein expression and purification

Expression plasmids coding for SpRodA or $SpRodA_{1\text{-}255}$ were used to transform *E. coli* BL21 (DE3) STAR (Invitrogen) competent cells. Four 2 L baffled Erlenmeyer flasks containing each 500 ml of auto-induction medium were inoculated with a $1/40^{th}$ dilution of overnight pre-cultures. Cultures were usually grown for 1 hour at

37°C and afterwards switched to 25°C for 24 hours to allow target protein overexpression. To enable sufficient aeration, cultures were grown in an incubator shaker usually at 230-250 rpm. After cultivation, cells were collected by centrifugation (6.000 rpm, 20 min, 4°C) and resuspended in Buffer A (50 mM Tris pH 8, 200 mM NaCl, 10% Glycerol) containing 1 mM protease inhibitors (PMSF, Pepstatin, Aprotinin and Leupeptin; Euromedex) and 200 μg/ml lysozyme (Fluka). Cells were subsequently broken by passing the sample six times through a pre-cooled cell disruptor (Constant Cell Disruption Systems) at 6.000 psi. Unbroken cells were removed by centrifugation (10.000 rpm, 10 min, 4°C) and membranes were afterwards collected by ultracentrifugation (40.000 rpm, 60 min, 4°C). The membrane resuspension was performed in Buffer A and if required, diluted to a final OD_{600nm} of 1 A.U. (parameter that enabled good detergent:protein ratios for subsequent solubilization). Solubilization of membranes was accomplished by the addition of LAPAO to a final concentration of 1%. After gentle incubation for 60 min at 4°C, non-solubilized material was removed by ultracentrifugation (40.000 rpm, 60 min, 4°C). The target protein was purified to homogeneity using the previously described protocol (see **Chapter 4**), with one modification: The gel filtration column used for analyzing the homogeneity of the samples was Superose 6 10/300 GL instead of Superdex 200 5/150 GL (GE Healthcare). Detergents (Affymetrix) that were used during the purification are listed in **TABLE 1**.

TABLE 1. List of detergents

DETERGENT	CMC* mM (%)	CMC* mM
n-Decyl-*β*-D-Maltopyranoside (DM)	1.8 (0.09)	3.6
n-Dodecyl-*β*-D-Maltopyranoside (DDM)	0.17 (0.009)	0.34
n-Nonyl-*β*-D-Glucopyranoside (NM)	6 (0.28)	12
Decyl Maltose Neopentyl Glycol (DMNG)	0.036 (0.0034)	0.072
Lauryl Maltose Neopentyl Glycol (LMNG)	0.01 (0.001)	0.02

* Approximate CMC in water at 20°C.

Thin layer chromatography (TLC)

TLC is a simple method that can be used to determine the detergent concentration in a membrane preparation. Detergent quantification was performed by spotting several concentrations of the reference detergent together with the purified protein sample on a silica plate (TLC Silica gel 60 F_{254}, Merck), taking care to set up the spots about 1 cm from the top edge of the plate. After drying of the spots, the plate was transferred into a sealed chromatographic chamber containing a solvent system composed of chloroform/methanol/water (65:25:4 by volume). This solvent enabled the detergent to move up the plate by capillary action. The TLC was developed until the solvent reached about 95% of the plate and then removed from the chamber to allow drying. The detergent was visualized by spraying the plate with a fine mist of sulfuric acid in a fume hood. The detergent concentration within the purified protein sample was determined by scanning the TLC plate and quantifying the spot intensities using the ImageJ software package (Schneider, Rasband et al. 2012).

Limited proteolysis

Limited proteolysis experiments were carried out using either trypsin, chymotrypsin or subtilisin. Protease stock solutions were prepared in PBS buffer at a final protease concentration of 1 mg/ml. The protease to protein ratio was adjusted to 1:100 (wt/wt) and incubated for up to 1 h at 4°C. Aliquots of 10 µl were removed after 15, 30, 60, 90 and 120 min. The reaction was stopped immediately by adding phenylmethanesulphoylfluoride (PMSF) to a final concentration of 1 mM. The proteolytic effect of the tested enzymes on the protein was analyzed by SDS-PAGE.

Crystallization in detergent-micelles

Detergent-based crystallization trials were performed using the high-throughput crystallization facility at the HTX lab (Partnership for Structural Biology, Grenoble). Protein samples were concentrated to 7-20 mg/ml. The protocol for crystallization setups was as described previously (Dimasi, Flot et al. 2007). Briefly, 100 nl of the sample was dispensed in each well of a sitting drop plate (Intelliplate, Art Robbins), followed by 100 nl of the crystallization condition (see **TABLE 2**). Plates were

afterwards transferred to an automated imaging robot at 4°C (RockImager, Formulatrix).

Crystallization in LCP

The lipid of choice for LCP crystallization setups was Monoolein (MO), purchased from Nu Check Prep. Inc. (Elysian, MN). Protein samples were concentrated to 10-40 mg/ml and mixed with molten MO in a ratio of 2/3 (v/v) using a lipid-mixing device as previously described (Cheng, Hummel et al. 1998, Caffrey and Cherezov 2009). The two components were mixed until the solution appeared clear and homogeneous. Once the components were well mixed, each well of a 96-well glass sandwich plate (Hampton Research) was loaded with 40 nl of the formed LCP followed by 800 nl of precipitant solution (see **TABLE 2**). Dispensing of the LCP was performed using the NT8 crystallization robot (Formulatrix). Plates were afterwards placed in a temperature-controlled chamber (RockImager, Formulatrix) for incubation and crystal visualization at 20°C.

Crystallization in bicelles

Bicelle preparations were purchased from Molecular Dimensions. Incorporation of the protein into bicelles was performed as previously described (Ujwal and Abramson 2012). Briefly, bicelle stock solutions were thawed at RT, subsequently placed on ice and vortexed to re-establish a homogeneous bicelle phase. Protein samples were concentrated at 8-14 mg/ml and mixed with bicelles at a 1:4 bicelle:protein ratio. To allow incorporation of the protein into bicelles, the mixture was further incubated for at least 30 min on ice. Crystallization trials were performed with the NT8 crystallization robot using 96-well hanging drop plates (CrystalQuick, Greiner). The standard setup was 100 nl of protein/bicelle mixture followed by 100 nl of crystallization solution (see **TABLE 2**). Plates were kept in an imaging system (RockImager, Formulatrix) at 20°C.

TABLE 2. **List of crystallization screens used in this study**

SCREEN	SUPPLIER	CRYSTALLIZATION METHOD
Index	Hampton Research	*in surfo*
Wizard I&II	Rigaku Reagents	*in surfo, in meso*
MemGold	Molecular Dimensions	*in surfo, in meso*
Crystal Screen I+II	Hampton Research	*in surfo, in meso*
The Classics II	Qiagen	*in surfo, in meso*
MemStart-MemSys	Molecular Dimensions	*in meso*
Salt Grid	Hampton Research	*in surfo*
The MbClass I+II	Qiagen	*in surfo*
FRAP screen pH 7+8	Home-made	LCP
MembFac	Hampton Research	*in meso*

Design of FRAP screens

The mobility of the protein within the LCP was analyzed under specific buffer and precipitant conditions that were previously described by Xu and co-workers (Xu, Liu et al. 2011). We designed four 96-well screens at different buffer conditions, including 0.1 M MES, pH 6.0, 0.1 M Tris pH 7.0, 0.1 M Tris pH 8.0 and 0.1 M Bis-Tris pH 8.5. Each screen was composed of 48 different salts (StockOption Salt kit, Hampton Research) at two different concentrations (100 mM in the upper 48 wells and 400 mM in the lower 48 wells) including a constant PEG 400 concentration of 30%.

High-Throughput LCP-Fluorescence Recovery after Photobleaching (HT LCP-FRAP)

Since diffusion of a membrane protein within the LCP is a prerequisite for crystallization, we performed HT LCP-FRAP assays to examine crystallization conditions conductive to diffusion of the protein. HT LCP-FRAP experiments were

performed as previously described (see **Fig. 2**) (Cherezov, Liu et al. 2008, Xu, Liu et al. 2011). Briefly, stock solutions of Cy3-mono NHS ester (GE Healthcare) at a final concentration of 5 mg/ml were prepared by adding 200 µl of dimethylformamide (DMF, Sigma) to a vial containing 1 mg of dye. Protein samples were labeled by incubating 25 µg Cy3-mono NHS with 500 µg of protein in 500 µl of Buffer E (25 mM HEPES (pH 7.5), 20 mM NaCl, 3% glycerol and 3.6 mM DM) at 4°C for 4 hours in the dark.

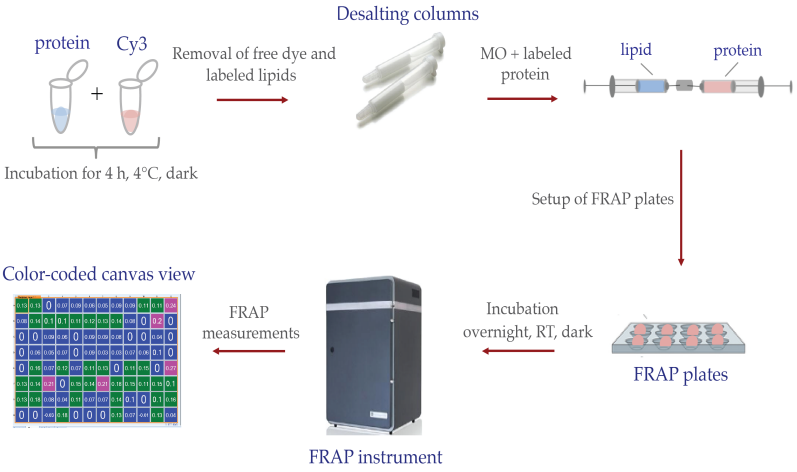

Fig. 2: Schematic representation of the LCP-FRAP workflow.

Membrane protein preparations from bacterial cells generally contain a portion of phosphatidylethanolamine (PE) lipids that can also be labeled with the Cy3-mono NHS ester. Labeled lipids and free dye were subsequently removed by applying the sample several times on a desalting column (PD MiniTrap G-25, GE Healthcare). The final elution fraction containing labeled protein was collected and concentrated to 4 mg/ml. HT LCP-FRAP experiments were afterwards performed according to the aforementioned protocol (see **Crystallization in LCP**), with the following modification: Samples were dispensed on glass sandwich plates optimized for FRAP studies (FRAP sandwich set, Hampton Research). Prior to FRAP data collections, plates were incubated at **r**oom **t**emperature (RT) overnight in the dark. FRAP measurements were performed using the LCP-FRAP instrument (Formulatrix).

FRAP data was collected in a fully automated mode, however, if protein labeling efficiencies were too low/high, exposure times for reading the fluorescence signal were increased/decreased. For each well a pre-bleached image was taken as the baseline fluorescence intensity. Each spot of the 96-well FRAP sandwich plate was afterwards photo-bleached and the fluorescence recovery within the spot was measured after 30 min. To allow evaluation of protein diffusion, we set up a negative control for each experiment in order to define the threshold level of mobile fraction. Here we used protein samples that were heated to 100°C prior to setting up FRAP experiments, which resulted in aggregation of the protein and lack of diffusion. The entire data was automatically presented as a color-coded 96-well grid, allowing direct visualization of positive hits.

RESULTS AND DISCUSSION

Auto-induction medium increases the expression yield of SpRodA

Structural studies require milligrams of homogeneous and active protein. Since membrane proteins are usually present at minute levels in natural biological membranes, it is often necessary to overexpress the membrane protein in question. This step requires generally extensive screening and is one of the major hurdles towards the structural characterization of a membrane protein. Previously we were able to show that fusion of Mistic to the N-termini of several SEDS proteins allows high-level overexpression of the proteins yielding up to 15 mg of protein per L of culture (see **Chapter 3**). One of these SEDS proteins, SpRodA, was successfully purified to homogeneity and was shown to actively transport fluorescently labeled Lipid II across model membranes (see **Chapter 4**).

Here, we further optimized the expression yield of SpRodA for downstream crystallization attempts. SpRodA was therefore subsequently overexpressed in auto-induction medium. Cultures reached extremely high cell densities when compared to the expression of SpRodA in TB medium (OD_{600nm} of 24 compared to OD_{600nm} 4, respectively), yielding up to 45 mg of protein per L of culture. Expression of SpRodA in auto-induction medium indicated therefore further boost of recombinant protein production resulting in a three-fold increase compared to the previously described expression yields (see **Chapter 3**). The overexpressed protein was afterwards

extracted from the membrane with LAPAO and further purified to homogeneity by a three-step purification pipeline, including immobilized metal affinity chromatography (IMAC), ion-exchange and size exclusion chromatography (SEC) (**Fig. 3**). Since the detergent choice has a great impact on crystallization success, we purified SpRodA in a panel of different detergents that had the ability to maintain the protein in a soluble and stable state after extraction and removal of the fusion tag (see **Chapter 4**). Each of the tested detergents was used at the concentration indicated in **TABLE 1**.

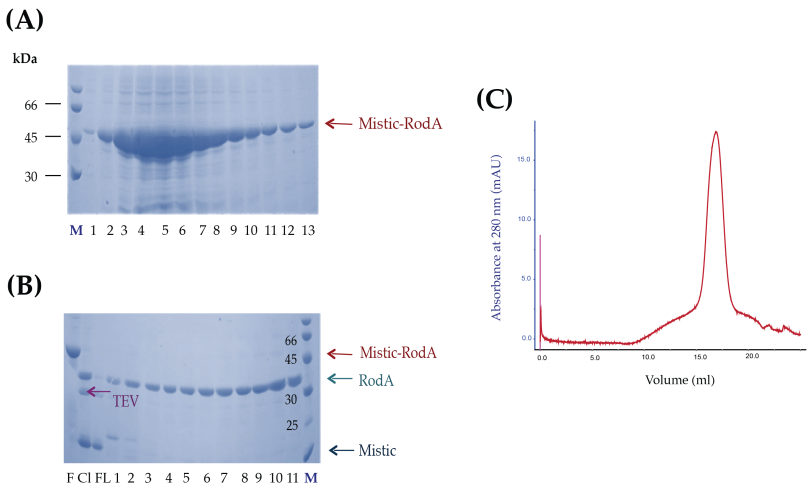

Fig. 3: Purification of SpRodA using an auto-induction medium. Solubilization of SpRodA was performed in 1% LAPAO. The detergent was exchanged for DM by **(A)** IMAC purification. After cleavage of Mistic, SpRodA was further purified using **(B)** cation-exchange chromatography. Sample homogeneity was analyzed by **(C)** gel filtration. Abbreviations: M, marker; F, uncleaved protein; Cl, cleaved protein; FL, flow through.

In surfo crystallization of SpRodA

After confirmation of the purity and homogeneity of the sample by the aforementioned methods, SpRodA was concentrated to 7 mg/ml. Since the detergent concentration of the sample plays a crucial role in the *in surfo* crystallization approach, we calculated the final detergent concentration of each sample prior to

crystallization trials. To determine the detergent concentration within the sample, we applied SpRodA as well as a wide range of detergent concentrations on a TLC plate and developed with sulfuric acid as described in Material and Methods. The result for SpRodA purified in DM is shown in **Fig. 4** (A). The intensity of each spot was quantified with ImageJ and plotted against the detergent concentration (**Fig. 4** (B)). Based on this standard curve, the calculated content of detergent within the sample was 0.5% and thus approximately 5-times higher than the CMC of DM. Detergent quantification of samples that were purified in different detergents led to similar results, except for DDM, where the calculated detergent content of the sample was 0.1% and therefore about 12-times the CMC of DDM (data not shown). However, the results indicated that concentration of the protein sample had only a minimal effect on the final detergent content within the sample. Detergent concentrations increased only about 2.7-5-fold compared to the initial detergent concentration.

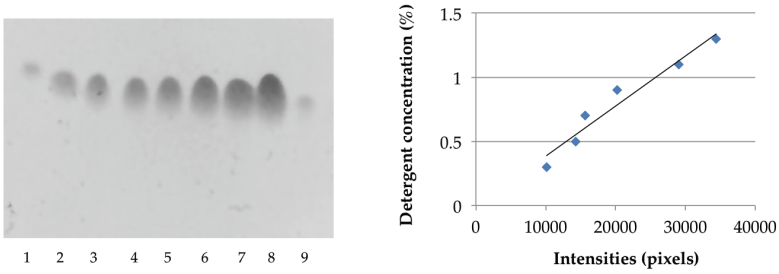

(A) **(B)**

Fig. 4: Detergent quantification of SpRodA in DM. **(A)** A 1/10 dilution of concentrated SpRodA (spot 1 and 9) was applied beside samples containing different concentrations of DM on a TLC plate. **(B)** Spot intensities were calculated with ImageJ and analyzed with Microsoft Excel, yielding a standard curve for the detergent. Abbreviations: 1, 1/10 dilution of SpRodA; 2, 0.3% DM; 3, 0.5% DM; 4, 0.7% DM; 5, 0.9% DM; 6, 1.1% DM; 7, 1.3% DM; 8, 1.5% DM; 9, 1/10 dilution of SpRodA.

Based on currently available membrane protein structures in the PDB, the calculated detergent concentration of the samples was in an acceptable range for further crystallization attempts. *In surfo* crystallization trials were therefore subsequently performed as described previously in this study (Material and Methods).

For six out of the seven tested crystallization screens (see **TABLE 2**) we did not observe any crystals even after extended periods of incubation. Nevertheless, we were able to identify four conditions within the Salt grid screen for protein samples purified in DM (**Fig. 5**).

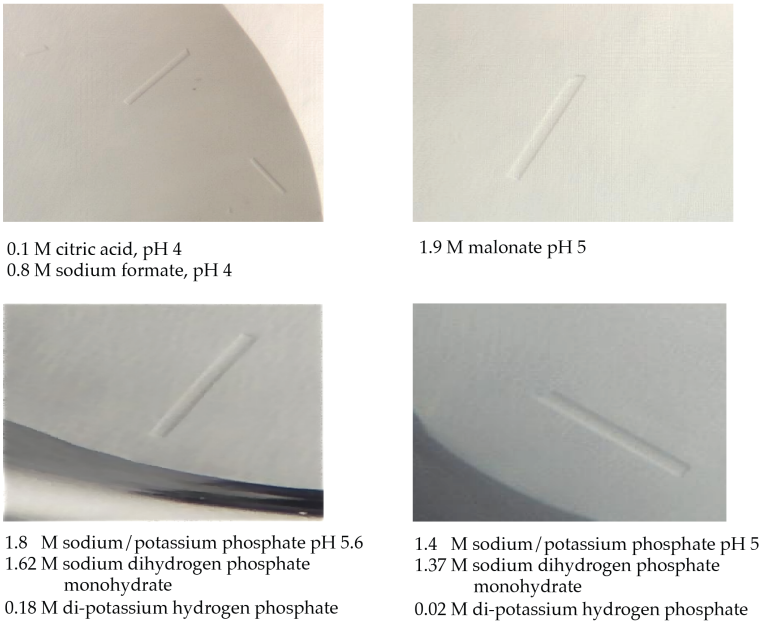

Fig. 5: *In surfo* crystals of SpRodA. Crystals were obtained after 3-14 days using the high-throughput facility at the HTX lab (Partnership for Structural Biology, Grenoble). Crystals were tested at ID23-2 (ESRF, Grenoble), but did not show any diffraction.

Crystals appeared within a few days and were fully grown after 3 weeks. Unfortunately, crystals were not of diffraction quality. Extensive efforts were made to optimize these conditions, but without any success. Possible explanations could be either that the detergent prevents the formation of potential crystal contacts or the protein has limited stability leading to rapid aggregation. Since detergent micelles are just a poor substitute for the protein's native environment and thus can result in

destabilization of the protein, we assumed that lipid based crystallization approaches could increase the likelihood of obtaining initial crystal hits for SpRodA.

Crystallization of SpRodA in LCP

Since we had inherent difficulties to obtain diffraction-quality crystals of SpRodA using the *in surfo* based crystallization approach, we pursued with an alternative approach, crystallization in LCP. This technique has the advantage that the protein of interest is incorporated in a membrane-like environment that not only stabilizes it but also supports crystal nucleation and growth. However, crystal nucleation requires sufficient protein mobility within the LCP and strongly depends on several parameters, including not only the structural features of the protein but also the geometric constraints of the curved LCP that is greatly affected by the chemical environment. To minimize the crystallization space, Xu and colleagues (Xu, Liu et al. 2011) established an automated high throughput pre-crystallization assay, further referred to as HT LCP-FRAP, that allows the identification of conditions that enable protein mobility in LCP. By using just a minimal amount of labeled protein, one can identify conditions that are non-conductive to protein diffusion and therefore not applicable for further crystallization trials.

To measure the mobility of SpRodA in LCP, we labeled the protein and set up the HT LCP-FRAP experiment as described in Material and Methods. The ability of SpRodA to diffuse within the LCP was assessed under conditions specifically designed for the FRAP experiment (see Material and Methods, Design of FRAP screens). Typical results are shown in **Fig. 6**. Depending on the concentration and identity of the salts, mobile fractions ranged from 0-39% for SpRodA at pH 7 and 0-24% for SpRodA at pH 8 (see **Fig. 6** (A)-(B)). Since the mobile fraction of the negative control was 17% (data not shown), which can be accounted for by natural lipid diffusion, we set a threshold level of 20% to evaluate the effect of the different salts on protein mobility. However, among all tested salts only high concentrations of ammonium acetate resulted in mobile fractions that were above the threshold level (see **Fig. 6** (A)+(B), red circle), leading to mobile fractions of 39 and 24% for pH 7 and 8, respectively. Since the stability of a protein is strongly related to its ability to diffuse in LCP (Xu, Liu et al. 2011), the difference of about 15% between mobile fractions obtained at pH 7 and 8 could indicate that a lower pH increases the stability of SpRodA. Indeed, HT LCP-FRAP data obtained at pH 6 and 8.5 revealed that

decrease of the pH led to increase of mobile fraction, whereas increase of pH decreased the mobile fraction drastically below the threshold level (**Fig. 6** (C)).

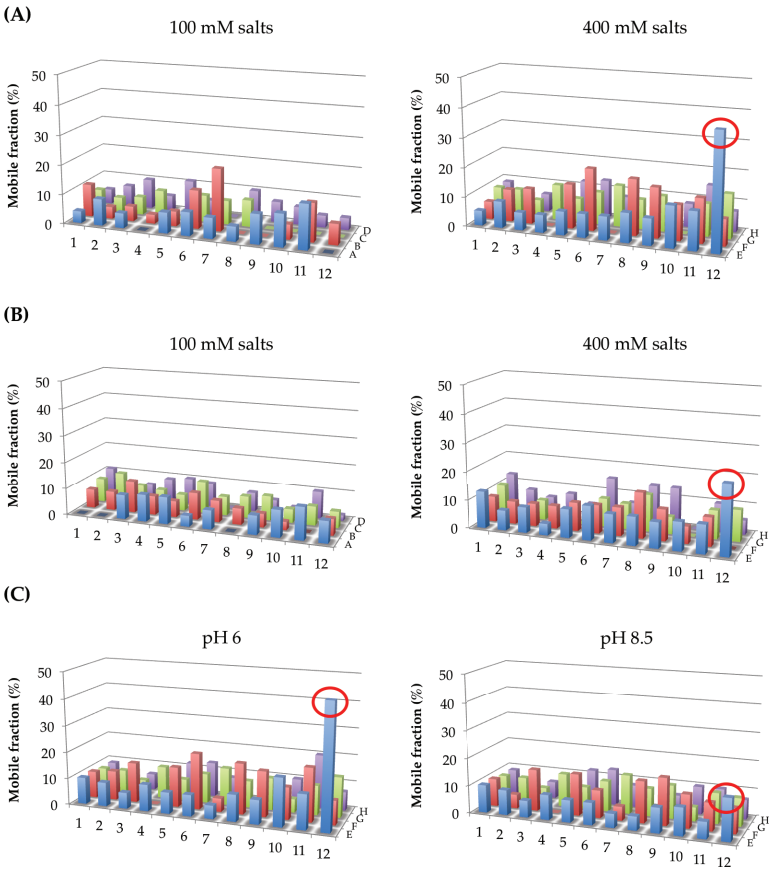

Fig. 6: LCP-FRAP experiments on SpRodA. HT LCP-FRAP experiments for SpRodA were performed under conditions described in Material and Methods. Fluorescence recovery for SpRodA was measured in **(A)** Tris pH 7 and **(B)** Tris pH 8. Each plate contained a constant concentration of PEG 400 at 30% and 48 different salts at two concentrations each (100 mM in rows A-D, 400 mM in rows E-H). **(C)** Fluorescence recovery for SpRodA under high salt concentrations at MES pH 6 (left) and Bis-Tris pH 8.5 (right). Mobile fractions in high concentrations of ammonium acetate are indicated as red circles.

The stability of SpRodA seems therefore to be highly dependent on the pH, which leads to destabilization of the protein in LCP and thus to loss of mobility at higher pH values. Since the mobility of a given protein in LCP is predictive of its crystallizability and only high concentrations of ammonium acetate resulted in mobile fractions above the threshold level, we pursued to set up crystallization trials of SpRodA by performing an extensive fine grid screen around this condition. However, this grid optimization did not lead to any crystal hits and neither did further attempts to crystallize SpRodA using commercially available crystallization screens (see **TABLE 2**). These results were not completely unexpected, since the ability of a given protein to diffuse in the LCP does not guarantee the formation of crystals. Reasons for this could be either a lack of protein-protein contacts that are required for crystal nucleation and growth or loss of protein mobility over time due to aggregation of the protein. Because the first hypothesis is difficult to prove, we investigated the stability of SpRodA in LCP over time. HT-LCP FRAP experiments were therefore performed in the condition resulting good initial mobile fractions (0.4 M ammonium acetate at pH 6 and 7) over the course of five days (**Fig. 7**).

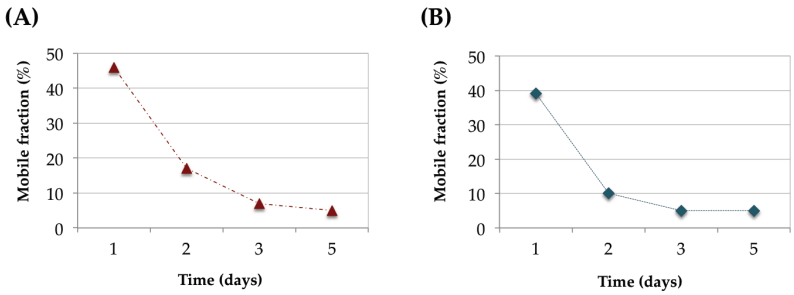

Fig. 7: Mobile fraction of SpRodA in 0.4 M ammonium acetate at different time points. Fluorescence recovery was measured at **(A)** pH 6 and **(B)** pH 7 at several time points over a period of five days. Under both tested conditions, diffusion of SpRodA completely stopped after two days.

Under both tested conditions SpRodA completely lost its mobility after two days, resulting in mobile fractions of 17% and 10% for pH 6 and pH 7, respectively. This drastic decrease in mobile fraction below the threshold level coincides well with the aforementioned speculation that crystallizability of SpRodA is hampered due to

relatively low stability of the protein, suggesting that this protein construct would not lead to the formation of crystals.

SpRodA displays high proteolytic susceptibility

Proteins can be described as modular entities that may contain regions of high conformational flexibility that can impede crystal growth. A useful biochemical approach to identify such flexible regions is limited proteolysis. This technique is based on the sensitivity of a given protein to proteolytic digestion. Well-ordered secondary structural elements, such as α-helices and β-sheets, are generally less prone to proteolytic digestion than solvent-exposed or disordered regions, such as loops. The key to this approach is therefore to identify a stable domain that resists proteolytic digestion and consequently can be more prone to crystallization.

Proteolytic digestion of SpRodA using three different endopeptidases (chymotrypsin, subtilisin and trypsin) led to the appearance of one fragment of approximately 28 kDa that was identical in each tested condition (see **Fig. 8** (A), red rectangle). This domain remained stable even after extended periods (4 weeks, 4°C) of incubation with the protease, indicating its resistance to proteolysis (**Fig. 8** (B), red rectangle). Interestingly, we observed a similar result when we analyzed a sample of SpRodA on SDS-PAGE that had been stored for five days at 4°C. SpRodA displayed partial cleavage, resulting in the appearance of a degradation fragment with an apparent molecular weight identical to that identified with protease treated SpRodA (see **Fig. 8** (B)). This domain seemed to have an extended half-life, since no further degradation was observed even after one year. To determine the boundaries of this major core domain, we performed a large-scale proteolysis experiment and subjected the proteolyzed fragment to peptide mass fingerprinting at the EMBL (Heidelberg, Germany). Analysis of the obtained data led to the identification of two major populations of peptides that provided the essential information to define the domain boundaries of the proteolyzed fragment (**Fig. 8** (C)). While the N-terminus of this fragment was only mildly affected by the proteolytic process (only three amino acids were removed, as compared to full-length SpRodA), the C-terminus was reduced by about 150 amino acids. Mapping both peptide populations onto the topology model of SpRodA highlighted that the C-terminal boundary of the fragment was predicted to be located in a large extracellular loop that connects transmembrane segment 7 and 8 (see **Fig. 8** (D)).

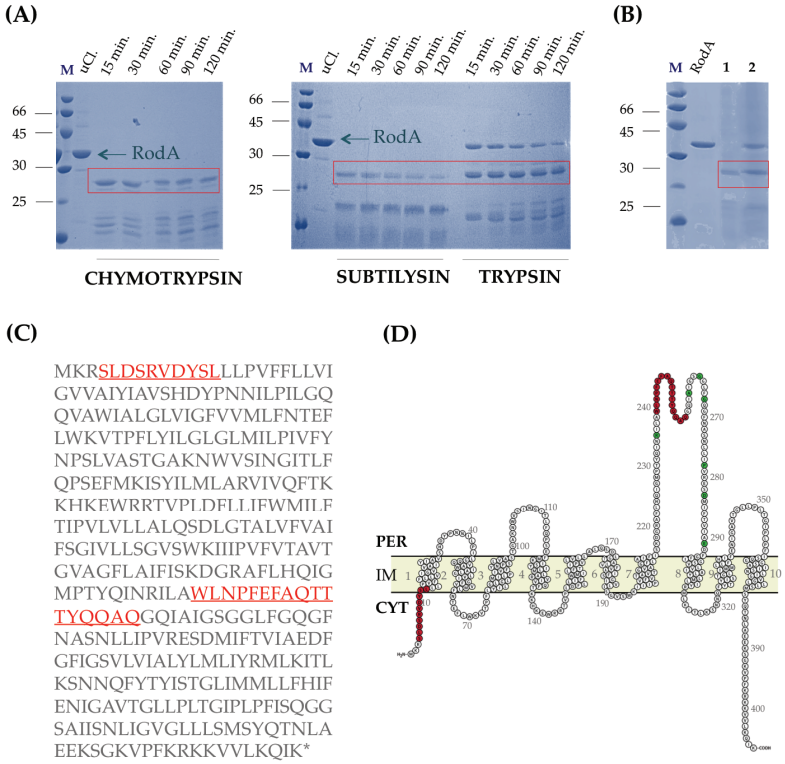

Fig. 8: Limited proteolysis and peptide mass fingerprinting of SpRodA. **(A)** Limited proteolysis experiments were performed at protease to protein ratios of 1:100 (wt/wt) with incubation for up to 1 hour at 4°C. In each tested condition one identical fragment appeared with an apparent molecular weight of 28 kDa (red rectangle). **(B)** This fragment was stable over an extended period of incubation with chymotrypsin (1) and seemed to be identical in size to naturally degraded SpRodA (2). **(C)** Peptide mass fingerprinting identified two peptide populations (red) that defined the N- and C- terminal boundaries of the proteolyzed fragment. **(D)** Mapping of the N- and C-terminal boundaries onto the topology model of SpRodA. The C-terminal boundary (highlighted in red) is located in a large periplasmic loop that contains many conserved residues (highlighted in green). Abbreviations: M, marker; uCL, uncleaved SpRodA; PER, periplasm; IM, inner membrane; CYT, cytoplasm.

Since this loop consists of many residues that are conserved among members of the SEDS protein family, it could probably serve as an interaction surface for other

proteins that form, together with SpRodA a discrete multi-enzyme complex that is required for cell wall growth. Consequently, in the absence of other protein partners, this loop is destabilized and prone to degradation.
Therefore, to enable increased stability of the protein, we performed site-directed mutagenesis to generate a variant of SpRodA lacking residues 256-407, further referred to as $SpRodA_{1\text{-}255}$.

Purification of $SpRodA_{1\text{-}255}$

$SpRodA_{1\text{-}255}$ was overexpressed in auto-induction medium and purified using the same protocol established for SpRodA. The expression yield of $SpRodA_{1\text{-}255}$ was similar to that of SpRodA, yielding up to 40 mg of protein per L of culture. Subsequent solubilization of $SpRodA_{1\text{-}255}$ with LAPAO and detergent exchange into DM by IMAC led to recoveries of approximately 80% pure protein (see **Fig. 9** (A)). Quantification of the protein using a NanoDrop apparatus resulted in total protein amounts of 75 mg. The condition for removal of Mistic was the same as the one described for SpRodA. Notably, we observed heavy precipitation of the sample after incubation with the protease; however, analysis of the sample by SDS-PAGE did not reveal any protein loss, so the reason for this precipitation remained unclear. Cleaved $SpRodA_{1\text{-}255}$ was subsequently subjected to cation exchange chromatography, resulting in complete removal of TEV and Mistic, leading to recoveries of 90-95% pure protein (**Fig. 9** (B)). The homogeneity of the sample was subsequently analyzed by gel filtration. Several injections of the same sample were made, with a time difference of fifty minutes between each run. The superposition of each elution profile clearly showed that the peak profile changed over time resulting in shorter retention times and the appearance of an elongated peak (see **Fig. 9** (C)).
Based on these results we assumed that $SpRodA_{1\text{-}255}$ partially oligomerizes in a time-dependent manner. This may be due to the presence of several species within the sample. However, by collecting just fractions of the main peak (see **Fig. 9** (C), grey shaded area) and analyzing it by gel filtration, we were able to obtain a pure, homogeneous sample (**Fig. 9** (D)).

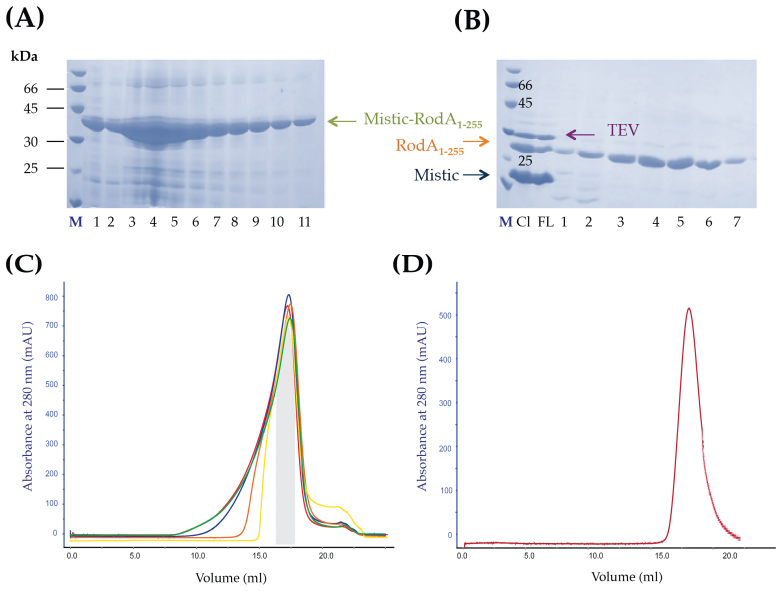

Fig. 9: Purification of SpRodA$_{1\text{-}255}$ from auto-induction medium. SpRodA$_{1\text{-}255}$ was solubilized in LAPAO and subsequently purified by **(A)** Ni-affinity chromatography. After removal of Mistic, SpRodA$_{1\text{-}255}$ was further purified using **(B)** cation-exchange chromatography to remove TEV and Mistic. **(C)** SEC analysis of SpRodA$_{1\text{-}255}$ demonstrated partial oligomerization of SpRodA$_{1\text{-}255}$ in a time-dependent manner. Careful selection of fractions in the peak center (grey shaded area) led to **(D)** the successful purification of homogeneous SpRodA$_{1\text{-}255}$, indicated by the elution of a well-defined peak. Abbreviations: M, marker; Cl, cleaved protein; FL, flow through.

SpRodA$_{1\text{-}255}$ does not crystallize in detergent micelles

Crystallization trials of SpRodA$_{1\text{-}255}$ in the presence of detergent micelles were set up using five different detergents (see **TABLE 1**), with protein concentrations ranging from 7-30 mg/ml as well as two different temperatures (4°C and 20°C). For each tested detergent we analyzed the final detergent concentration in the sample by TLC, resulting in detergent concentrations that were approximately four to six times the CMC (data not shown). Crystallization trials for each protein preparation was set up using a panel of different commercially available screens that cover a broad range of precipitants, pH and salts (see **TABLE 2**).

However, despite significant efforts, SpRodA$_{1\text{-}255}$ failed to crystallize under each tested condition. Since we verified the homogeneity of each protein preparation by size exclusion chromatography and the protein seemed to be stable over extended periods indicating no proteolytic degradation, we excluded the possibility that the absence of crystals was due to the quality of the protein preparations. A more likely explanation could be that SpRodA$_{1\text{-}255}$ failed to form protein-protein interactions essential for crystal nucleation and growth. Considering that, in this specific case, the protein's hydrophobic core is surrounded by a detergent belt that prevents protein-protein interactions, formation of crystal contacts can only be achieved through interaction between the protein's hydrophilic portions. This requires that the detergent micelle fits optimally into the lattice of the crystal. Consequently, the detergent micelle should be as small as possible but still big enough to allow sufficient protection of the proteins hydrophobic transmembrane segments. Therefore, even though we tested crystallizability of SpRodA$_{1\text{-}255}$ in detergents with rather short alkyl chains (NM and DM), we could not exclude that the micelle sizes of these detergents were still too large to allow the formation of potential crystal contacts. On the other hand, failure to crystallize SpRodA$_{1\text{-}255}$ could have also been caused due to scarcity of large hydrophilic surfaces available for protein-protein interactions.

Crystallization of SpRodA$_{1\text{-}255}$ in LCP

Failure of SprodA$_{1\text{-}255}$ to crystallize with the traditional *in surfo* approach led us to the assumption that the detergent environment was not conducive to its crystallization, and we thus chose to proceed with crystallization trials using LCP as the host medium. The advantage of this approach over the one involving crystallization in detergent micelles is that it is generally well suited for integral membrane proteins that contain only small hydrophilic portions, such as SpRodA$_{1\text{-}255}$. However, successful crystallization in LCP requires diffusion of the protein within the three-dimensional lattice of the cubic phase (Cherezov, Liu et al. 2008).
Prior to crystallization attempts we therefore measured the ability of SpRodA$_{1\text{-}255}$ to diffuse freely within the LCP by using the HT LCP-FRAP assay. Experiments were performed under similar conditions as for SpRodA. Since the mobile fraction of the negative control was 20% (data not shown), we set a threshold level of 25% to be able

to distinguish protein from lipid diffusion. Analysis of the results clearly indicated increased mobility of SpRodA$_{1\text{-}255}$ as compared to SpRodA. While only one salt generated mobile fractions for SpRodA that were above the threshold level, approximately 95% of all tested conditions for SpRodA$_{1\text{-}255}$ led to mobile fractions that could be accounted to diffusion of the protein (see **Fig. 10**).

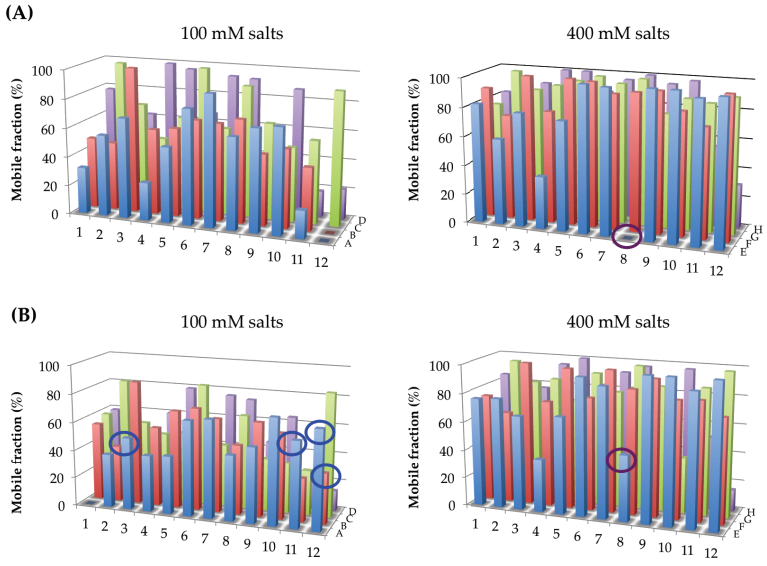

Fig. 10: HT LCP-FRAP results for SpRodA$_{1\text{-}255}$. Fluorescence recovery for SpRodA$_{1\text{-}255}$ was measured in **(A)** Tris pH 7 and **(B)** Tris pH 8. Each plate contained 48 different salts (Stock option Salt kit, Hampton research) at two concentrations each (100 mM in rows A-D, 400 mM in rows E-H). The concentration of PEG 400 was kept constant at 30% (v/v).

Comparative analysis of mobile fractions obtained at pH 7 and pH 8 revealed that the mobility of SpRodA$_{1\text{-}255}$ was not significantly affected by the pH. Diffusion of the protein was generally induced by the same set of salts. However, except for a few conditions (see **Fig. 10** (B), blue circles), mobile fractions increased by about 5-20% at lower pH values (**Fig. 10** (A), left). In addition, HT LCP-FRAP data indicated that mobility of SpRodA$_{1\text{-}255}$ further increased at high salt concentrations, leading to mobile fractions that were in 90% of the conditions higher than 70% (**Fig. 10** (A) and

(B), right). The only exception was ammonium nitrate which led either to a similar or higher mobile fraction at low salt concentrations (**Fig. 10** (B), purple circles). Nevertheless, based on the high diffusion properties of $SpRodA_{1-255}$, we hypothesized that the protein was stable over a wide range of different conditions. Each of the 48 different salts led to mobile fractions that were above the given threshold level in at least one tested concentration value.

Therefore, since $SpRodA_{1-255}$ demonstrated higher mobility in 0.4 M salt concentrations, we initiated crystallization trials of $SpRodA_{1-255}$ using these conditions. Protein concentrations ranged from 10-40 mg/ml. However, these conditions did not lead to any initial crystal hits. Since three of the salts that promoted high protein mobility (mobile fractions > 90%) had buffering capacity (sodium phosphate, potassium phosphate and potassium citrate), we prepared new screens in which we exchanged the Tris buffer either for sodium phosphate, potassium phosphate or potassium citrate buffer at pH 7. Unfortunately, crystallization trials also failed for these screens.

To exclude that these results were caused due to potential stability issues of $SpRodA_{1-255}$, we monitored over the course of five days mobile fractions of six conditions that resulted in initial mobile fractions of 100% (**Fig. 11**). Salts with such high mobile fractions were: ammonium tartrate, ammonium sulfate, lithium acetate, sodium citrate, sodium chloride and sodium phosphate. The data revealed that, depending on the identity of the salt, mobile fractions decreased only by 8-25%, hence still 50-67% above the given threshold level. Consequently, mobile fractions were expected to completely stop after a decay time of 14-40 days. These results indicated therefore that all tested salts were able to keep $SpRodA_{1-255}$ in a mobile state for an extended period of time, reflecting high stability of the protein under these conditions. The reason why $SpRodA_{1-255}$ did not crystallize in LCP remained thus unclear.

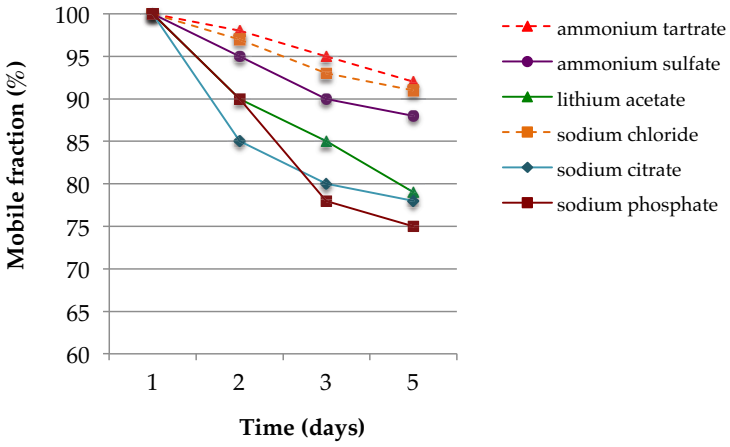

Fig. 11: Mobile fractions of SpRodA$_{1\text{-}255}$ at different incubation times. Fluorescence recovery of SpRodA$_{1\text{-}255}$ was measured for the same drop over a period of five days. The effect of incubation time on the mobile fraction was analyzed in six different salts that led at high concentrations of salt to initial mobile fractions of 100%. The HT LCP-FRAP experiments were performed in Tris pH 7. Each tested condition indicated only a slow decrease in mobile fraction.

Crystallization of SpRodA$_{1\text{-}255}$ in bicelles

Another attractive lipidic medium for the crystallization of membrane proteins are bicelles. The major advantage of this crystallization medium is given by its unique phase behavior. Below their transition temperature (approximately 30°C), bicelles maintain a liquid state that allows manipulation using standard crystallization equipment.

Since most of the membrane protein structures solved by this technique were crystallized in the presence of approximately 8% bicelles 2.9:1 DMPC:CHAPSO (Ujwal and Bowie 2011), we initiated crystallization trials of SpRodA$_{1\text{-}255}$ using this condition as a starting point. Crystallization trials were performed with protein concentrations of 10 mg/ml. Due to the high probability of bicelles to form non-proteinaceous crystals, we carefully inspected each crystallization setup using UV-microscope.

This technique proved to be the best one for $SpRodA_{1\text{-}255}$, since we were able to identify several conditions that led to initial crystal hits. Depending on the condition, crystals appeared after 1-15 weeks and grew to their maximum size after 2-24 weeks (see **TABLE 3** (A)). Diffraction analysis of crystals grown in condition 1, 5, 6, 7 and 8 did not reveal any proteinaceaous diffraction pattern. Crystals that resulted in early identification of positive hits (**TABLE 3** (A), condition 2-4) were on the average not large enough for direct diffraction analysis and were therefore subjected to further optimization. Each optimization step included extensive fine screening of the crystallization parameters, also including the final concentration of bicelles. Optimization of condition 3 led to several crystal hits (see **TABLE 3** (B)). Each of these crystals was tested for diffraction on micro-focus beamlines at the ESRF. Crystals were prior to X-ray analysis cryoprotected in their crystallization condition supplemented with 30% glycerol. Using regular oscillation techniques, we were not able to identify an X-ray diffraction pattern for these crystals. Possible reasons for this outcome could be either that the cryoprotectant or cryocooling procedure damaged the crystal or the crystals were insufficient in size and rather disordered to allow X-ray diffraction.

We thus turned to serial protein crystallography, a recently developed approach that has the potential to circumvent these drawbacks. This approach allows room temperature raster-scanning data collection of micro-sized crystals that are sandwiched between two silicon nitride (Si_3Ni_4) wafers (Coquelle, Brewster et al. 2015). Conditions 3.2, 3.3 and 3.4 were tested in collaboration with J-P. Colletier (Institut de Biologie Structurale (IBS), PSB, France) on beamline ID13 at the ESRF (Grenoble, France) using a crystalline slurry obtained directly from the crystallization plate. The slurry was deposited between two Si_3Ni_4 wafers and presented to the X-ray beam by mounting the Si_3Ni_4 sandwich onto an *xyz* translation table on ID13, followed by data collection. Analysis of the data using the recently developed pre-processing software *NanoPeakCell* (Coquelle, Brewster et al. 2015) clearly indicated that crystals produced in condition 3.1 diffracted X-rays and displayed a possible protein lattice of 50 X 50 X 80 Å (see **Fig. 12**).

TABLE 3. **Crystals of SpRodA$_{1\text{-}255}$ in bicelles.**

(A) Initial crystal hits

#	CRYSTAL	CONDITIONS	#	CRYSTAL	CONDITIONS
1	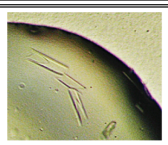	0.1 M HEPES, pH 7.5 0.5 M $(NH_4)_2SO_4$ 30% MPD (24 weeks)	5	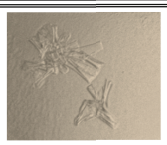	0.1 M Bis-Tris, pH 6.5 0.2 M $CaCl_2$ 45% MPD (10 weeks)
2		0.056 M Na_3PO_4 1.344 M K_3PO_4 (3 weeks)	6		0.1 M Bicine, pH 9 2 M $MgCl_2$ (15 weeks)
3	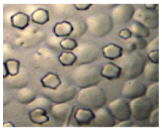	0.2 M $(NH_4)_2SO_4$ 10% PEG 8000 (2 weeks)	7	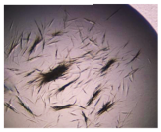	0.1 M HEPES, pH 7.5 1.5 M Li_2SO_4 (10 weeks)
4		0.1 M HEPES, pH 7.5 1 M Li_2SO_4 (2 1/2 weeks)	8	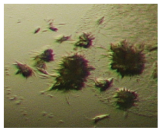	0.1 M Tris, pH 8.5 1.5 M Li_2SO_4 (7 weeks)

(B) Optimization condition 3

#	CRYSTAL	CONDITIONS	#	CRYSTAL	CONDITIONS
3.1	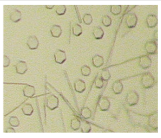	8-10% PEG 8000 0 – 0.07 M $(NH_4)_2PO_4$ 8-12 mg/ml protein 8% bicelles	3.3		10% PEG 8000 0.05 M $(NH_4)_2PO_4$ 0.18 M 2.5-Hexandiol 8 mg/ml protein 8% bicelles
3.2	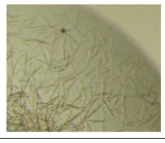	12% PEG 8000 0.05 – 0.09 M $(NH_4)_2PO_4$ 8-12 mg/ml protein 8% bicelles	3.4		3% PEG 400 0.05 M $(NH_4)_2PO_4$ 12 mg/ml protein 8% bicelles

The diffraction pattern indicated a hexagonal space group; interestingly, crystals that were produced in condition 3.1 displayed also hexagonal shape (**TABLE 3** (B)).

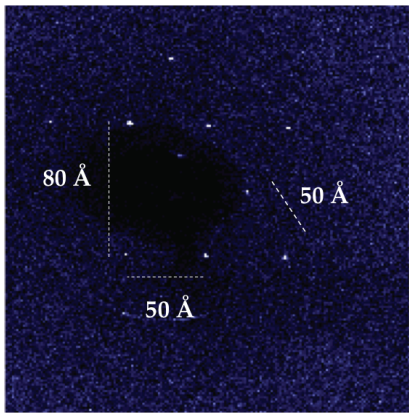

Fig. 12: Protein diffraction of $SpRodA_{1\text{-}255}$ in condition 3.1. A crystalline slurry of condition 3.1 was gently deposited between two Si_3Ni_4 wafers and presented to the X-ray beam (ID13, ESRF). Data analysis showed protein diffraction with possible unit cell parameters of 50 X 50 X 80 Å.

At the moment, we are proceeding with further optimization of condition 3.1 in order to improve diffraction quality. This effort includes modification of salt and precipitant concentrations, as well as protein concentration and crystallization temperature, but also the addition of ligands, such as Lipid II, which may enhance stability of $SpRodA_{1\text{-}255}$ and aid the crystallization process. X-ray diffraction analyses of optimized crystals are planned for the near future.

CONCLUSION

The path towards the structural characterization of a protein by X-ray diffraction requires the production of well-ordered crystals. This demonstrates to be in particular challenging for membrane proteins, requiring generally extensive screening.

The data presented here reports the first successful crystallization of a bacterial flippase that already led to initial diffraction data analysis. This information may therefore pave the way to unravel the first structure of a bacterial flippase.

ACKNOWLEDGEMENTS

We would like to thank J. Marquez and the HTX Lab team (Partnership for Structural Biology (PSB), PSB, France) for access to and help with high throughput crystallization, F. Dupeux (IBS, PSB) for access to and help with LCP and bicelle crystallization, and the European Synchrotron Radiation Facility (ESF, PSB) for access to beamlines. We thank J-P. Colletier (IBS, PSB) for helpful advice in bicelle crystallization and for raster-scanning serial protein crystallography data collection.

REFERENCES

Caffrey, M. (2000). "A lipid's eye view of membrane protein crystallization in mesophases." Curr Opin Struct Biol **10**(4): 486-497.

Caffrey, M. (2003). "Membrane protein crystallization." J Struct Biol **142**(1): 108-132.

Caffrey, M. and V. Cherezov (2009). "Crystallizing membrane proteins using lipidic mesophases." Nat Protoc **4**(5): 706-731.

Cheng, A., et al. (1998). "A simple mechanical mixer for small viscous lipid-containing samples." Chem Phys Lipids **95**(1): 11-21.

Cherezov, V., et al. (2002). "Membrane protein crystallization in meso: lipid type-tailoring of the cubic phase." Biophys J **83**(6): 3393-3407.

Cherezov, V., et al. (2006). "Room to move: crystallizing membrane proteins in swollen lipidic mesophases." J Mol Biol **357**(5): 1605-1618.

Cherezov, V., et al. (2008). "LCP-FRAP Assay for Pre-Screening Membrane Proteins for in Meso Crystallization." Cryst Growth Des **8**(12): 4307-4315.

Cherezov, V., et al. (2004). "A robotic system for crystallizing membrane and soluble proteins in lipidic mesophases." Acta Crystallogr D Biol Crystallogr **60**(Pt 10): 1795-1807.

Cherezov, V., et al. (2007). "High-resolution crystal structure of an engineered human β2-adrenergic G protein-coupled receptor." Science **318**(5854): 1258-1265.

Cherezov, V., et al. (2006). "In meso structure of the cobalamin transporter, BtuB, at 1.95 Å resolution." J Mol Biol **364**(4): 716-734.

Coquelle, N., et al. (2015). "Raster-scanning serial protein crystallography using micro- and nano-focused synchrotron beams." Acta Crystallogr D Biol Crystallogr **71**(Pt 5): 1184-1196.

Dimasi, N., et al. (2007). "Expression, crystallization and X-ray data collection from microcrystals of the extracellular domain of the human inhibitory receptor expressed on myeloid cells IREM-1." Acta Crystallogr Sect F Struct Biol Cryst Commun **63**(Pt 3): 204-208.

Faham, S., et al. (2005). "Crystallization of bacteriorhodopsin from bicelle formulations at room temperature." Protein Sci **14**(3): 836-840.

Faham, S. and J. U. Bowie (2002). "Bicelle crystallization: a new method for crystallizing membrane proteins yields a monomeric bacteriorhodopsin structure." J Mol Biol **316**(1): 1-6.

Hanson, M. A., et al. (2008). "A specific cholesterol binding site is established by the 2.8 Å structure of the human β2-adrenergic receptor." Structure **16**(6): 897-905.

Jaakola, V. P., et al. (2008). "The 2.6 angstrom crystal structure of a human A2A adenosine receptor bound to an antagonist." Science **322**(5905): 1211-1217.

Johansson, L. C., et al. (2009). "Membrane protein crystallization from lipidic phases." Curr Opin Struct Biol **19**(4): 372-378.

Katona, G., et al. (2003). "Lipidic cubic phase crystal structure of the photosynthetic reaction centre from *Rhodobacter sphaeroides* at 2.35Å resolution." J Mol Biol **331**(3): 681-692.

Landau, E. M. and J. P. Rosenbusch (1996). "Lipidic cubic phases: a novel concept for the crystallization of membrane proteins." Proc Natl Acad Sci U S A **93**(25): 14532-14535.

Li, D. and M. Caffrey (2011). "Lipid cubic phase as a membrane mimetic for integral membrane protein enzymes." Proc Natl Acad Sci U S A **108**(21): 8639-8644.

Malinauskaite, L., et al. (2014). "A mechanism for intracellular release of Na+ by neurotransmitter/sodium symporters." Nat Struct Mol Biol **21**(11): 1006-1012.

Moraes, I., et al. (2014). "Membrane protein structure determination - the next generation." Biochim Biophys Acta **1838**(1 Pt A): 78-87.

Ostermeier, C. and H. Michel (1997). "Crystallization of membrane proteins." Curr Opin Struct Biol **7**(5): 697-701.

Pebay-Peyroula, E., et al. (1997). "X-ray structure of bacteriorhodopsin at 2.5 angstroms from microcrystals grown in lipidic cubic phases." Science **277**(5332): 1676-1681.

Rasmussen, S. G., et al. (2007). "Crystal structure of the human β2 adrenergic G-protein-coupled receptor." Nature **450**(7168): 383-387.

Sanders, C. R. and R. S. Prosser (1998). "Bicelles: a model membrane system for all seasons?" Structure **6**(10): 1227-1234.

Schneider, C. A., et al. (2012). "NIH Image to ImageJ: 25 years of image analysis." Nat Methods **9**(7): 671-675.

Stroud, R. M. (2011). "New tools in membrane protein determination." F1000 Biol Rep **3**: 8.

Studier, F. W. (2005). "Protein production by auto-induction in high density shaking cultures." Protein Expr Purif **41**(1): 207-234.

Tiefenbrunn, T., et al. (2011). "High resolution structure of the ba3 cytochrome c oxidase from *Thermus thermophilus* in a lipidic environment." PLoS One **6**(7): e22348.

Ujwal, R. and J. Abramson (2012). "High-throughput crystallization of membrane proteins using the lipidic bicelle method." J Vis Exp(59): e3383.

Ujwal, R. and J. U. Bowie (2011). "Crystallizing membrane proteins using lipidic bicelles." Methods **55**(4): 337-341.

Ujwal, R., et al. (2008). "The crystal structure of mouse VDAC1 at 2.3 Å resolution reveals mechanistic insights into metabolite gating." Proc Natl Acad Sci U S A **105**(46): 17742-17747.

Wadsten, P., et al. (2006). "Lipidic sponge phase crystallization of membrane proteins." J Mol Biol **364**(1): 44-53.

Xu, F., et al. (2011). "Development of an Automated High Throughput LCP-FRAP Assay to Guide Membrane Protein Crystallization in Lipid Mesophases." Cryst Growth Des **11**(4): 1193-1201.

CHAPTER 6

Summarizing discussion

This thesis describes the application of several biochemical and structural approaches aimed at gaining more insight into the complex process of peptidoglycan biosynthesis. The first part of the work concentrated on the characterization of a complex between a Lytic Transglycosylase (LT) and a Penicillin-Binding Protein (PBP) from *Pseudomonas aeruginosa*, with the objective of characterizing the necessary elements for this interaction, which is crucial for peptidoglycan biosynthesis regulation. In the second, major part of this work, the focus was on developing strategies for the purification and crystallization of Lipid II flippases.

$CaCl_2$-dependency of PBP2-SltB1 interaction

Safe enlargement of the stress-bearing peptidoglycan sacculus requires the coordinated action of murein hydrolases and synthases (Holtje 1998). **Chapter 2** describes interaction studies of these two antagonistic proteins. SltB1 (murein hydrolase) and soluble PBP2 (lacking its transmembrane anchor, murein synthase) were purified and surface plasmon resonance studies were performed. Analysis of the data clearly indicated interaction of the proteins, however, in the presence of EDTA the interaction seemed to be completely abolished. Only the addition of $CaCl_2$ could restore the PBP2-SltB1 interaction, pointing out that the presence of Ca^{2+} could be required for the interaction.

Interestingly, structural determination of SltB1 revealed that the protein carries a classical EF-hand like Ca^{2+} binding loop. This EF-hand motif was shown to be essential for stability of *Escherichia coli* Slt35, a close homolog of SltB1, and was proposed to potentially participate in interactions with other proteins (van Asselt and Dijkstra 1999). In eukaryotic systems, on the other hand, it was shown that EF-hand domains often undergo conformational changes upon binding Ca^{2+}, an essential event in signal transduction (Ikura 1996, Grabarek 2006). Ca^{2+}-dependency of the SltB1-PBP2 interaction is therefore likely due to structural rearrangement and/or stabilization of the EF-hand upon binding of Ca^{2+} which might lead to exposure of the EF-hand and thus in the ability of SltB1 to interact with PBP2.

Overexpression of SEDS proteins

The identity of the protein mediating Lipid II transport during peptidoglycan biosynthesis was for a long time a matter of controversy. Members of the SEDS (**S**hape, **E**longation, **D**ivision and **S**porulation) protein family are essential for cell wall growth during division (FtsW), elongation (RodA) and spore cortex formation (SpoVE) and have been proposed as being responsible for transbilayer movement of Lipid II across the cytoplasmic membrane to the periplasmic space (Ishino, Park et al. 1986, Ikeda, Sato et al. 1989, Boyle, Khattar et al. 1997, Henriques, Glaser et al. 1998, Holtje 1998). *In vitro* studies of Mohammadi and colleagues provided the first biochemical evidence that FtsW functions as the Lipid II flippase in *E. coli* (Mohammadi, van Dam et al. 2011). In addition, it was shown that specific, charged residues (R145 and K153) in the fourth predicted transmembrane domain were essential for the transport activity of FtsW (Mohammadi, Sijbrandi et al. 2014). Mutations of these residues to uncharged amino acids did not only completely abolish the transport activity of FtsW *in vitro*, but also led to loss of its *in vivo* activity, which was reflected by the inability of these substitution mutants to complement temperature-sensitive FtsW mutant strains (Mohammadi, Sijbrandi et al. 2014).

Recent *in vivo* studies by Sham and colleagues, however, did not confirm the role of FtsW in Lipid II translocation, but suggested that MurJ, a protein from the MOP (multidrug/oligo-saccharidyl-lipid/polysaccharide) exporter superfamily, was proposed to mediate this function (Sham, Butler et al. 2014). In this work, inactivation of MurJ led to accumulation of peptidoglycan precursors in the *E. coli* cytoplasm and cell lysis. However, accumulation of peptidoglycan precursors is not necessarily due to impaired Lipid II translocation, since it could be also due to a defect in the recycling mechanism of the isoprenoid carrier. Notably, if MurJ were involved in Lipid II translocation, its function would have been confirmed by the *in vitro* assay used to verify FtsW flipping activity, which was not the case (Mohammadi, van Dam et al. 2011). Moreover, if MurJ were the Lipid II flippase, MurJ homologs from other cell wall producing organisms would likely be essential as well. However, deletion of four identified MurJ homologs in *Bacillus subtilis* did not lead to any shape or growth defects (Fay and Dworkin 2009). Moreover, it was reported that *B. subtilis* requires the presence of a newly identified Lipid II flippase (AmJ) for cell wall biogenesis, shedding therefore doubt on the identification of MurJ as the Lipid II flippase (Fay and Dworkin 2009, Meeske, Sham et al. 2015).

Taking into consideration the literature at hand, which presents somewhat controversial data for the new flippase candidate MurJ, SEDS proteins remain the most extensively characterized Lipid II translocating proteins. However, despite the crucial role of Lipid II flippases in the synthesis of peptidoglycan, only little is known about the translocation process. Structural determination of the first bacterial flippase would provide an important step towards understanding the mechanism of Lipid II translocation at a molecular level.

The first step towards the structural characterization of the Lipid II flippase required the overexpression of sufficient yields of recombinant proteins. In **Chapter 3** the expression yield of ten SEDS homologs was evaluated in two expression hosts using various fusion tags, culture conditions and expression strains. Fusion of SEDS proteins to a conventional poly His-tag led in all tested conditions either to poor expression yields, degradation of the protein or strongly hampered cell growth resulting in loss of cell viability and cell death (**TABLE 1**). In addition, other fusion tags that were previously reported to enhance the overexpression of several membrane proteins, such as Thioredoxin (Trx) or the glycerol-conducting channel protein (GlpF) (Begum, Newbold et al. 2000, Ishihara, Goto et al. 2005, Neophytou, Harvey et al. 2007), did not result in successful overexpression of SEDS proteins; in fact expression of these chimeras led to an extremely reduced growth phase that was followed by loss of cell viability (**TABLE 1**).

Failure to overexpress foreign membrane proteins in *E. coli* is presumably associated with their complex biogenesis. Correct insertion of the protein into the membrane generally requires the assistance of the Sec translocon machinery. This translocation machinery can be quickly saturated during membrane protein overexpression. The limiting capacity of the Sec translocon to process a massive load of nascent, heterologously expressed protein results often in destabilization of the host's balance that may lead to activation of stress responses and eventually to cell death. To circumvent this drawback, SEDS proteins were fused to Mistic, a small integral membrane protein from *B. subtilis* that was proposed to have the unique ability to fold itself and its cargo proteins into the membrane without the assistance of the Sec translocon (Roosild, Greenwald et al. 2005). Expression of the SEDS proteins in fusion to Mistic resulted in tremendous increase of expression for six out of the ten tested homologs, resulting in expression levels of 2 to 15 mg of protein/L of culture depending on the SEDS homolog (see **TABLE 1**). Overexpression of the SEDS proteins in fusion to Mistic seemed to have no effect on the host's balance,

suggesting that Mistic may have chaperoned folding of the SEDS into the membrane in a Sec-independent manner.

TABLE 1. Protein yields obtained with the small-scale expression test

	E. coli based expression				Cell-free expression	
PROTEIN NAME	His-tag	Trx-tag	GlpF-tag	Mistic-tag	N-terminal His-tag	C-terminal His-tag
S. pneumoniae RodA	◆◆	⦸	⦸	◆◆◆◆◆◆	◆	⦸
E. coli FtsW	◆◆	⦸	⦸	◆◆◆◆	◆	⦸
E. coli RodA	⦸	⦸	⦸	◆◆◆◆	n.t	n.t
T. maritima FtsW	⦸	⦸	⦸	◆◆◆◆◆	n.t	n.t
P. aeruginosa RodA	⦸	⦸	⦸	◆◆◆◆	n.t	n.t
B. subtilis FtsW	◆◆	⦸	⦸	◆◆◆◆	n.t	n.t
B. subtilis RodA	◆◆	⦸	⦸	⦸	n.t	n.t
B. subtilis SpoVE	❖	⦸	⦸	⦸	n.t	n.t
A. aeolicus FtsW	⦸	⦸	⦸	⦸	n.t	n.t
A. aeolicus RodA	⦸	⦸	⦸	⦸	n.t	n.t

For each protein, the yield obtained is expressed in mg of target protein/liter of culture. Abbreviations: ⦸, not detectable; ❖, degraded; n.t, not tested; ◆, < 0.1 mg/L; ◆◆, 0.1-0.4 mg/L; ◆◆◆, 0.4-2 mg/L; ◆◆◆◆, 2-5 mg/L; ◆◆◆◆◆, 5-10 mg/L; ◆◆◆◆◆◆, > 10mg/L.

Purification of SEDS proteins

Once sufficient yields of SEDS proteins were obtained, the protein had to be extracted from the membrane in a stable and functionally active form, which is described in **Chapter 4**. SEDS homologs that displayed high expression yields in **Chapter 3** (5-15 mg of protein/L of culture), including *Streptococcus pneumoniae* RodA (SpRodA), *E. coli* FtsW (EcFtsW) as well as *Thermatoga maritima* FtsW (TmFtsW), were solubilized in a panel of different detergents. Whereas nonionic detergents, such as DDM, β-OG and Triton–X100, resulted in poor solubilization of the proteins, detergents with anionic (Sarcosine) and zwitterionic (Fos-choline 12 and LAPAO) properties were capable to efficiently extract all three tested SEDS proteins from the membrane, with LAPAO being the most effective. Anionic and zwitterionic detergents are known to be more effective in the solubilization of membrane proteins than nonionic, mainly due to their charged character; however, it was still somehow

unclear why DDM and β-OG showed very low solubilization efficiencies given their success in the structural characterization of several membrane proteins (Raman, Cherezov et al. 2006). It is therefore likely that the three tested SEDS proteins had relatively strong affinities to the lipid bilayer which required the use of more harsh detergents for effective extraction from the membrane.

Since the detergent used for the solubilization of the SEDS proteins does not necessarily have the ability to maintain the proteins in a stable and functional active form, we performed extensive detergents exchange screenings of all three SEDS homologs previously solubilized in LAPAO (most effective detergent for solubilization) and bound to an Ni-affinity resin. Whereas all three SEDS homologs showed heavy aggregation in alkyl PEGs (C_8E_4, C_8E_6, $C_{12}E_8$ and $C_{12}E_9$) and β-OG, the proteins were successfully maintained in a soluble state upon detergent exchange into maltopyranoside (NM, DM and DDM), MNG (LMNG and DMNG) or zwitterionic (LAPAO and Anzergent 3-14) detergents. However, subsequent removal of Mistic led to heavy precipitation of the samples in the presence of zwitterionic detergents, indicating stability issues of the cleaved proteins in these detergents. Interestingly, the only detergents that were able to maintain the SEDS proteins in soluble and stable form were therefore sugar-based detergents that contained all a maltoside-based head group. Maltoside-based detergents were shown to be effective in inhibiting protein denaturation and aggregation thereby enabling preservation of the native protein structure (Prive 2007). The reason for this could be the reduced ability of maltoside-based detergents to disrupt protein:protein interactions that are essential for maintaining the native structure of a protein.

The homogeneity and functional state of the protein with respect to different detergents was further analyzed by solubilizing in parallel the best behaving SEDS candidate, SpRodA, in the three most efficient detergents for extraction (LAPAO, Sarcosine and Fos-choline 12) and subsequently exchanging these detergents for a maltoside-based detergent (DM). Purification of SpRodA did not reveal any significant differences in protein recoveries when solubilized either in LAPAO, Sarcosine or Fos-choline 12; however, analysis of the samples by size exclusion chromatography (SEC) indicated that only LAPAO led to homogeneity of SpRodA, whereas Fos-choline and Sarcosine resulted in aggregation of the protein.

Activity assays of SpRodA reflected the same result; the protein did not show any transbilayer movement of fluorescent labeled Lipid II when solubilized in Fos-choline 12 or Sarcosine, whereas transport activity was observed for LAPAO-

extracted SpRodA. Moreover, it was shown that transport activity was abolished when SpRodA was still in fusion to Mistic, indicating that fusion to Mistic might render SpRodA catalytically inactive. Since Mistic was thought to chaperone SEDS proteins into the membrane, it is likely that specific protein:protein interactions required for this process could be preventing accessibility of SpRodA's active site when the protein is still bound to Mistic.

The data presented in **Chapter 4** therefore clearly indicated that homogeneity and functionality of SEDS proteins coincide and are highly dependent on the choice of detergent. Additionally, the data provided the first biochemical evidence that RodA exerts Lipid II flipping activity which has been until today only reported for *E. coli* FtsW (Mohammadi, van Dam et al. 2011, Mohammadi, Sijbrandi et al. 2014).

Crystallization of SpRodA

Since SpRodA was successfully purified in functional and homogeneous form, its crystallization was pursued with the intent of obtaining diffraction-quality crystals, viewing eventual structure solution (**Chapter 5)**. Crystallization experiments generally consume very large amounts of purified protein that are required for testing a panel of different conditions. Expression conditions of SpRodA were therefore optimized by expressing the protein in auto-induction medium, yielding 45 mg of protein/L of culture. This high cell density medium resulted therefore in a three-fold increase of protein production when compared to the abovementioned expression yields (**Chapter 3**). SpRodA was afterwards purified in six different maltoside-based detergents that were previously shown (**Chapter 4**) to enable stability of the protein. Homogeneity of the samples was confirmed by SEC analysis. Crystallization of SpRodA in the presence of detergents resulted in the identification of several conditions that led to the formation of crystals. However, these crystals were not of diffraction-quality and extensive efforts to optimize these conditions failed. Detergents cannot always provide an adequate substitute for the protein's native environment, and it is therefore likely that the protein displayed only limited stability within detergent micelles resulting in rapid aggregation of the protein and thus in failure to crystallize. Another possibility could be that the detergent could have masked most of the protein's surface, preventing the formation of potential protein-protein contacts that are required for crystal growth.

To circumvent these obstacles, SpRodA was subjected to crystallization trials using the lipidic cubic phase (LCP) methodology that provides a more native-like environment and therefore could increase the likelihood of obtaining initial crystal hits of SpRodA. Crystal nucleation, however, requires sufficient mobility of the protein within the LCP and can be strongly influenced by several factors. By using a specifically designed pre-crystallization assay (HT LCP-FRAP) that measures the mobility of labeled protein within the LCP, it is possible to minimize the crystallization space by identifying conditions that are non-conductive to protein diffusion (Xu, Liu et al. 2011). For this purpose, SpRodA was labeled with Cy3-mono NHS ester to enable detection of crystallization conditions that promote protein diffusion. The ability of SpRodA to diffuse within the LCP was assessed under conditions that included a constant PEG 400 concentration, a panel of different salts at low (0.1 M) and high (0.4 M) concentration as well as different pH (pH 7+8). Mobility of SpRodA was only detected in high concentrations of ammonium acetate, however, several attempts to crystallize SpRodA within these conditions failed. A HT LCP-FRAP time course experiment of SpRodA under these conditions revealed that mobility of SpRodA was completely suppressed after two days. This short time window reflected therefore the low stability of SpRodA that clearly hampered crystallization of the protein.

Subsequently, by using limited proteolysis, it was possible to identify a stable domain of SpRodA that was highly resistant to proteolytic digestion. Interestingly, the appearance of a similar fragment was observed within a SpRodA sample that was stored for five days at 4°C. Analysis of the fragment by peptide mass fingerprinting led to the definition of the boundaries of the proteolyzed fragment. Mapping the N- and C-terminal boundaries onto the topology model of SpRodA, highlighted that the C-terminus was lacking transmembrane helices 8-10 and a major part of the large extracellular loop connecting transmembrane helices 7 and 8. Proteolytic digestion of this loop reflected therefore its high flexibility that may require stabilization by other protein partners. Localization of several conserved residues within this loop strengthened this hypothesis.

Based on the findings that the proteolyzed fragment displayed increased stability, a variant of SpRodA lacking residues 256-407 ($SpRodA_{1-255}$) was generated. However, despite significant efforts, $SpRodA_{1-255}$ failed to crystallize in the presence of detergents or in LCP. Since crystallization of membrane proteins in detergents is based on the formation of crystal contacts between hydrophilic domains (Ostermeier

and Michel 1997), it is likely that despite the use of relatively short alkyl chains (DM and NM), the detergent could have masked most of the protein's surface, including the hydrophilic domains which were rather small in $SpRodA_{1-255}$. This would have prevented potential protein-protein interactions and consequently results in lack of crystals. Why, however, $SpRodA_{1-255}$ failed to crystallize within the LCP remained elusive.

However, bicelles provided an excellent host medium for the crystallization of $SpRodA_{1-255}$. Crystallization in bicelles did not only result in the identification of several conditions that led to initial crystal hits, but also and more importantly, to the identification of one condition in which crystals diffracted X-rays. The fact that $SpRodA_{1-255}$ successfully crystallized with bicelles, but not within another lipidic environment such as the LCP, could indicate that a specific lipid composition of the host system is required. While monoolein is the major constituent of the LCP, bicelles are composed of a well-defined lipid-amphiphile mixture, mainly DMPC:CHAPSO. It could be that DMPC has the ability to more closely mimic the native environment of $SpRodA_{1-255}$ than monoolein, indicating that $SpRodA_{1-255}$ may require specific lipid-protein interactions. These conditions will continue to be explored and improved in the laboratory, with the goal of obtaining a complete diffraction data set that can be phased, leading eventually to the structural determination of the first bacterial flippase.

Concluding remarks

The peptidoglycan is a unique structure of the bacterial cell wall and is essential for bacterial survival. One central event during its biosynthesis is the translocation of Lipid II from the inner to the outer leaflet of the cell. For a number of years SEDS proteins have been proposed as being responsible for Lipid II translocation across membranes. However, to date, flippase activity could be only incontestably shown for *E. coli* FtsW.

In this thesis we provided the first biochemical evidence that *S. pneumoniae* RodA, a close homolog of *E. coli* FtsW, also functions as Lipid II flippase. In addition, we crystallized the protein and obtained initial diffraction data. Further determination of the structure will not only provide insight into the mechanism of lipid transport across cellular compartments but also serve as a new target for the development of antimicrobial agents.

REFERENCES

Begum, R. R., et al. (2000). "Purification of the membrane binding domain of cytochrome b5 by immobilised nickel chelate chromatography." J Chromatogr B Biomed Sci Appl **737**(1-2): 119-130.

Boyle, D. S., et al. (1997). "ftsW is an essential cell-division gene in *Escherichia coli*." Mol Microbiol **24**(6): 1263-1273.

Fay, A. and J. Dworkin (2009). "*Bacillus subtilis* homologs of MviN (MurJ), the putative *Escherichia coli* lipid II flippase, are not essential for growth." J Bacteriol **191**(19): 6020-6028.

Grabarek, Z. (2006). "Structural basis for diversity of the EF-hand calcium-binding proteins." J Mol Biol **359**(3): 509-525.

Henriques, A. O., et al. (1998). "Control of cell shape and elongation by the rodA gene in *Bacillus subtilis*." Mol Microbiol **28**(2): 235-247.

Holtje, J. V. (1998). "Growth of the stress-bearing and shape-maintaining murein sacculus of *Escherichia coli*." Microbiol Mol Biol Rev **62**(1): 181-203.

Ikeda, M., et al. (1989). "Structural similarity among *Escherichia coli* FtsW and RodA proteins and *Bacillus subtilis* SpoVE protein, which function in cell division, cell elongation, and spore formation, respectively." J Bacteriol **171**(11): 6375-6378.

Ikura, M. (1996). "Calcium binding and conformational response in EF-hand proteins." Trends Biochem Sci **21**(1): 14-17.

Ishihara, G., et al. (2005). "Expression of G protein coupled receptors in a cell-free translational system using detergents and thioredoxin-fusion vectors." Protein Expr Purif **41**(1): 27-37.

Ishino, F., et al. (1986). "Peptidoglycan synthetic activities in membranes of *Escherichia coli* caused by overproduction of penicillin-binding protein 2 and rodA protein." J Biol Chem **261**(15): 7024-7031.

Meeske, A. J., et al. (2015). "MurJ and a novel lipid II flippase are required for cell wall biogenesis in *Bacillus subtilis*." Proc Natl Acad Sci U S A **112**(20): 6437-6442.

Mohammadi, T., et al. (2014). "Specificity of the transport of lipid II by FtsW in *Escherichia coli*." J Biol Chem **289**(21): 14707-14718.

Mohammadi, T., et al. (2011). "Identification of FtsW as a transporter of lipid-linked cell wall precursors across the membrane." EMBO J **30**(8): 1425-1432.

Neophytou, I., et al. (2007). "Eukaryotic integral membrane protein expression utilizing the *Escherichia coli* glycerol-conducting channel protein (GlpF)." Appl Microbiol Biotechnol **77**(2): 375-381.

Ostermeier, C. and H. Michel (1997). "Crystallization of membrane proteins." Curr Opin Struct Biol **7**(5): 697-701.

Prive, G. G. (2007). "Detergents for the stabilization and crystallization of membrane proteins." Methods **41**(4): 388-397.

Raman, P., et al. (2006). "The Membrane Protein Data Bank." Cell Mol Life Sci **63**(1): 36-51.

Roosild, T. P., et al. (2005). "NMR structure of Mistic, a membrane-integrating protein for membrane protein expression." Science **307**(5713): 1317-1321.

Sham, L. T., et al. (2014). "Bacterial cell wall. MurJ is the flippase of lipid-linked precursors for peptidoglycan biogenesis." Science **345**(6193): 220-222.

van Asselt, E. J. and B. W. Dijkstra (1999). "Binding of calcium in the EF-hand of *Escherichia coli* lytic transglycosylase Slt35 is important for stability." FEBS Lett **458**(3): 429-435.

Xu, F., et al. (2011). "Development of an Automated High Throughput LCP-FRAP Assay to Guide Membrane Protein Crystallization in Lipid Mesophases." Cryst Growth Des **11**(4): 1193-1201.

APPENDIX

NEDERLANDSE SAMENVATTING

De peptidoglycaan laag van de celwand is uniek voor bacteriën en essentieel voor de bacterie om te kunnen overleven. Het is verantwoordelijk voor het in stand houden van de vorm van de cel en zorgt ervoor dat de bacterie het hoge osmotische drukverschil tussen de binnen en buitenkant van de cel kan weerstaan. De peptidoglycaan laag wordt continu vergroot gedurende de groei van de bacterie tot aan de deling in twee dochtercellen. Dit dynamische proces heeft een goed gecontroleerde coördinatie van de biosynthese, transport en assemblage van al de betrokken componenten nodig. In de afgelopen decennia is er al veel voortgang geweest in het begrijpen van essentiële processen binnen de biosynthese van peptidoglycaan. Echter, door de hoge mate van complexiteit van deze biosynthese route, waarbij een groot aantal verschillende eiwitten samenwerken, is het exacte mechanisme van de celwandsynthese en de controle daarvan nog steeds niet duidelijk.

In dit proefschrift gebruiken we verscheidene biochemische en structurele aanpakken om meer inzicht te krijgen in het complexe proces van de biosynthese van peptidoglycaan en de regulatie daarvan. Het eerste deel van dit proefschrift (Hoofdstuk 2) richt zich op de karakterisering van de interactie van eiwitten die antagonistische functies uitoefenen gedurende de groei van de celwand. Voor dit doel werden lytic transglycosylase SltB1 en PBP2 van *Pseudomonas aeruginosa* gezuiverd en werd met behulp van surface plasmon resonance metingen aangetoond dat deze eiwitten een interactie vertonen die zeer afhankelijk is van de aanwezigheid van Ca^{2+}. Opheldering van de structuur van SltB1 tot hoge resolutie gaf aan dat dit eiwit een zogenaamd EF-hand motief heeft wat mogelijk participeert in de interactie met PBP2.

In **Hoofdstuk 3-5** werd de focus verplaatst naar de ontwikkeling van strategieën om Lipid II flippases van de SEDS (**S**hape, **E**longation, **D**ivision and **S**porulation) eiwitfamilie tot expressie te laten komen, te zuiveren, en te kristalliseren. SEDS eiwitten zijn integrale membraan eiwitten die acht tot tien membraan overspannende segmenten hebben en ze zijn essentieel voor de groei van de celwand tijdens de celdeling, cel elongatie en eventuele spore-vorming. In **Hoofdstuk 3** is de opbrengst van de expressie van SEDS homologen geëvalueerd in twee expressieplasmiden en gebruikmakend van verschillende zuiveringstags, groeicondities en expressiestammen. We konden aantonen dat alleen voor een fusie

met Mistic een hoog expressieniveau van de SEDS eiwitten kon worden gehaald. Dit resulteerde in expressieniveaus van 2 tot 15 mg eiwit per liter cultuur voor zes van de tien geteste SEDS homologen.

In **Hoofdstuk 4** zijn drie van deze SEDS homologen, RodA van *Streptococcus pneumoniae* (SpRodA), FtsW van *Escherichia coli* (EcFtsW) en FtsW van *Thermatoga maritima* (TmFtsW) uit de membraan geextraheerd met behulp van een paneel van verschillende detergenten. Voor elk van de geteste SEDS eiwitten bleek dat zowel anionische (Sarcosine) als zwitterionische (Fos-choline 12 en LAPAO) detergenten zeer efficiënt waren in het extraheren van de SEDS eiwitten uit het membraan, waarbij LAPAO het meest efficiënt was. Uit vervolg experimenten met uitwisselen van detergenten bleek dat de SEDS eiwitten, na verwijdering van de zuiveringstag, alleen stabiel waren in op maltose gebaseerde detergenten. Uit additionele zuivering studies van het zich best gedragende eiwit, SpRodA, bleek dat de homogeniteit en functionaliteit van het gezuiverde SpRodA sterk afhankelijk was van het detergens dat voor de extractie uit het membraan gebruikt was: alleen na extractie met behulp van LAPAO behield SpRodA zijn actieve vorm. Het gebruik van Sarcosine en Fos-choline 12 leidde uiteindelijk tot aggregatie van het eiwit.

Na de succesvolle zuivering van SpRodA in pure en homogene vorm is verder gegaan in **Hoofdstuk 5** met pogingen om het eiwit te kristalliseren door gebruik te maken van verschillende kristallisatiemethodes. Hiervoor is eerst de expressie van SpRodA verder geoptimaliseerd zodat een opbrengst kon worden gehaald van 45 mg eiwit per liter cultuur door gebruik te maken van een auto-inductie medium. Vervolgens is SpRodA gezuiverd gebruikmakend van zes verschillende op maltose gebaseerde detergenten (**Hoofdstuk 4**) om stabiliteit van het eiwit te garanderen. Voor elk van de detergenten werd de homogeniteit van de eiwitoplossing geverifieerd met behulp van gelfiltratie chromatografie. Kristallisatie pogingen van SpRodA vanuit de kubische lipide fase (lipidic cubic phase, LCP) resulteerde niet in kristallen die een diffractie patroon gaven. Uit metingen van de mobiliteit van SpRodA in de kubische lipide fase met behulp van FRAP (fluorescentie herstel na fotobleaching) kwam naar voren dat SpRodA niet stabiel was in dit lipide systeem. Dit bleek uit een volledige afwezigheid van mobiliteit van het eiwit na twee dagen. Met behulp van gelimiteerde proteolyse kon een stabiel fragment van SpRodA worden geïdentificeerd dat in hoge mate stabiel was tegen verdere proteolytische afbraak. Een vergelijkbaar fragment kon worden gedetecteerd in een gezuiverd preparaat van SpRodA dat vijf dagen lang was opgeslagen bij 4 ºC. Uit analyse van

dit fragment met behulp van massa spectrometrie bleek dat dit fragment een C-terminaal stuk mist bestaande uit membraanhelices (8-10) alsmede een groot deel van de periplasmatische loop tussen membraanhelices 7 en 8. Omdat bleek dat dit proteolytische fragment verhoogde stabiliteit vertoonde, is een vergelijkbare variant van SpRodA gemaakt welke de aminozuren 256-407 ($SpRodA_{1-255}$) mist. Hoewel $SpRodA_{1-255}$ ook niet kristalliseerde vanuit de kubische lipide fase, bleek dat bicellen een uitermate geschikt medium waren voor kristallisatie van dit fragment, waarbij één conditie leidde tot kristallen die een diffractie patroon gaven.

Samenvattend is in dit proefschrift een eerste kader geschetst voor het begrijpen van de relatie tussen eiwitten die antagonistische functies uitoefenen tijdens de biosynthese van de celwand. Tevens is voor het eerst vastgelegd dat SpRodA functioneert als een Lipide II flippase. Dit was tot nu toe alleen voor EcFtsW aangetoond. Ook is SpRodA gekristalliseerd en is initiële diffractie data van deze kristallen verkregen. Opheldering van de driedimensionale structuur van SpRodA zal niet alleen inzicht geven in het transportmechanisme van lipiden over cellulaire compartimenten maar zal ook nieuwe wegen openen voor rationeel ontwerp van medicijnen.

ACKNOWLEDGEMENTS

The path to becoming a doctor included for me not only overcoming several hurdles, but also and more importantly working with and getting to know a lot of amazing people that had a great influence on my scientific and personal life, making my Ph.D. an unforgettable experience.

First and foremost, I would like to thank my advisors Andrea Dessen and Eefjan Breukink for their continuous support and encouragement during the past five years.

I gratefully acknowledge the funding received towards my Ph.D. from the Netherlands Organisation for Health Research and Development that made my Ph.D. work possible for such a long period.

I greatly appreciate the support and advice from members of the Patbac group, specifically Viviana, for sharing with me her broad knowledge about molecular biology and biochemistry, Alex, for always having to purify for me tons of TEV protease and of course Carlito, for the countless discussions about how to improve crystals.

I have been very privileged to get to know and work with two amazing Ph.D. students, Marko and my dearest friend Fedex. Your enthusiasm and friendship made the last years of my Ph.D. unforgettable and I wish you all the best for finishing up your Ph.D.! Fedex, my little crazy Italian, I am grateful for all your support you gave me since I had the pleasure to get to know you, the long discussions we had about all aspects of life and your craziness that made me always smile and pushed me through hard times. Thanks for being my friend!

Other past group members that I had the pleasure to work with and get to know are Thierry Izore, who did not only share with me his broad technical know-how, but was also a friend, Karen Fulan-Discola, who was always thinking positive and taught me never to give up, David Neves, our dearest '*Junior boss*', who's good mood was always contagious and last but not least Steve Wong and Munan Shaik, two former postdocs who very much impressed me with their deep understanding of cutting-edge techniques.

My Ph.D. would not have been possible without the contribution of the platforms of the Partnership for Structural Biology. A special thanks goes here to Florine Dupeux, who was always helpful and set up for me countless crystallization plates.

I am also particularly indebted to Jacques-Phillippe Colletier for his invaluable advice and feedback on my bicelles crystals.

I greatly appreciate the collaboration with Tamimount Mohammadi, who shared with me her broad knowledge and passion about the flippase and performed several activity assays.

My time in Grenoble, especially the last two years, was made enjoyable in large part due many friends that became a part of my life. I am especially grateful for the Denfer '*gang*' Sonja, Yann, Fedex, Marko, Silvia, Charles, Wilek, Albert, Javier, Joyce and many more, who were always up for a beer, sometimes even until the birds start singing.

Schließlich möchte ich mich ganz besonders bei meiner Familie bedanken, ohne die ich heute nicht da wäre wo ich bin. Danke, dass ihr mich in allen meinen Entscheidungen immer unterstützt habt, danke, dass ihr immer da wart wenn ich nicht wusste wie es weitergehen soll, danke, dass ihr mir beigebracht habt nie das Ziel aus den Augen zu verlieren und nie aufzugeben. Durch eure Hilfe und Kraft war es mir möglich alle Herausforderungen zu bewältigen, DANKE, dafür, dass es euch gibt! Last but not least, I am grateful for my boyfriend Jon. He was always there for me when I thought there is no way out, he tried to motivate me, make me laugh, even I made it very hard for him, but he never gave up. Thanks for always being so positive when I couldn't and listening to me when I needed it. Thank you for being my light in the dark!

Julia

CURRICULUM VITAE

Ioulia Nikolaidis was born on January 25th 1982 in Oelde, Germany. In 2004 she obtained her Abitur from the Einstein-Gymnasium in Rheda-Wiedenbrück, Germany. In the same year she began her bachelor studies in Bioinformatics and Genome Research at the University Bielefeld, Germany. After she obtained her Bachelor degree in 2007, she continued to pursue a Masters degree in Genome Based Systems Biology at the University Bielefeld. A research project was attended in the group of Prof. dr. Turlough Finan at the McMaster University in Canada under the supervision of Prof. dr. Anke Becker from the University Bielefeld. The research project was based on the molecular and functional analysis of members of the *Sinorhizobium meliloti* phosphate uptake regulon. In 2010 she obtained her masters degree and in the same year she began her Ph.D. in the Membrane Biochemistry and Biophysics group at the University Utrecht (the Netherlands) under the supervision of Prof. dr. Antoinette Killian, dr. Eefjan Breukink and dr. Andrea Dessen (Institut de Biologie Structurale, France). The research was performed at the Institut de Biologie Structurale, France, and resulted in this thesis.

LIST OF PUBLICATIONS

1. V. Lantez, **I. Nikolaidis**, M. Rechenmann, T. Vernet and M. Noirclerc-Savoye (2015) Rapid automated detergent screening for the solubilization and purification of membrane proteins and complexes. Engineering in Life Sciences **15** (1): 39-50.
2. **I. Nikolaidis**, S. Favini-Stabile and A. Dessen (2013) Resistance to antibiotics targeted to the bacterial cell wall. Protein Science **23** (3): 243 – 259.
3. **I. Nikolaidis**, T. Izore, V. Job, N. Thielens, E. Breukink and A. Dessen (2012) Calcium–dependent complex formation between PBP2 and lytic transglycosylase SltB1 of *P. aeruginosa*. Microb Drug Resist **18** (3): 298 – 305.

ABBREVIATIONS

Å	Angstrom
A.U.	Arbitrary Units
ADP	Adenosine diphosphate
Ala	Alanine
anhMur*NA*c	1,6-anhydroMur*NA*c
Anzergent 3-14	*n*-tetradeyl-N,N-dimethyl-3-ammonio-1-propanesulfonate
Arg	Arginine
Asp	Asparagine
ASPRE	Active-site serine penicillin-recognizing enzymes
ATP	Adenosine triphosphate
BSA	Bovine serum albumin
$C_{12}E_8$	Octaethylene glycol monooctyl ether
$C_{12}E_9$	Polyoxyethylene (9) dodecyl ether
C_8E_4	Tetraethylene glycol monooctyl ether
C_8E_6	Hexaethylene glycol monooctyl ether
CHAPS	3-[(3-Cholamidopropyl)dimethylammonio]-1-propanesulfonate hydrate
CHAPSO	3-([3-cholamidopropyl]dimethylammonio)-2-hydroxy-1-propanesulphonate
cm	centimeter
CM	Cytoplasmic membrane
CMC	Critical micelle concentration
ColM	Colicin M
CYT	Cytoplasm
dcw	*division and cell wall*
DDM	*n*-dodecyl-*β*-D-maltopyranoside
DM	*n*-decyl-*β*-D-maltopyranoside
DMF	Dimethylformamide
DMNG	Decyl maltose neopentyl glycol
DMPC	1,2-dimyristoyl-*sn*-glycero-3-phosphocholine
DTT	Dithiothreitol
e.g.	For example
EcFtsW	*Escherichia coli* FtsW
EDTA	Ethylenediaminetetraacetic acid
ESRF	European Synchrotron Facility
FOS12	Fos-choline 12
FPLC	Fast protein liquid chromatography
FRET	Fluorescence resonance energy transfer
Glc*NA*c	*N*-acetyl glucosamine

GlpF	Glycerol-conducting channel protein
Glu	Glutamate
Gly	Glycine
GPCRs	G-protein-coupled receptors
GT	Glycosyltransfer
h	hours
His	Histidine
HMM	High-molecular mass
HT LCP-FRAP	High-throughput LCP-Fluorescence recovery after photobleaching
IBS	Institut de Biologie Structurale
IM	Inner membrane
IMAC	Immobilized metal affinity chromatography
IPTG	Isopropyl β-D-1-thiogalactopyranoside
k_a	Association rate constant
k_d	Dissociation rate constant
K_D	Equilibrium dissociation constant
kDa	Kilodalton
L	Liter
LAPAO	3-laurylamido-N,N′-dimethylpropyl amine oxide
LB	Luria-Bertani medium
LCP	Lipidic Cubic Phase
LMM	Low-molecular mass
LPS	Lipopolysaccharide
LT	Lytic transglycosylase
LUVs	Large unilamellar vesicles
Lys	Lysine
M	Molar
M9	Minimal medium
MATE	Multidrug and toxic compound extrusion
meso-A_2pm	2,6-diaminoheptanedioic acid
mg	Milligram
min	Minutes
Mistic	Membrane-integrating sequence for translating inner membrane protein constructs
ml	Milliliter
mM	millimolar
MNG	Maltose neopentyl glycol
MO	Monoolein
MOP	Multidrug/oligo-saccharidyl-lipid/polysaccharide exporter
Mur*NA*c	*N*-acetyl muramic acid
MWCO	Molecular-weight cutoff

Mg	Microgram
µM	Micromolar
NADPH	Nicotinamide adenine dinucleotide phosphate
NAG	Glc*NA*c
NAM	Mur*NA*c
NBD	7-nitro-2,1,3-benzoxandiazol-4-yl
Ni	Nickel
nM	Nanomolar
nm	Nanometer
NM	*n*-nonyl-*β*-D-maltopyranoside
NMNG	Lauryl maltose neopentyl glycol
nPB	
OD	Optical Density
OM	Outer membrane
PBP	Penicillin Binding Protein
PCR	Polymerase chain reaction
PDB	Protein Data Bank
PDC	Protein-detergent complex
PE	Phosphatidylethanolamine
PEG	Polyethylene glycol
PEP	Phosphoenolpyruvate
PER	Periplasm
PG	Peptidoglycan
Phe	Phenylalanine
pI	Isoelectric point
PMSF	Phenylmethanesulphoylfluoride
PP-M_{pep5}-G	
PSB	Partnership for Structural Biology
rpm	Rounds per minute
RT	Room temperature
s	Seconds
Sarcosine	Sodium lauroyl sarcosine
SDS-PAGE	Sodium dodecyl sulfate-polyacrylamide gel electrophoresis
SEC	Size-exclusion chromatography
SEDS	Shape, Elongation, Division and Sporulation
Ser	Serine
SPR	Surface Plasmon Resonance
SpRodA	*Streptococcus pneumoniae* RodA
TB	Terrific broth medium
TEV	Tobacco etch virus
TLC	Thin layer chromatography
TM	transmembrane
TmFtsW	*Thermatoga maritima* FtsW

TMR	Tetramethylrhodamine cadaverine
TP	Transpeptidation
Triton-X-100	polyoxyethylene octyl phenyl ether
tRNA	transfer RNA
Trx	Thioredoxin
Tyr	Tyrosine
UDP	Uridine diphosphate
v/v	Volume/volume
VDAC	Voltage-dependent anion channel
wt/wt	Weight/weight
β-OG	*n*-octyl-*β*-D-glucopyranoside